

Process Characterization of Electrical Discharge Machining of Highly Doped Silicon

by

Gregory Allan Crawford

B.A. Chemistry

University of Idaho, 1995

M.A. Organizational Management

The George Washington University, 2005

SUBMITTED TO THE DEPARTMENT OF MECHANICAL ENGINEERING IN
PARTIAL FULLFILLMENT OF THE REQUIREMENTS FOR THE DEGREES OF

Naval Engineer

and

Master of Science in Mechanical Engineering

at the

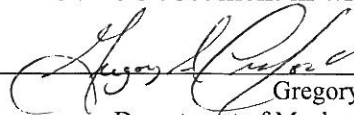
Massachusetts Institute of Technology

June 2012

© Gregory Allan Crawford, 2012. All rights reserved.

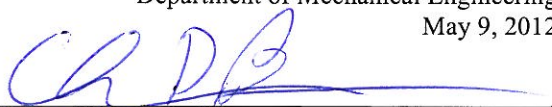
The author hereby grants to MIT and Draper Laboratory permission to reproduce and
distribute publicly paper and electronic copies of this thesis document in whole or in part.

Signature of Author: _____



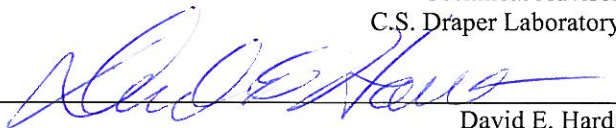
Gregory Allan Crawford
Department of Mechanical Engineering
May 9, 2012

Certified by: _____



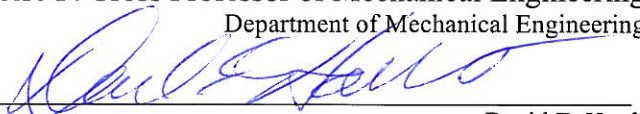
Dr. Christopher DiBiasio
Technical Advisor
C.S. Draper Laboratory

Certified by: _____



David E. Hardt
Ralph E. and Eloise F. Cross Professor of Mechanical Engineering
Department of Mechanical Engineering

Accepted by: _____



David E. Hardt
Chairman, Committee for Graduate Students
Department of Mechanical Engineering

Report Documentation Page			Form Approved OMB No. 0704-0188		
Public reporting burden for the collection of information is estimated to average 1 hour per response, including the time for reviewing instructions, searching existing data sources, gathering and maintaining the data needed, and completing and reviewing the collection of information. Send comments regarding this burden estimate or any other aspect of this collection of information, including suggestions for reducing this burden, to Washington Headquarters Services, Directorate for Information Operations and Reports, 1215 Jefferson Davis Highway, Suite 1204, Arlington VA 22202-4302. Respondents should be aware that notwithstanding any other provision of law, no person shall be subject to a penalty for failing to comply with a collection of information if it does not display a currently valid OMB control number.					
1. REPORT DATE 01 JUN 2012		2. REPORT TYPE		3. DATES COVERED	
4. TITLE AND SUBTITLE Process Characterization of Electrical Discharge Machining of Highly Doped Silicon				5a. CONTRACT NUMBER	
				5b. GRANT NUMBER	
				5c. PROGRAM ELEMENT NUMBER	
6. AUTHOR(S)				5d. PROJECT NUMBER	
				5e. TASK NUMBER	
				5f. WORK UNIT NUMBER	
7. PERFORMING ORGANIZATION NAME(S) AND ADDRESS(ES) Massachusetts Institute of Technology, Washington, DC, 20052				8. PERFORMING ORGANIZATION REPORT NUMBER	
9. SPONSORING/MONITORING AGENCY NAME(S) AND ADDRESS(ES)				10. SPONSOR/MONITOR'S ACRONYM(S)	
				11. SPONSOR/MONITOR'S REPORT NUMBER(S)	
12. DISTRIBUTION/AVAILABILITY STATEMENT Approved for public release; distribution unlimited.					
13. SUPPLEMENTARY NOTES The original document contains color images.					
14. ABSTRACT					
15. SUBJECT TERMS					
16. SECURITY CLASSIFICATION OF:			17. LIMITATION OF ABSTRACT	18. NUMBER OF PAGES 128	19a. NAME OF RESPONSIBLE PERSON
a. REPORT unclassified	b. ABSTRACT unclassified	c. THIS PAGE unclassified			

(THIS PAGE INTENTIONALLY LEFT BLANK)

Process Characterization of Electrical Discharge Machining of Highly Doped Silicon

**by
Gregory Allan Crawford**

**Submitted to the Department of Mechanical Engineering on May 11, 2012
in Partial Fulfillment of the Requirements for the Degrees of**

**Naval Engineer
and
Master of Science in Mechanical Engineering**

Abstract

Electrical Discharge Machining (EDM) is an advanced machining process that removes material via thermal erosion through a plasma arc. The machining process is accomplished through the application of high frequency current (typically through a fine wire or some other electrode) to a conductive workpiece. The electrode is physically separated from the workpiece by some small distance and the potential difference is commonly discharged through an insulating dielectric material such as deionized water or oil. This short duration application of current produces a spark across the gap between the electrode and workpiece, causing vaporization and melting of local material in both the electrode and workpiece. The EDM process is most frequently used for conductive substrates (i.e. metals); however, research has shown that the process may be successfully used on semiconductor substrates such as doped silicon wafers¹. The purpose of this research was to characterize the EDM process using Design of Experiments (DOE) statistical methodology on highly doped silicon wafer workpieces for material removal rate (MRR) and surface roughness (R_a) for both Wire EDM (WEDM) and die sinker EDM machines. Once process characterization was completed, confirmation testing was conducted for each machine. The applied spark energy had a significant impact on processing speed for both machines as expected, with the WEDM processing also heavily dependent on selected control speed. Surface roughness was also found to be highly dependent on spark energy for both machines. Evaluation of minimum obtainable feature sizes for some specific geometries as well as evaluation of various effects on the processing of silicon were also conducted.

Thesis Supervisor: David E. Hardt
Ralph E. and Eloise F. Cross Professor of Mechanical Engineering
Professor of Engineering Systems

¹ (Reynaerts, Heeren and Van Brussel 1997)

(THIS PAGE INTENTIONALLY LEFT BLANK)

Table of Contents

Abstract.....	3
Table of Contents.....	5
List of Figures.....	7
List of Tables	10
Biographical Note.....	12
Acknowledgements.....	13
1.0 Introduction.....	15
1.1 EDM Process Description	15
1.1.1 EDM Theory.....	17
1.2 Wire EDM	18
1.3 Die sinking EDM.....	20
1.4 Thesis Scope.....	22
2.0 Characterization of Silicon Wafer Processing on the Wire EDM for Material Removal Rate and Surface Roughness	23
2.1 Introduction.....	23
2.11 Wire EDM Research and Equipment	23
2.12 Experimental Design	24
2.13 Conduct of WEDM experiments.....	29
2.14 Analysis of WEDM Results	30
2.15 Confirmation of Experiment Results	41
3.0 Characterization of Silicon Wafer Processing on the Die Sinker EDM for Material Removal Rate and Surface Roughness.....	43
3.1 Die Sinker Experiment	43
3.11 Die Sinker Setup and Research	43
3.12 Experimental Design	46
3.13 Conduct of die sinker experiments.....	51

3.14 Analysis of Die Sinker EDM Results	51
3.15 Confirmation of Experiment Results	88
4.0 Processing Testing and Production Examples	89
4.1 Effect of Doping Type in Die Sinker Processing	89
4.2 Effect of Resistivity on Die Sinker Processing	90
4.3 Cantilever Beam Width Using the Roboform 240 WEDM	91
4.4 Hemisphere Negatives using Die Sinker EDM	93
4.5 A Complex Processing Example.....	97
5.0 Machinist's Guidance and Lessons Learned	99
5.1 General guidelines	99
5.2 WEDM specific information	100
5.3 RAM EDM specific pointers.....	100
5.4 Fixturing and Handling	101
6.0 Conclusions and Future Work.....	103
6.1 General Conclusions.....	103
6.2 Areas for Future Study	103
6.2.1 WEDM	103
6.2.2 Die Sinker EDM	103
6.2.3 General Areas.....	104
Bibliography.....	107
Appendix A – Literature Search Summation	109
Appendix B – WEDM Roughing Experiment Data	116
Appendix C – WEDM Finishing Experiment Data.....	118
Appendix D – Die Sinker Roughing Experiment Data	119
Appendix E – Die Sinker Finishing Experiment Data	123
Appendix F – Hemispherical Geometry Data	126

List of Figures

Figure 1: EDM Spark Process for Resistive Spark Generator Circuit.....	17
Figure 2: Typical WEDM Setup	19
Figure 3: Typical Die Sinker Setup	21
Figure 4: Graphic of Sample Coupon for WEDM Experiments.....	30
Figure 5: Normal Probability Plot of WEDM Roughing Experiment MRR R-Values	33
Figure 6: Input Effects for WEDM Roughing Experiment MRR S/N	34
Figure 7: Normal Probability Plot of WEDM Roughing R_a R-Values	35
Figure 8: WEDM Roughing Experiment Input Effects for R_a S/N	36
Figure 9: WEDM Finishing Experiment Input Effects for MRR S/N	38
Figure 10: Normal Probability Plot for WEDM Finishing MRR R-Values	39
Figure 11: WEDM Finishing Experiment Input Effects for R_a S/N	40
Figure 12: Normal Probability Plot for WEDM Finishing Experiment R_a R-Values	40
Figure 13: Die Sinker Roughing Mean Cut Speed Input Effects.....	54
Figure 14: Normal Probability Plot of Die Sinker Roughing Experiment Mean Cut Speed R-Values	54
Figure 15: Die Sinker Roughing Mean Cut Speed ANOVA	55
Figure 16: Interaction Plots for Die Sinker Roughing Mean Cut Speed	57
Figure 17: Die Sinker Roughing Cut Speed S/N Input Effects	58
Figure 18: Normal Probability Plot of Die Sinker Cut Speed S/N R-Values	59
Figure 19: Die Sinker Roughing Experiment Cut Speed S/N ANOVA	60
Figure 20: Die Sinker Cut Speed S/N Interaction Plots.....	61
Figure 21: Die Sinker Roughing Experiment Cut Speed Standard Deviation Input Effects	62
Figure 22: Normal Probability Plot of Cut Speed S/N Standard Deviation R-Values	63
Figure 23: Die Sinker Roughing Experiment Cut Speed Standard Deviation Interaction Plots.....	63
Figure 24: Die Sinker Roughing Experiment Cut Speed Standard Deviation ANOVA ..	64
Figure 25: Die Sinker Roughing Experiment Mean R_a Input Effects.....	66
Figure 26: Normal Probability Plot of Die Sinker Roughing Experiment Mean R_a R- Values	66

Figure 27: Die Sinker Roughing Experiment R_a ANOVA	67
Figure 28: Die Sinker Roughing Experiment R_a S/N R-Values	68
Figure 29: Normal Probability Plot for Die Sinker Roughing Experiment R_a S/N R- Values	68
Figure 30: Die Sinker Roughing Experiment R_a S/N ANOVA	69
Figure 31: Die Sinker Roughing Experiment R_a Standard Deviation R-Values	70
Figure 32: Die Sinker Roughing Experiment R_a Standard Deviation ANOVA	71
Figure 33: Die Sinker Finishing Cut Speed Input Effects	74
Figure 34: Normal Probability Plot of Die Sinker Finishing Experiment Mean Cut Speed R-Values	74
Figure 35: Die Sinker Finishing Experiment Cut Speed ANOVA	75
Figure 36: Die Sinker Finishing Experiment Cut Speed S/N Input Effects	76
Figure 37: Normal Probability Plot of Die Sinker Cut Speed S/N R-Values	76
Figure 38: Die Sinker Finishing Experiment Cut Speed S/N ANOVA	77
Figure 39: Die Sinker Finishing Experiment Cut Speed Standard Deviation Input Effects	78
Figure 40: Normal Probability Plot of Die Sinker Finishing Experiment Cut Speed Standard Deviation R-Values	78
Figure 41: Die Sinker Finishing Experiment Cut Speed Standard Deviation ANOVA...	79
Figure 42: Die Sinker Finishing Experiment Cut Speed Standard Deviation Interaction Plots.....	80
Figure 43: Die Sinker Finishing Experiment Mean R_a Input Effects	81
Figure 44: Normal Probability Plot of Die Sinker Finishing Experiment Mean R_a R- Values	81
Figure 45: Die Sinker Finishing Experiment R_a ANOVA	82
Figure 46: Die Sinker Finishing Experiment R_a Interaction Plots.....	83
Figure 47: Die Sinker Finishing Experiment R_a S/N Input Effects	84
Figure 48: Normal Probability Plot of Die Sinker Finishing Experiment R_a S/N R-Values	84
Figure 49: Die Sinker Finishing Experiment R_a S/N ANOVA	85
Figure 50: Die Sinker Finishing Experiment R_a S/N Interaction Plots.....	85

Figure 51: Die Sinker Finishing Experiment R_a Standard Deviation Input Effects	86
Figure 52: Normal Probability Plot of Die Sinker Finishing Experiment Standard Deviation R-Values.....	87
Figure 53: Die Sinker Finishing Experiment R_a Standard Deviation ANOVA.....	87
Figure 54: Effect of Silicon Resistivity on Processing Time.....	91
Figure 55: Cantilever beams in Silicon.....	92
Figure 56: Cantilever Beams, reduced magnification.....	93
Figure 57: 0.015" Radius Hemispherical Cut and Electrodes	94
Figure 58: Hemisphere #8, $R_a = 21.4 \mu\text{inches}$ (top), and #9, $R_a = 13.6 \mu\text{inches}$ (bottom)....	95
Figure 59: SEM photos of Hemisphere #4, no R_a taken, but estimated at 90-120 μinches	96
Figure 60: SEM of Hemisphere #12, avg R_a 10.5 μinches . Note the chipping around feature edge.	96

List of Tables

Table 1: Roboform 240 WEDM Controllable Inputs	25
Table 2: WEDM Roughing Experiment Settings	27
Table 3: WEDM Finishing Experiment Settings	27
Table 4: Taguchi L12 Array used for WEDM Roughing Experiment	28
Table 5: Taguchi L8 Array used for WEDM Finishing Experiment	28
Table 6: WEDM Roughing Experiment Data Summary	32
Table 7: WEDM Roughing Experiment MRR S/N ANOVA.....	32
Table 8: WEDM Roughing Experiment MRR R-Values	32
Table 9: WEDM Roughing Experiment R_a S/N ANOVA.....	34
Table 10: WEDM Roughing Experiment R_a R-Values	34
Table 11: WEDM Finishing Experiment Data Summary.....	37
Table 12: WEDM Finishing Experiment MRR S/N.....	38
Table 13: WEDM Finishing Experiment R_a S/N.....	39
Table 14: Roboform 350 Die Sinker EDM Controllable Inputs.....	46
Table 15: Die Sinker EDM Roughing Experiment Settings.....	49
Table 16: Die Sinker EDM Roughing Experiment Design	49
Table 17: Die Sinker EDM Finishing Experiment Settings.....	50
Table 18: Die Sinker EDM Finishing Experiment Design	50
Table 19: Die Sinker EDM Roughing Experiment Data Summary.....	53
Table 20: Die Sinker Roughing Experiment Mean Cut Speed R-Values.....	54
Table 21: Die Sinker Roughing Experiment Cut Speed S/N R-Values.....	58
Table 22: Die Sinker Roughing Experiment Cut Speed Standard Deviation R-Values ...	62
Table 23: Die Sinker Roughing Experiment Mean R_a R-Values.....	65
Table 24: Die Sinker Roughing Experiment R_a S/N R-Values	67
Table 25: Die Sinker Roughing Experiment R_a Standard Deviation R-Values.....	70
Table 26: Die Sinker Finishing Experiment Mean Cut Speed R-Values.....	72
Table 27: Die Sinker EDM Finishing Experiment Data Summary	73
Table 28: Die Sinker Finishing Experiment Cut Speed S/N R-Values	75
Table 29: Die Sinker Finishing Experiment Cut Speed Standard Deviation R-Values....	78
Table 30: Die Sinker Finishing Experiment Mean R_a R-Values	80

Table 31: Die Sinker Finishing Experiment R_a S/N R-Values	83
Table 32: Die Sinker Finishing Experiment R_a Standard Deviation R-Values	86
Table 33: Dopant Test Input Parameter Settings	90
Table 34: Resistivity Test Data.....	90
Table 35: Cantilever Beam Settings	91
Table 36: 0.015” Radius Hemisphere Settings	94

Biographical Note

Lieutenant Commander Greg Crawford was born in Columbus, Ohio in 1970. He enlisted in the Navy in 1991 as a nuclear Electricians Mate. He graduated from University of Idaho in 1996 with a Bachelor of Arts in Chemistry and received his commission following completion of Officer Candidate School in Pensacola, Fl. After commissioning, LCDR Crawford reported to the USS GEORGIA (GOLD) (SSBN 729) where he served as Chemistry and Radiological Controls Assistance and Tactical Systems Officer. Following his Junior Officer tour, he served as Shift Engineer and Staff Training Officer on the Daniel Webster (MTS-626) in Charleston, SC. He was accepted into the Navy DC Intern Program and attended The George Washington University, where he completed a Masters degree in Organizational Management. He served as Engineer Officer on board USS HELENA and as Navigator on PCU TEXAS. After joining the Engineering Duty Officer community, LCDR Crawford reported to Supervisor of Shipbuilding, Conversion and Repair, Newport News where he served as an Assistant Project Officer, delivering the USS NORTH CAROLINA (SSN 777) and supervising the 2008 USS ENTERPRISE (CVN-65) EDSRA. He reported to MIT for the graduate program in Naval Construction and Engineering in 2009. He is married to Denise Komenda.

Acknowledgements

My very special thanks go to all of the Draper Laboratory shop personnel for their patience and assistance throughout this yearlong project. Their knowledge and skills were invaluable in throughout the conduct of this thesis. Specifically, Paul Boselli's invaluable assistance and patience with my never-ending questions and requests for electrode manufacture were a true blessing. We even had a little fun. Paul, my apologies for developing some new work for you to do!

Thanks also to Chris DiBiasio as my research advisor for dealing with my occasional impatience when frustrated and his keen questioning of approach and thoughtfulness in considering some of the more difficult questions.

Thanks to Professor David Hardt at MIT for taking the time away from busy departmental and teaching duties to answer my sometimes-basic questions on statistical analysis and keeping me asking the right questions about the data I had acquired.

Most of all, my deepest thanks and love to Denise, who made all of this possible by putting up with me and being so supportive over the last three years. Without her, this would all be rather pointless.

This thesis was prepared at the Charles Stark Draper Laboratory, Inc., under the Internal Research and Development Program. Project ID 26546 Activity ID 001.

Publication of this thesis does not constitute approval by Draper or the sponsoring agency of the findings or conclusions contained herein. It is published for the exchange and stimulation of ideas.

(THIS PAGE INTENTIONALLY LEFT BLANK)

1.0 Introduction

This research applies the basic principles of Electrical Discharged Machining (EDM) to the processing of highly doped silicon substrate for use in Microelectromechanical Systems (MEMS). While the processing of silicon by EDM has been demonstrated in various works² and is well documented in published literature, true characterization of the process with respect to the various input variables has evidently not been previously conducted. The primary research objective was to characterize the processing of silicon in Wire EDM and die sinker EDM machines for use in rapid prototyping of MEMS.

1.1 EDM Process Description

Electrical discharge machining (EDM) is a common machining process typically used on conductive materials—metals³. The process utilizes spark erosion to melt and vaporize material from the workpiece via the application of a high frequency current in a dielectric fluid. Forming stresses to the worked material are minimized due to the physics of the process, which in certain applications can be highly desirable. In addition, unique geometric configurations can be created as well as potentially very small-scale and high aspect ratio structures depending on the machine design.

The spark erosion process removes material through the application of a series of electrical sparks between an electrode connected to a spark generator and the workpiece in some dielectric fluid. This fluid is usually some type of oil or deionized water. The application of a single spark creates a melt zone in the work material, with a portion of the melted workpiece removed by the dielectric fluid. The remainder of the melt pool re-solidifies on the work piece as a recast layer. The spark is usually generated by a resistive or relaxation (resistive-capacitive) circuit. The spark in a direct current generator application is a function of the potential difference (V) between the electrode

² (Heeren, et al. 1997)(Kunieda and Ojima 2000)(Reynaerts, Heeren and Van Brussel 1997)

³ (Guitrau 1997)

and workpiece, the current (I), and the spark duration or on time (A). These parameters define the Spark Energy (E) as shown in Equation 1 for a purely resistive spark generator circuit. Units for spark energy are typically in μ Joules. The diagram in Figure 1 depicts the generic change in these parameters over time. Additionally, discharge voltage (Aj), current off time (B), delay time (Td), and period (T) are also depicted.

$$E = I * V * A$$

Equation 1

Equation 2 defines the spark energy for a relaxation-style (resistive-capacitive) spark generation circuit, where C is circuit capacitance. Values are typically also in μ Joules. Processing here is similar to that depicted in Figure 1, but without the uniform square wave shown for voltage.

$$E = \frac{1}{2} * C * V^2$$

Equation 2

Some of the other more common machine parameters that can affect material processing speed and cut quality are the type of electrode material selected, electrode renewal rate (via Wire Speed in a Wire EDM machine or by electrode replacement in a Die Sinker machine), current off time (B), type of dielectric fluid used, and various flushing effects determined by other machine input parameters. Specific inputs used for each of the experiments conducted for this thesis and their associated impacts on the desired output parameters are discussed in the applicable thesis sections.

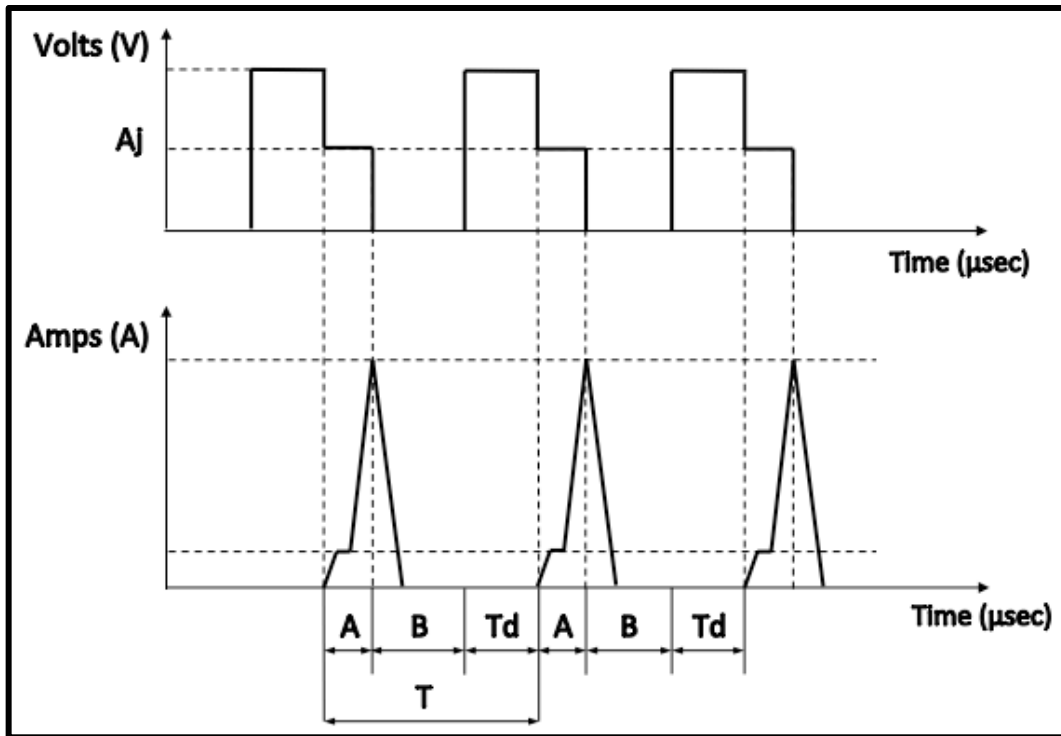


Figure 1: EDM Spark Process for Resistive Spark Generator Circuit⁴

EDM processes are divided into subcategories based on machine design. Wire EDM uses a wire electrode to cut the workpiece material and die sinker uses a manufactured electrode of varying configuration that is then pressed into the workpiece to achieve the desired geometry. The physics of the spark process is identical for each type of machine when viewed on the microscopic level however.

1.1.1 EDM Theory

The individual spark process and physics associated with material removal is the same for both the die-sinking EDM and wire EDM machines when examined on a microscopic level. For the purpose of this discussion, assume that the electrode is the cathode (negatively charged) and that both the workpiece and bench together comprise the anode (positively charged). The electrode approaches the workpiece through the

⁴ Adapted from (Depraz n.d.)

dielectric fluid, which serves as both an insulator (preventing inadvertent or continuous discharges) and as a cooling agent to the machined surface and electrode. The electrode is charged with some high magnitude potential voltage and, as it nears the workpiece, this potential voltage causes the dielectric fluid to begin to break down. As the dielectric becomes sufficiently polarized electrical resistance decreases. Once the resistance levels have fallen sufficiently, a plasma channel is formed in the dielectric fluid⁵ and electrically connects the anode and cathode, allowing current to flow during the machine on time (A). A small gas bubble surrounds the plasma channel during the discharge. Due to the dielectric density, the plasma channel is confined and concentrates the transfer of energy to a very small volume within the dielectric fluid. Melting and vaporization of the workpiece and electrode material commences, and the dielectric begins to be contaminated with both workpiece and electrode material. At the end of the on time, the voltage is removed from the electrode, and the plasma channel and gas bubble violently collapse as current drops rapidly to zero. This collapse drives off a majority of the melt pool and vaporization residue into the surrounding dielectric fluid, with some small amount of the melt pool being deposited in a recast layer on both the workpiece and the electrode. A small pit is left in the workpiece. During the subsequent off time, the dielectric fluid undergoes reionization⁶ and any programmed flushing action removes the contamination from the gap between the electrode and the workpiece.

1.2 Wire EDM

Wire EDM (WEDM) uses a fine wire electrode that is run through a pulley system while moving in a transverse direction across a workpiece to affect the desired cut geometry. Electrode material composition and diameter vary according to the material selected for processing, output requirements, cost, and machine design. The dielectric fluid is typically deionized water for WEDM. A typical configuration utilized by this type of mechanism is shown in Figure 2 showing the wire feed panel where the spool of

⁵ (DiBitonto, et al. 1989)

⁶ (Guitrau 1997)

electrode wire is contained, the upper head, the workpiece, the lower head that collects the expended electrode, the spark generator, and the computer-controlled servos—used to position the workpiece relative to the electrode.

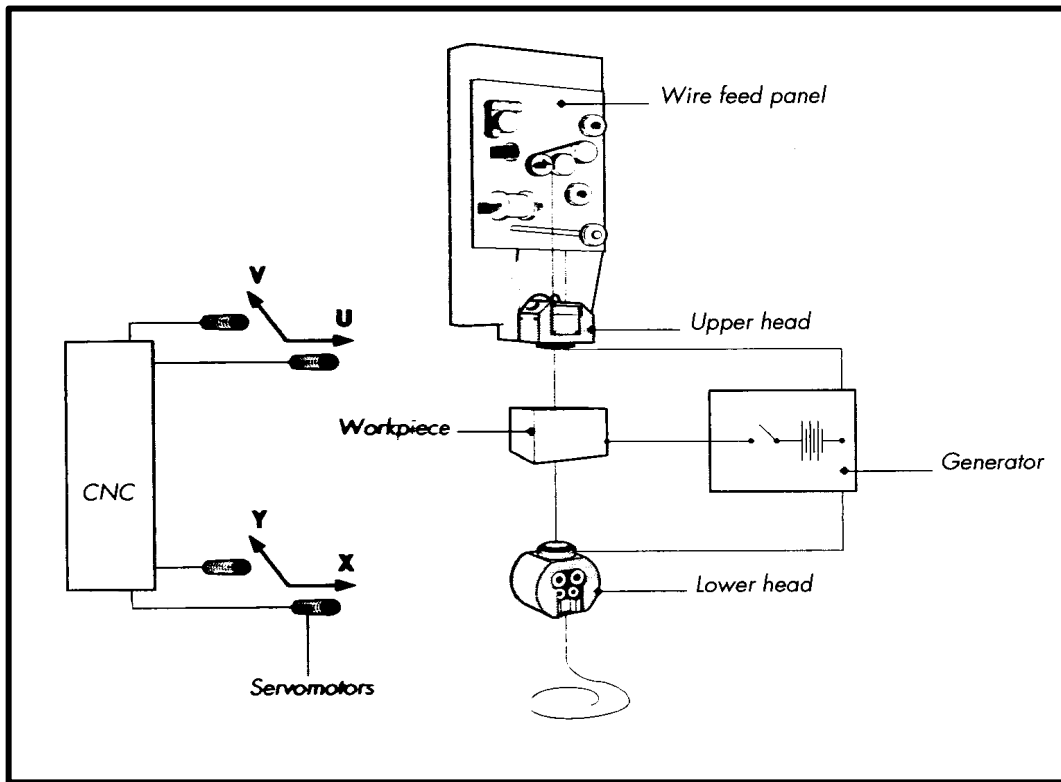


Figure 2: Typical WEDM Setup

Wire EDM has several advantages as a machining process: it generally removes less material from the workpiece than die sinker EDM and consequently results in much shorter processing times; the wire motion results in insignificant wear to the electrode due to its being continuously renewed by the pulley and spool system; and the electrode tends to be much less expensive than the complex electrodes that are frequently utilized in a die sinking application. Wire EDM's major disadvantage is the fact that it will generally only make ruled cuts. This limits the geometric complexity of machined pieces as well as the thickness of the piece being processed based on machine dimensions – specifically the maximum clearance between the upper and lower heads as seen in Figure 2. Additionally, the wire may bend or break during workpiece processing (sometimes repeatedly), especially in sharp feature corners, resulting in a loss of feature accuracy,

damage to the workpiece due to the fact that the wire is under tension, and or increased processing time.⁷

1.3 Die sinking EDM

Die sinking EDM utilizes either metallic or graphitic electrodes that approach the workpiece along the operator-selected axis. The electrode can be any shape or size desired by the operator provided it can be purchased or accurately machined, and is pressed into the workpiece material. Depending on the electrode configuration and the desired cut shape, the electrode may also be spun around an axis of rotation to allow for more even wear to the electrode during workpiece processing and a more even feature in the workpiece. Wear to the electrode during die sinker EDM is of particular concern, as the electrode is not automatically replenished during processing as in Wire EDM. This wear can result in significant feature inaccuracies unless accounted for during processing set up by the machine operator. This accounting is typically performed through the use of multistep processing utilizing multiple electrodes that are used to remove workpiece material in incremental steps. Multistep processing may also be used to impart a particular finish to a workpiece through the use of disparate machine settings designed to impart a particular surface finish to the completed workpiece. A typical die-sinking setup is shown below in Figure 3.

⁷ (Reynaerts, Heeren and Van Brussel 1997)

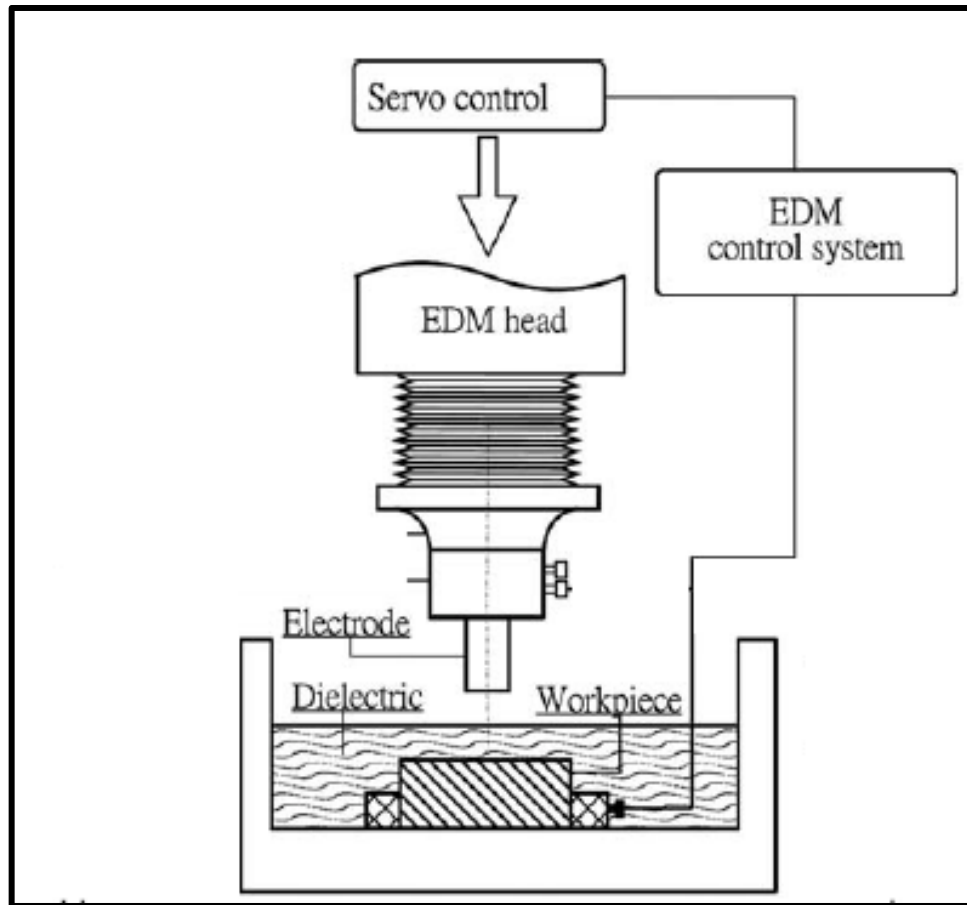


Figure 3: Typical Die Sinker Setup⁸

Die sinking EDM has the ability to render shapes along multiple axes depending on machine construction, and allows for much more complicated feature geometries than can be readily achieved using WEDM. Die sinking EDM typically uses kerosene or oil as the dielectric medium, an advantage of which is the fact that the recast layer on metal surfaces is typically much harder than that of the parent workpiece. Disadvantages of die sinking EDM are typically longer processing times due to feature complexity and quantities of material removed, cost and time associated with the manufacture of complex electrodes, and the previously discussed electrode wear issues during workpiece processing.

⁸ Adapted from (Lin, et al. 2006)

1.4 Thesis Scope

This thesis was undertaken in an attempt to mitigate risk associated with rapid prototyping of Microelectromechanical (MEMS) silicon components. Currently, MEMS devices are constructed only via micro fabrication techniques. Processing via EDM has the potential to reduce risk through reduction of technical risk, shortening of production timelines (and hence cost), and clarification of technical requirements.

The intent of this thesis is to characterize the processing of silicon via both wire and die sinker EDM and to evaluate the impact of this characterization on some of the representative geometries and structures typically associated with MEMs. The results of this work will allow shop operators to readily understand the machine capabilities with respect to processing silicon as well as provide the knowledge base needed to pose the appropriate queries to the engineers or external customers when beginning an associated project.

Chapter 2 describes the characterization of processing highly doped silicon using the WEDM. Chapter 3 describes the characterization of processing silicon using die sinker EDM. Chapter 4 utilizes the information from chapters 2 and 3 in an attempt to evaluate the effect of external properties on processing silicon using EDM as well as evaluating potential geometries for use in silicon MEMS components. Chapter 5 captures lessons learned and pointers for machine operations developed over the course of this thesis for easy use and reference by machine operators. Chapter 6 discusses conclusions and areas of potential future work.

2.0 Characterization of Silicon Wafer Processing on the Wire EDM for Material Removal Rate and Surface Roughness

Charles Stark Draper Laboratory currently owns and operates both Roboform 240 WEDM and Roboform 350 Die-Sinker EDM machines manufactured by GF AgieCharmilles, Inc. All experimentation and silicon processing was conducted on Draper Laboratory equipment.

2.1 Introduction

The goal of this section was to characterize the process outputs of Material Removal Rate (MRR) and Surface Roughness (R_a) for the WEDM based on the numerous input variables available to the machine operator. These two process outputs were selected for characterization based on an understanding of the physics of the erosion process developed during the literature review, the desire to be able to process silicon quickly, and the fact that surface roughness would be a direct indicator of both material damage during processing as well as feature dimensional accuracy—a common requirement in the manufacturing of individual components

2.11 Wire EDM Research and Equipment

The AgieCharmilles Roboform 240 Wire EDM is preprogrammed with specific recommended settings designed to efficiently perform EDM processing operations on well-established electrode-material pairings. These preprogrammed settings, called technique tables, allow for processing of steel, titanium, aluminum, copper, polycrystalline diamond, carbide and graphite without significant input manipulation or guesswork by the machine operator. Silicon, however, is not an available preprogrammed selection on this machine, and so there are no technical tables or guidelines available for silicon processing. A literature review was conducted to compile

an approximate range of input parameters that had been used to process silicon with EDM successfully and to identify any specific technical challenges. Appendix A – Literature Search Summation compiles the basic findings of that search for both the WEDM and the die sinker EDM processes, including both the general characteristics and parameters used in the previous research found during the search as well as any available data concerning these previously analyzed inputs. Specific problems associated with the processing of silicon that were discovered during the literature search and were of immediate concern were the potential lack of ohmic contact between the workpiece and the EDM machine and how to improve this contact⁹ for resistivity over 50 ohm-cm, material damage due to cracking and spalling from excessive spark energy (dependent on workpiece resistivity), and material damage during die sinker when the electrode passes through the lower face of the workpiece.

The Roboform 240 Wire EDM allows the operator to program and adjust the input settings listed in Table 1 within the allowed range of the preprogrammed technical tables once the workpiece-electrode pair is selected. Spark Mode data for the Roboform 240 was specifically unavailable outside of a few of the many settings available on the machine, but are broken up into settings used for roughing, finishing and polishing of the workpiece. The known settings available provided the bounds on this research in this case.

2.12 Experimental Design

For the characterization of the WEDM the use of orthogonal arrays of a Taguchi¹⁰ design were selected. This decision was based on a number of factors. Discussions with an experienced machine operator and the literature research showed for WEDM that there were few potential interaction effects in the WEDM process with a relatively high number of input variables. Of these inputs, only a few were anticipated to be significant to the process—rendering even a fractional factorial design excessively expensive in time

⁹ (Kunieda and Ojima 2000)

¹⁰ (Fraley, et al. 2007)

and cost. Any interactions present would therefore play a relatively small part in the examined process outputs when compared to the main effects based on the heredity principal¹¹, which states that a two-factor interaction is unlikely to be of significance

Table 1: Roboform 240 WEDM Controllable Inputs

Parameter	Units	Range	Parameter Description
Spark Mode (M)	N/A	Unknown	Determines spark shape
Voltage (V)	Volts	± 80 -200 Volts	No-load applied voltage
*Spark Ignition Intensity (IAL)	Amps	1-20 Amps	Spark current
*Pulse On Time (A)	μsec	0.2-2 μsec	Duration of spark
*Short A Time (TAC)	μsec	< A time	Shortened spark duration should machine detect a short during sparking
*Pulse Off Time (B)	μsec	0.2-20 μsec	Time delay between sparks
*Set Value of Average Machining Voltage (A_i)	Volts	% of V	Voltage maintained during spark discharge
*Frequency (FF)	%	1-100%	Reduction in settings following automatic rethreading due to a wire break (prevented in this research)
*Injection Pressure (INJ)	N/A	0-4	Dielectric injection pressure
*Wire Tension (WB)	N/mm ²	Wire dependent	Tension applied to the electrode wire. Range of tension is based on the type of wire installed in the machine
*Wire Speed (WS)	m/min	1.0-15 m/min	Feed rate of the electrode wire
*Control Speed (S)	N/A	0.0-10.0	Relative speed of electrode to work piece

unless both parents are significant. Also, considering the large number of input parameters available for consideration on the Roboform 240 WEDM, it was desired to be as efficient as possible and to minimize time cost in this portion of the thesis. Taguchi orthogonal arrays specifically allow for this efficiency by allowing for an experimental design that uses the minimum amount of experimental treatments for a given number of input parameters while providing sufficient data to be extracted to determine significance of inputs.

All automatic machine actions for the WEDM such as rethreading or parameter optimization attempts were specifically prevented for these tests. As such, both

¹¹ (Wu and Hamada 2000)

Frequency (FF) and number of automatic rethreads allowed were both eliminated as input parameters for the WEDM experiments.

Spark mode selection also played a fairly significant role in the overall experimental design. Available machine literature lacked complete detailed descriptions of the available spark modes with the exception of three specific modes – two specifically designed for roughing cuts, and one designed for finishing cuts. Additional spark mode descriptions were not made available for this investigation due to the proprietary nature of that information.

When a roughing mode is selected on the Roboform 240, all of the input parameters of Table 1 are available for operator manipulation within the available parameter's design range either during the job setup (all) or during the job execution phase (those marked with an asterisk in column one of Table 1) with the range of available adjustment is determined by the selection of wire-workpiece material pairing. For the finishing settings, set average value of machining voltage (A_j) must be set to zero for processing to occur (the machine delivers an error otherwise, and will not process the job). Based on these requirements and the lack of additional information on other spark modes available, two orthogonal array experiments were utilized – one utilizing roughing settings and one utilizing finishing settings. The control parameters and the selected values are included in Table 2 and Table 3.

Table 2: WEDM Roughing Experiment Settings

Roughing	Variable	Low	High
P1	Spark Mode (M)	M1	M21
P2	NL Voltage (V)	80V	100V
P3	Intensity (IAL)	4 A	8 A
P4	On Time (A)	0.3 μ s	0.5 μ s
P5	Duty Cycle	2%	8%
P6	Gap Voltage (Aj)	30 V	60 V
P7	Injection pressure (INJ)	1 L/min	2 L/min
P8	Wire Speed (WS)	3 m/min	6 m/min
P9	Control Speed (S)	0.3	3

Table 3: WEDM Finishing Experiment Settings

Finishing	Variable	Low	High
P1	NL Voltage (V)	80V	100V
P2	Intensity (IAL)	4 A	8 A
P3	On Time (A)	0.3 μ s	0.5 μ s
P4	Duty Cycle	2%	8%
P5	Injection pressure (INJ)	1 L/min	2 L/min
P6	Wire Speed (WS)	3 m/min	6 m/min
P7	Control Speed (S)	0.1	0.4

Note: Spark mode setting was M7 for finishing experiments.

For the Roughing portion of the experiment, an L12 array¹² (Table 4) was selected based on having nine experimental input parameters of interest. For the Finishing experiment, having only seven input variables allowed for the use of an L8 array¹³ (Table 5). Duty cycle, the ratio of on time to off time, was selected based on the fact that some on time to off time pairs were not available and the fact that the literature search indicated that low Duty Cycles were generally used. Other input parameter ranges were also selected based on availability of settings and literature research. Where possible, high or low limits of a particular setting were avoided as well. Treatment run order was randomized to confound any noise inputs, and four replicates were conducted at each treatment level for both experiments. Replicate number was selected based on: 1) ensuring an adequate number for detection of variation within the treatments; 2) providing adequate physical separation between replicates to prevent loss of material during processing, and; 3) allowing an entire treatment to be conducted on a single coupon to ensure maximum consistency within the treatment.

¹² (Fraley, et al. 2007)

¹³ (Fraley, et al. 2007)

Table 4: Taguchi L12 Array used for WEDM Roughing Experiment

Experiment	P1	P2	P3	P4	P5	P6	P7	P8	P9
1	-1	-1	-1	-1	-1	-1	-1	-1	-1
2	-1	-1	-1	-1	-1	1	1	1	1
3	-1	-1	1	1	1	-1	-1	-1	1
4	-1	1	-1	1	1	-1	1	1	-1
5	-1	1	1	-1	1	1	-1	1	-1
6	-1	1	1	-1	1	1	-1	1	-1
7	-1	1	1	1	-1	1	1	-1	1
8	1	-1	1	-1	1	1	1	-1	-1
9	1	-1	-1	1	1	1	-1	1	1
10	1	1	1	-1	-1	-1	-1	1	1
11	1	1	-1	1	-1	1	-1	-1	-1
12	1	1	-1	-1	1	-1	1	1	1

Table 5: Taguchi L8 Array used for WEDM Finishing Experiment

Experiment	P1	P2	P3	P4	P5	P6	P7
1	-1	-1	-1	-1	-1	-1	-1
2	-1	-1	-1	1	1	1	1
3	-1	1	1	-1	-1	1	1
4	-1	1	1	1	1	-1	-1
5	1	-1	1	-1	1	-1	1
6	1	-1	1	1	-1	1	-1
7	1	1	-1	-1	1	1	-1
8	1	1	-1	1	-1	-1	1

Workpiece material, electrode choice and other machining conditions outside of the input parameters were as follows:

1. Electrode selection: half-hard brass wire with an outer diameter of 0.25 mm (0.01"). Half-hard brass was selected as a compromise between material strength and flexibility. Wire tension was maintained for each treatment at 1000 N/mm².
2. Workpiece: 500 μm ($\pm 25 \mu\text{m}$) thick silicon cut from four-inch P-type (Boron), <100> crystal orientation test wafers with doping levels of $\sim 10^{-2}$ ohm-cm (verified).
3. Cutting length: 0.45" straight-line cuts, with each replicate started from 0.02" from the edge of the support plate used to clamp the workpiece to the EDM.

4. Dielectric fluid: Deionized water with conductivity maintained below 5 μS in accordance with the WEDM machine operating manuals.

2.13 Conduct of WEDM experiments

Prior to conduct of the two WEDM experiments, the settings expected to correspond to the slowest material removal rate were selected, and replicates were conducted with successively higher control speeds (S) until wire breaks were experienced or the cut length was measured as incomplete. For Roughing settings, wire breaks were not experienced, but incomplete cuts were experienced at a Control Speed (S) of 5.0. Wire breaks occurred for finishing settings at Control Speed of 0.6. Margin was subjectively taken off the speed at which the wire breaks or incomplete cuts occurred, and this determined the higher Control Speed setting for the experiment (S=4.0 and S=0.4 for roughing and finishing respectively). These choices were made to ensure complete cuts were received in each treatment. This ensured that data comparisons would all be for continuous cuts only. As depicted in Figure 4, sample wafers were diced into quarters. Treatment replicates were cut perpendicular to the flat edge of each coupon and were evenly spaced. The workpiece was fully supported and clamped to an aluminum support plate with pre-cut slots of 0.02" width to ensure cutting was only of the workpiece but that full support was also provided. Contact resistance was measured between the wafer coupon and support plate to ensure ohmic contact and was approximately 11 ohms. Time to complete each replicate cut was recorded by the operator and utilized to calculate material removal rates in accordance with Equation 3 directly in conjunction with cut dimensions as measured using a 100x Falcon optical microscope and assuming a uniform wafer thickness of 500 μm . Surface roughness for each replicate was measured using a profilometer by breaking the workpieces to allow cut surface access.

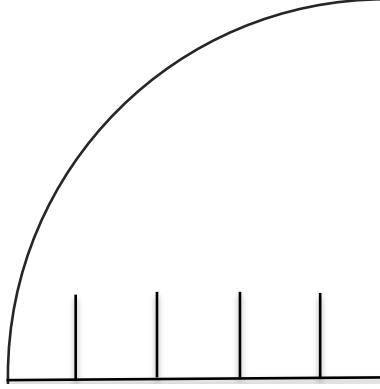


Figure 4: Graphic of Sample Coupon for WEDM Experiments

$$MRR = \frac{l * w * t}{time} \quad (mm^3/min)$$

Equation 3

Where:

l = length of actual cut

w = width of cut

t = wafer thickness

$time$ = time to complete replicate

2.14 Analysis of WEDM Results

When utilizing the Taguchi method for experimental design, signal-to-noise ratio (S/N) – where signal is the desired output characteristic and noise represents the variation of the output – is calculated. S/N is typically denoted as η and has units of decibels (dB).

S/N is calculated in two ways depending on whether the output variable is to be minimized or maximized. For an output characteristic that has an observed value that is better when higher (e.g. MRR) the method of Equation 4, below is used. For output characteristics where the observed value is better when lower (e.g. R_a), the method of Equation 5 is used.

$$\eta = -10 * \log_{10} \left[\frac{1}{n} * \sum \frac{1}{y_i^2} \right]; \quad i=1,2,\dots,n$$

Equation 4

$$\eta = -10 * \log_{10} \left[\frac{1}{n} * \sum y_i^2 \right]; \quad i=1,2,\dots,n$$

Equation 5

Once S/N for each output characteristic is determined, the significance of each input parameter must be determined, either using analysis of variation (ANOVA) or by direct determination of the individual input parameters effect (R-Value) on output at each level of the input. The R-value, or range of the main effect, is calculated by averaging S/N at each level of the input parameter. In this case, that means the average S/N of the output when the input of interest is low, and the average S/N when the input of interest is high. The range is then the magnitude of the difference between these two average values. The larger the magnitude of the R-value, the larger the apparent effect of that input parameter on the process output¹⁴. These R-Values were then plotted on a normal probability plot in order to determine if the output was caused by noise. Effects due solely to noise would plot on the normal line of the normal probability plot. ANOVA was also implemented where sufficient degrees of freedom existed using MATLAB's statistical toolbox function and analyzed using a 90% confidence interval as the standard for statistical significance.

2.141 WEDM Roughing Experiment

Table 6 shows the WEDM Roughing experiment summary results for both material removal rate (MRR) and surface roughness (R_a). Complete data and calculations for the WEDM roughing experiment are contained in Appendix B – WEDM Roughing Experiment Data. Input parameter significance was evaluated both by ANOVA analysis using MATLAB and by R-value calculation and analysis. ANOVA results are included in Table 7 and Table 9, with statistically significant inputs highlighted (using a 90%

¹⁴ (Fraley, Oom and Terrien)

confidence interval). R-values are included in Table 8 and Table 10, with the better S/N ratio (between the high and low input level) highlighted as well. R-values were then plotted on a normal probability plot using MATLAB to further analyze significance of the data.

Table 6: WEDM Roughing Experiment Data Summary

Treatment	Mean MRR (mm ³ /min)	MRR σ (mm ³ /min)	η (MRR) (dB)	Mean R _a (μ in)	R _a σ (μ in)	η (R _a) (dB)
1	0.03373	0.00070	-49.45	168.463	14.397	-39.39
2	0.03394	0.00108	-29.35	104.980	10.186	-38.90
3	0.00350	0.00005	-29.04	136.772	5.660	-43.46
4	0.00343	0.00005	-49.00	106.788	5.761	-42.58
5	0.00337	0.00007	-49.70	93.215	1.340	-39.31
6	0.03560	0.00144	-49.12	112.668	5.249	-42.73
7	0.00355	0.00003	-28.99	134.415	6.673	-41.04
8	0.03414	0.00123	-49.05	88.120	1.701	-40.49
9	0.03534	0.00081	-29.16	148.777	8.133	-44.06
10	0.00328	0.00010	-29.39	92.164	6.121	-40.45
11	0.03484	0.00011	-49.30	159.194	11.330	-40.41
12	0.00353	0.00011	-29.44	105.627	7.875	-44.55

Table 7: WEDM Roughing Experiment MRR S/N ANOVA

MRR S/N Analysis of Variance					
Source	Sum Sq.	d.f.	Mean Sq.	F	Prob>F
Mode	0.0057354	1	0.0057354	0.067902	0.81879
V	0.042954	1	0.042954	0.50854	0.54975
IAL	0.069795	1	0.069795	0.82632	0.45929
A	0.1811	1	0.1811	2.1441	0.28071
DC	0.0017289	1	0.0017289	0.020468	0.89935
Aj	0.0062203	1	0.0062203	0.073643	0.81155
Inj	0.10992	1	0.10992	1.3014	0.37216
WS	0.007106	1	0.007106	0.084128	0.79909
S	498.9779	1	498.9779	5907.4583	0.00016923
Error	0.16893	2	0.084466		
Total	1205.4191	11			
Constrained (Type III) sums of squares.					

Table 8: WEDM Roughing Experiment MRR R-Values

MRR	Mode	V	IAL	A	DC	Aj	Inj	WS	S
Low S/N	-40.66	-37.21	-39.28	-40.79	-37.29	-37.27	-40.74	-41.16	-49.27
High S/N	-37.27	-40.71	-39.21	-37.10	-40.64	-40.66	-37.17	-37.88	-29.23
R-Value	3.40	-3.50	0.07	3.69	-3.35	-3.40	3.57	3.28	20.04
Effect Rank	5	4	7	2	5	5	3	6	1

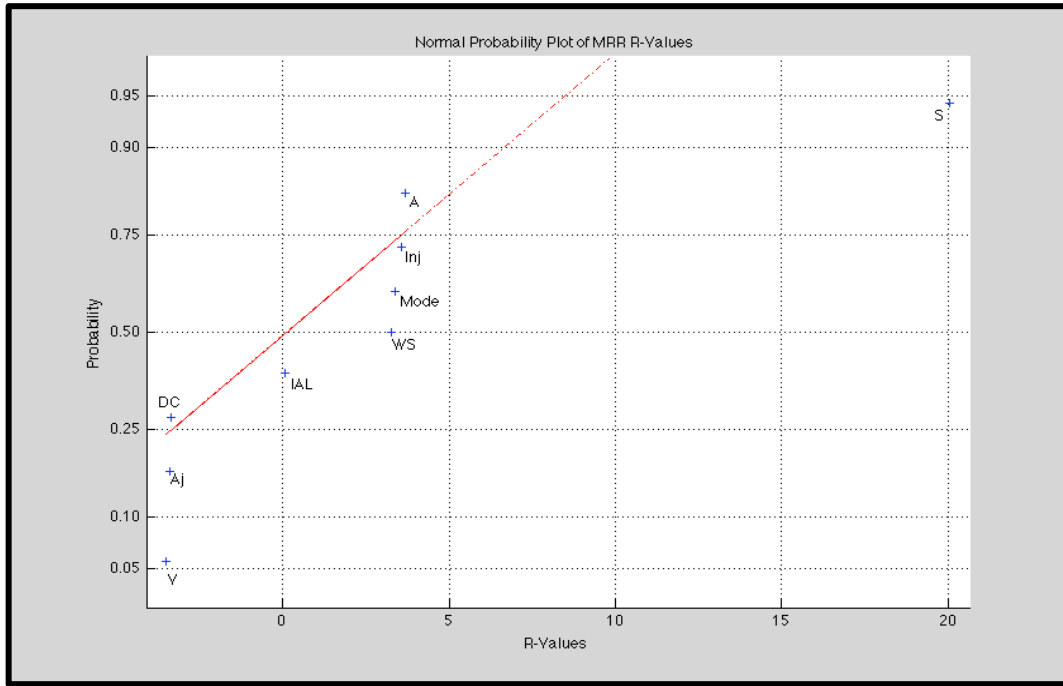


Figure 5: Normal Probability Plot of WEDM Roughing Experiment MRR R-Values

Significance testing by ANOVA testing for WEDM roughing MRR indicates that servo (S) is the only statistically significant input parameter (90% confidence interval). R-value testing also shows that servo is the most significant input. The normal probability plot of the R-values (Figure 5) shows visually that although servo is the dominant factor for MRR as demonstrated by ANOVA analysis, that the other machine inputs, while not statistically significant to a 90% confidence interval, have contributions to the output that are most likely not the result of system noise, and do contribute to overall the MRR (noise factors should plot on the red line under the assumption that noise is normally distributed). This finding agrees with the known physics of the process in that the spark energy applied (defined by current, voltage and on time per Equation 1) largely contributes to the resulting MRR. Figure 6 depicts the parametric response graph for MRR. Based on this response for MRR, the optimal combination of input parameters for MRR is $M_2V_1IAL_2A_2DC_1Aj_1Inj_2WS_2S_2$ (where 1 corresponds to a low setting and 2 to a high setting) with the statistically significant parameter, servo, primarily controlling the response. It is critical to note here, that although the servo input is directly limited by

the erosion capability that results from the selection of the other inputs – the machine can only go as fast as the erosion process will allow.

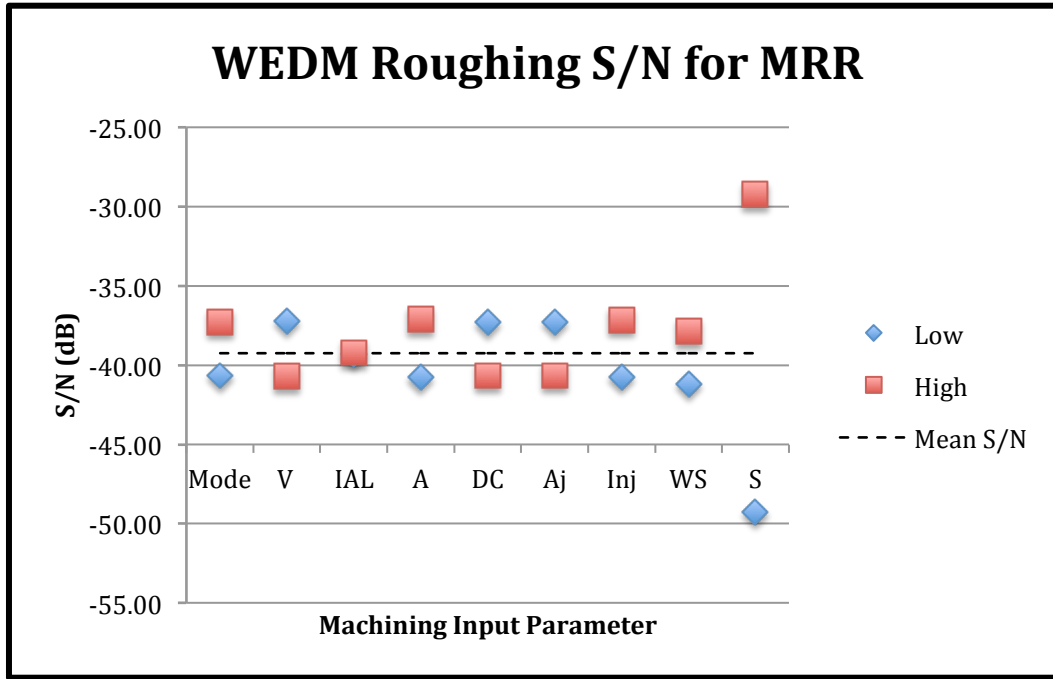


Figure 6: Input Effects for WEDM Roughing Experiment MRR S/N

Table 9: WEDM Roughing Experiment R_a S/N ANOVA

R_a S/N Analysis of Variance					
Source	Sum Sq.	d.f.	Mean Sq.	F	Prob>F
Mode	0.13476	1	0.13476	0.14871	0.73693
V	0.17413	1	0.17413	0.19216	0.70393
IAL	4.2279	1	4.2279	4.6655	0.16337
A	0.0022799	1	0.0022799	0.0025158	0.96456
DC	0.012041	1	0.012041	0.013287	0.91876
Aj	0.22463	1	0.22463	0.24788	0.66793
Inj	4.8535	1	4.8535	5.3559	0.14671
WS	4.5582	1	4.5582	5.03	0.15413
S	0.8502	1	0.8502	0.93819	0.43493
Error	1.8124	2	0.90621		
Total	23.3677	11			
Constrained (Type III) sums of squares.					

Table 10: WEDM Roughing Experiment R_a R-Values

R_a	Mode	V	IAL	A	DC	Aj	Inj	WS	S
Low Input	-41.06	-41.26	-41.65	-40.83	-40.04	-42.09	-41.40	-40.96	-40.82
High Input	-41.99	-41.58	-41.25	-42.31	-42.45	-40.99	-41.51	-41.80	-42.08
R-Value	0.94	0.32	0.40	1.48	2.41	1.10	0.11	-0.84	1.26
Effect Rank	5	8	7	2	1	4	9	6	3

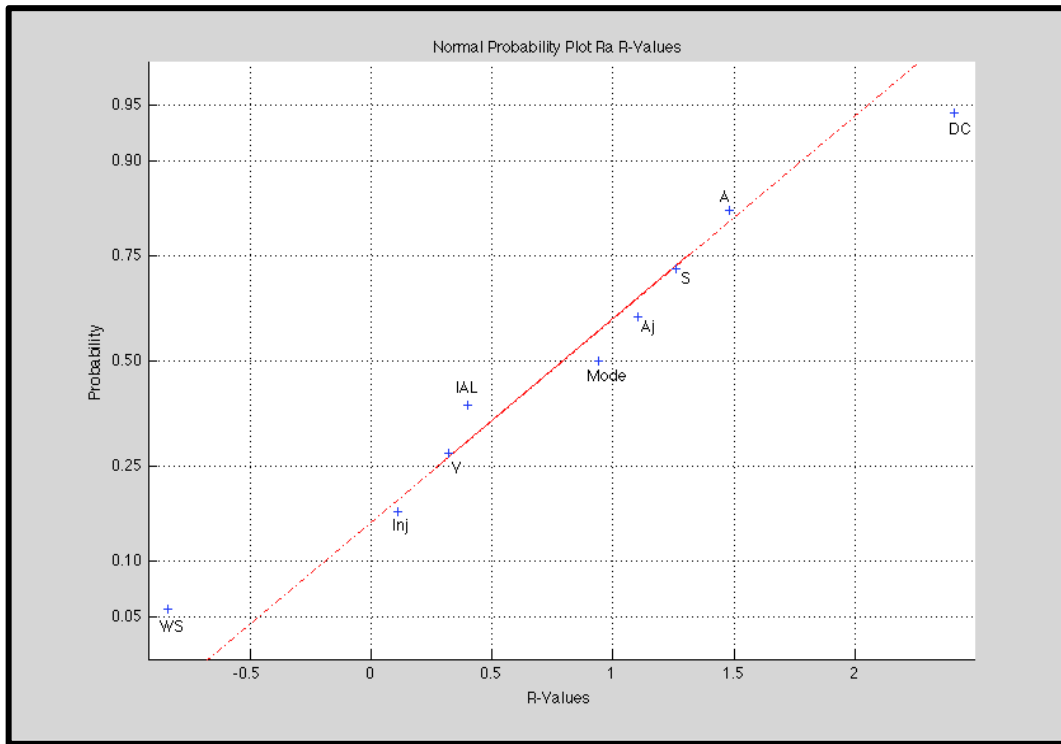


Figure 7: Normal Probability Plot of WEDM Roughing R_a R-Values

Significance testing by ANOVA for WEDM roughing surface roughness (R_a) yields results that there are no inputs significant to a 90% confidence interval based on the data gathered. Analysis to an 80% confidence interval shows that wire speed (WS), Injection (INJ) and current (IAL) are significant, with WS and INJ significant to an 85% confidence interval. Examination of the R-values for surface roughness provides a completely different picture, with duty cycle (DC), on time (A), and servo (S) having the largest magnitude effects, while mode (M) and average spark voltage (Aj) closely follow in magnitude. Examination of these R-values by normal probability plot helps to clarify the input importance, showing that the on-time and servo inputs are likely due to noise rather than actual significance. This plot also reinforces the ANOVA analysis results that point to the significance of current in surface roughness results (which also agrees with the accepted physics of the process). Figure 8 depicts the parametric response graph for WEDM roughing surface roughness. Based on this response graph for R_a , the best

combination of input parameters for R_a would be $M_1V_1IAL_2A_1DC_1Aj_2Inj_1WS_1S_1$, with the most significant parameters primarily controlling the output response.

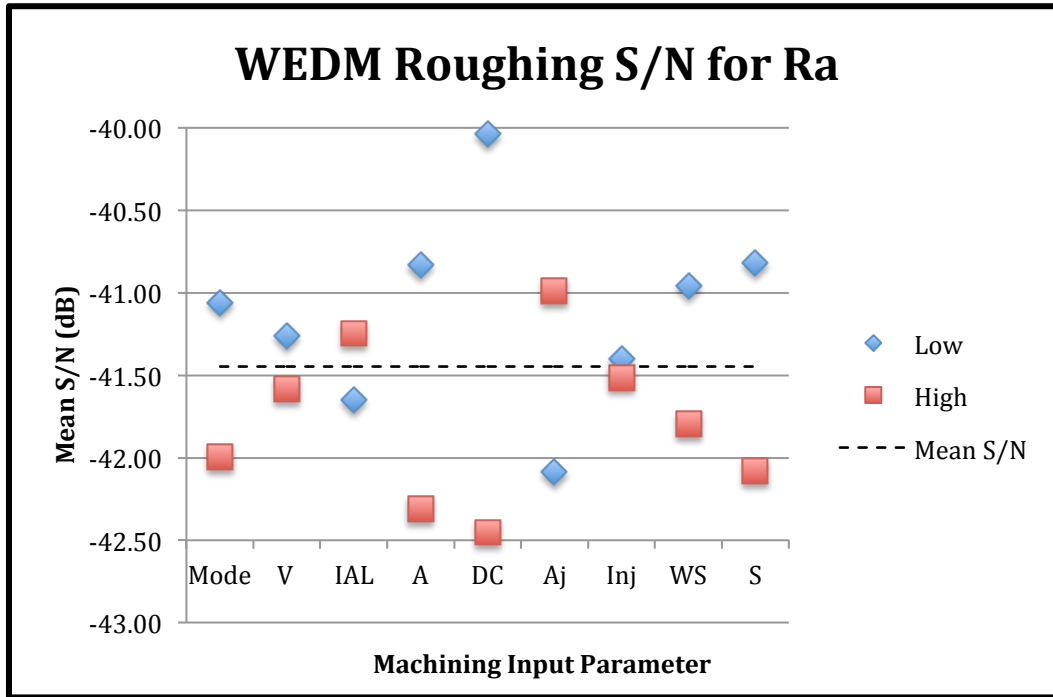


Figure 8: WEDM Roughing Experiment Input Effects for R_a S/N

However, the optimum setting for IAL here is contrary to that generated based on the basic physics of the process, since the melt pool size for an individual spark is well-known to be directly proportional to the spark energy as shown in Equation 1, and a smaller individual melt pool results in a smaller individual pit. Given the well-documented physics of the EDM process, utilizing $M_1V_1IAL_1A_1DC_1Aj_2Inj_1WS_1S_1$ instead of the experimentally indicated best settings when surface roughness is the operator's primary concern would be more appropriate.

2.142 WEDM Finishing Experiment

The finishing settings shown in Table 3 completed the required cuts in four to fifteen minutes, also based largely on the selected input parameter servo speed (S) as seen in the roughing experiment. Surface roughness measurements ranged from just over 24

μinches to 41 μinches, a fairly significant improvement over the roughing experiment, which was also expected. Table 11 provides the summary of experimental results for both material removal rate (MRR) and surface roughness (R_a) for the finishing settings of the experiment. Complete data for the experiment is provided in Appendix C – WEDM Finishing Experiment Data. Input parameter significance results for the WEDM finishing experiment were evaluated solely using R-value determination calculation and normal probability plot of the R-values as ANOVA results were not calculable due to the lack of sufficient degrees of freedom in experimental design.

Table 11: WEDM Finishing Experiment Data Summary

Experiment	MRR	MRR σ	η	Mean R_a	$R_a \sigma$	η
	(mm ³ /min)		(dB)	(μin)		(dB)
1	0.0010376	0.0000080	-59.6801092	24.1635000	2.4049015	-27.6953417
2	0.0041487	0.0001218	-47.6504426	31.8182500	3.2880222	-30.0881699
3	0.0042140	0.0000675	-47.5086649	34.9742500	2.7343612	-30.8948322
4	0.0011327	0.0000080	-58.9180717	40.9525000	4.4323657	-32.2835971
5	0.0041378	0.0000348	-47.6653909	32.3592500	3.9175513	-30.2474480
6	0.0010633	0.0000305	-59.4748543	24.8592500	0.9488784	-27.9145034
7	0.0011210	0.0000163	-59.0096357	36.7207500	0.7851944	-31.2997199
8	0.0041966	0.0000434	-47.5430212	29.8055000	1.9230324	-29.4994661

Significance testing for the WEDM finishing settings for MRR indicate that servo speed (S) is again the most significant parameter affecting MRR on the wire, with current (IAL) and Injection Pressure (Inj) following as the next most significant parameters. As expected, this is similar to the MRR results of the roughing testing in that spark energy and flushing directly impact MRR. Figure 9 graphically depicts the parametric response for MRR while using finishing settings on the WEDM, and again shows the overwhelming significance of servo speed for material removal rate. Figure 10 is the normal probability lot for these R-values. Based on this response for MRR, the best combination of input parameters for MRR are $V_2IAL_2A_2DC_2Inj_2WS_2S_2$, with the most significant and significant parameters primarily governing the response. It is important to note that other than servo (S), that the analysis shows that the other settings may be changed with little impact on resulting MRR.

Table 12: WEDM Finishing Experiment MRR S/N

MRR S/N	V	IAL	A	DC	Inj	WS	S
Low S/N	-53.44	-53.62	-53.47	-53.47	-53.55	-53.55	-59.27
High S/N	-53.42	-53.24	-53.39	-53.40	-53.31	-53.41	-47.59
R-Value	0.02	0.37	0.08	0.07	0.24	0.14	11.68
Effect Rank	7	2	5	6	3	4	1

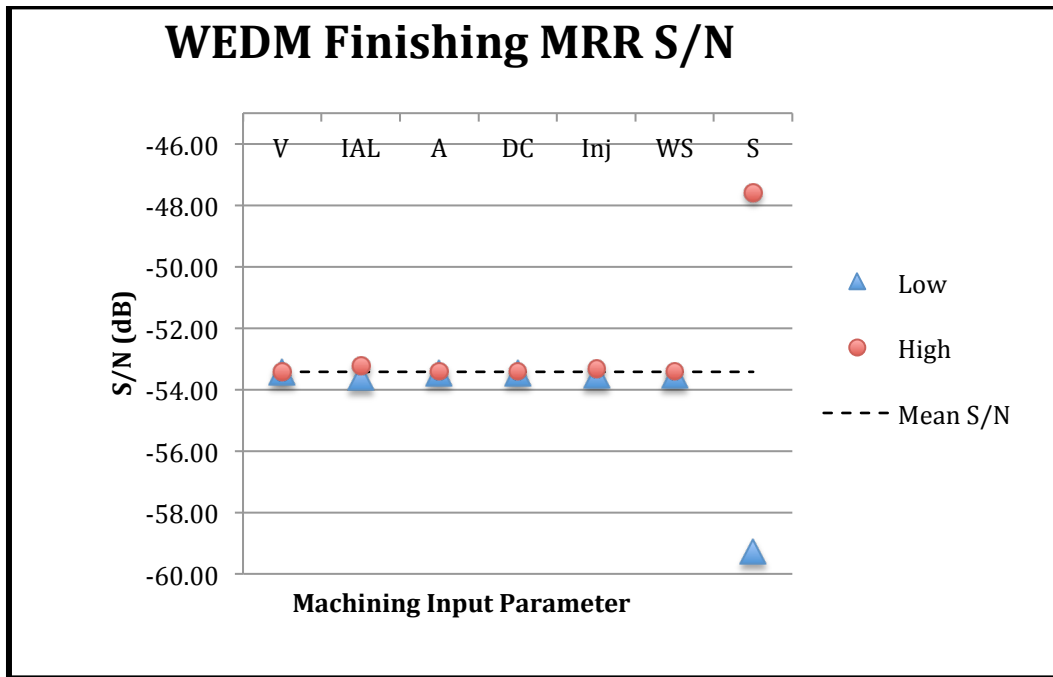


Figure 9: WEDM Finishing Experiment Input Effects for MRR S/N

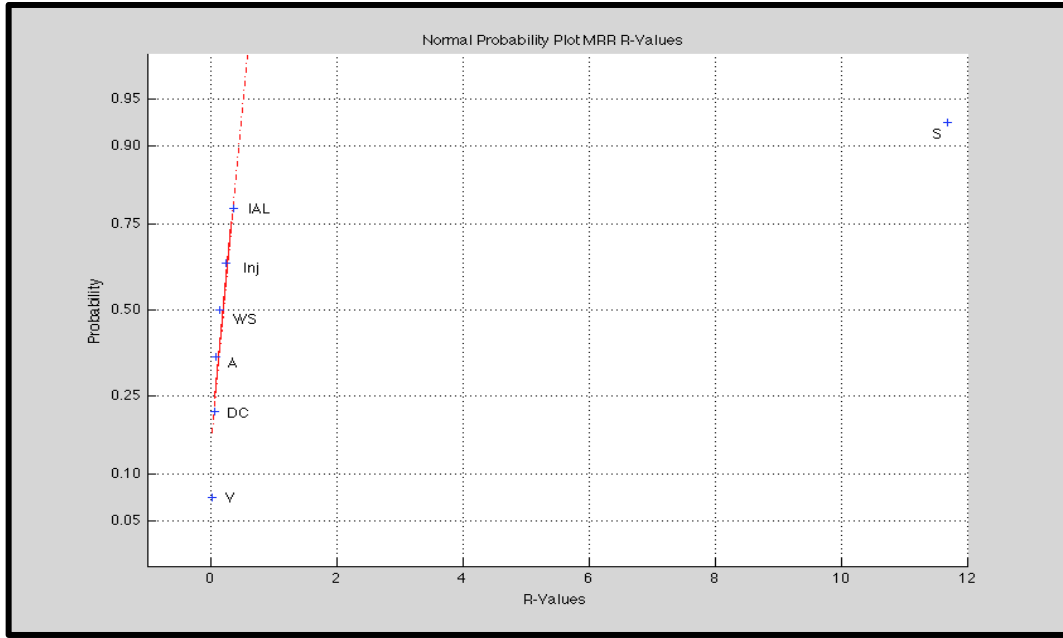


Figure 10: Normal Probability Plot for WEDM Finishing MRR R-Values

Significance testing results for the WEDM finishing experiment for surface roughness (R_a) indicate that current (IAL), Injection Pressure (Inj) and on time (A) are the most significant parameters affecting R_a . Figure 11 shows the parametric response graph for surface roughness. The normal probability plot of the R-values is given in Figure 12. Based on this response for R_a , the optimal combination of input parameters for R_a are $V_2IAL_1A_1DC_2Inj_1WS_1S_1$, with the most significant and significant parameters primarily controlling the output response. In this experiment, the current response and on time were as expected based on the known physics of the removal process, with lower current and lower on time resulting in better surface roughness.

Table 13: WEDM Finishing Experiment R_a S/N

Ra S/N	V	IAL	A	DC	Inj	WS	S
Low S/N	-30.24	-28.99	-29.65	-30.03	-29.00	-29.93	-29.80
High S/N	-29.74	-30.99	-30.34	-29.95	-30.98	-30.05	-30.18
R-Value	0.50	2.01	0.69	0.09	1.98	0.12	0.38
Effect Rank	4	1	3	7	2	6	5

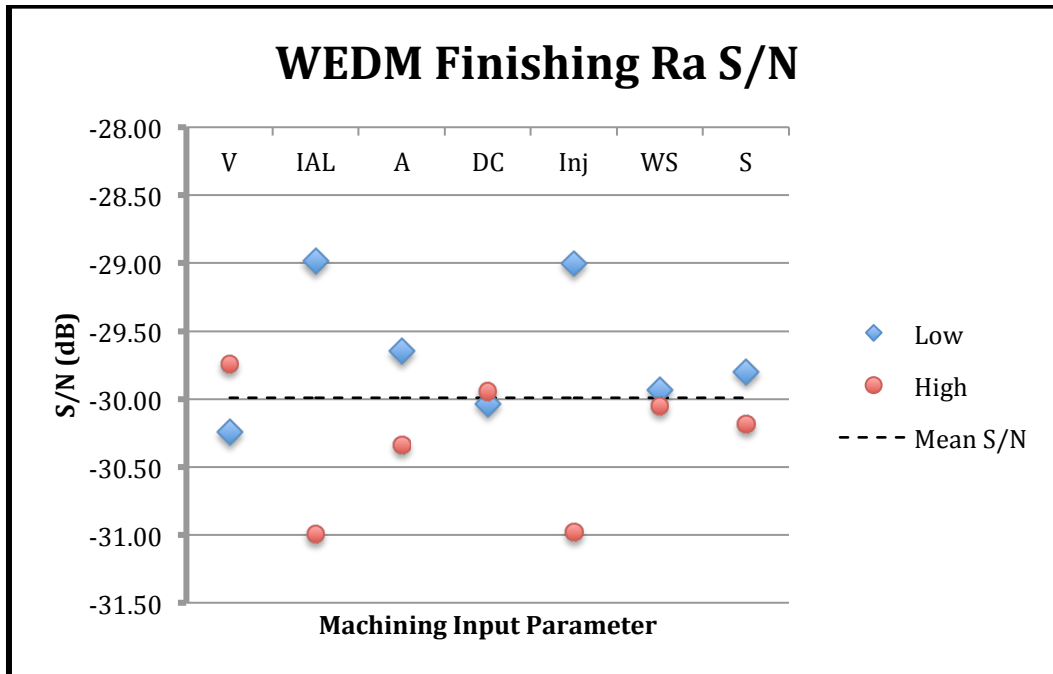


Figure 11: WEDM Finishing Experiment Input Effects for R_a S/N

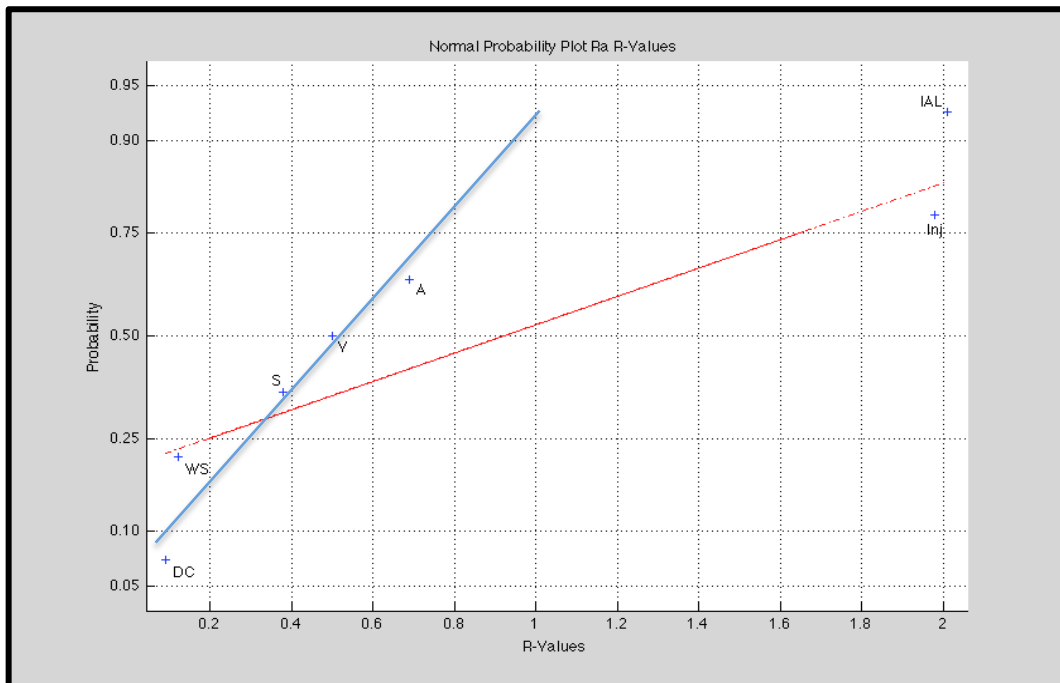


Figure 12: Normal Probability Plot for WEDM Finishing Experiment R_a R-Values

***Note: Blue line indicates a better fit for the normal plot and better indication of the significance of both IAL and Inj.**

2.15 Confirmation of Experiment Results

2.151 WEDM Roughing Experiment

Using the experimental results discussed in 2.141 WEDM Roughing Experiment, a confirmation experiment was conducted using the determined best settings for both MRR and R_a . The MRR confirmation experiment allowed complete cuts of the same length (0.45”) to be cut between 10 and 13 seconds (as opposed to a previous fastest time of 30 seconds), and an average S/N of -21.55 decibels. This was an over seven-decibel improvement from any of the setting combinations used in the baseline experiment, and a fairly significant improvement in processing speed. (Data collected is included at the bottom of the table in Appendix B – WEDM Roughing Experiment Data.)

The surface roughness confirmation experiment provided surface roughness results between 93 and 110 μ inches with a mean of 104 μ inches and an average S/N of -40.37 decibels. This was worse than the best trial experiment (Treatment #2 - average R_a of 88.12 μ inches, S/N -38.90 decibels). The only differences in the settings used for the confirmation run and the treatment were injection pressure (high for the treatment, low for the confirmation) and control speed (high for the treatment, low for the confirmation). Given the results of the experiment, and the normal probability plot, it seems most likely that a higher injection pressure may be more appropriate for better results. However, the physics of the process logically suggests that lower control speed, allowing all of the potential material to be removed along a cut for a specific spark energy, would be better for better surface roughness than higher speeds that may leave some material behind that would be removed at the slower processing speed. Another possible explanation is that the response surface for R_a may be relatively “flat” across the evaluated range for these inputs, resulting in insignificant statistical improvement for a measurement that is, in itself, a statistical measurement. Unfortunately, insufficient time remained to further test these evaluations prior to completion of this thesis.

2.152 WEDM Finishing Experiment

With the experimental results from Section 2.142 WEDM Finishing Experiment, another pair of confirmation runs were conducted on the WEDM—one for MRR, and one for R_a .

The MRR confirmation run completed all of its cuts in under a minute – approximately one quarter of the time needed for the fastest treatments settings. MRR S/N was -36.41 dB, over a 10 dB improvement in processing speeds.

Similarly, the R_a confirmation run failed to provide improvement in the baseline surface roughness on the WEDM, yielding surface roughness of approximately 38 μ inches (the best treatment achieved approximate 24 μ inches) and a R_a S/N of 31.65 dB, approximately 4 dB worse than the best surface roughness achieved during the characterization process (treatment #1). The differences here were in no-load voltage (low in treatment #1, vice high in confirmation) and duty cycle (low in treatment #1, vice high in confirmation).

3.0 Characterization of Silicon Wafer Processing on the Die Sinker EDM for Material Removal Rate and Surface Roughness

3.1 Die Sinker Experiment

The die sinker characterization experiments were conducted by drilling a series of holes in similar wafer coupons as the WEDM experiments using a 0.09” diameter solid copper electrode rotating at 50 rpm. Based on the diameter of each replicate and coupon size, three replicates per treatment were cut, with one treatment being performed per each wafer coupon. Using only one treatment per wafer served to minimize the chances of any need to repeat a treatment due to subsequent breakage of the work piece. The replicate diameter was chosen to limit the quantity of material being removed during each replicate, thus limiting total processing time, while allowing a hole of sufficient diameter to allow for some reasonable quality of surface roughness measurements to be taken on the laboratory’s available equipment.

Initial attempts to cut silicon on the die sinker machine used in this experiment had been unsuccessful due to test material being broken during the initial approach and contact of the electrode. As such, the first step of the experimentation process consisted of determining how to prevent workpiece breakage.

3.11 Die Sinker Setup and Research

There was specific concern that workpiece breakage was the result of either the work piece resistivity or the presence of high contact resistance and a failure of the machine to recognize a surface that could be machined by a reduction in detected resistance. The first concern was minimized by the use of highly doped silicon. Contact resistance between the workpiece and the support table were also measured, with an average resistance of approximately 30 Ω , the same order of magnitude as that found when contact resistance was measured during the WEDM experiments.

The speed of approach of the electrode to the work piece was examined for potential adjustment, but machine design prevented this from being changed by the operator. As a result, alternate methods to prevent work piece breakage were examined. Based on the fact that the process for calibration of the vertical axis did not result in workpiece breakage for the same thickness of workpiece (the process includes contact with the work piece), methods of reinforcing the strength of the individual wafer coupon were considered.

Kunieda et al¹⁵ had previously documented success in improving the efficiency of the EDM processing of silicon through the use of metallic plating of the work piece—a process also discussed in other literature. On examination, a variation of this method appeared to have potential as a technique to both protect the workpiece from breakage by the electrode on initial approach while also serving to improve the processing of the workpiece. Initial tests of this potential method utilized front and back support plates of 0.02” thick copper, with the silicon work piece sandwiched in between the copper plates. Tests were repeated replacing the copper with aluminum with no discernable difference in processing speed or quality. Although the plating practice prevented workpiece breakage as desired, the interface of the two different materials (metal-silicon) apparently resulted in undesirable machine shutdowns due to detection of bad machining.

Bad machining is defined as a condition where the EDM circuitry detects what is evaluated as abnormal sparking and excessive contamination in the dielectric fluid and initiates an automatic shutdown of processing. The machine monitors the voltage across the gap during the on time (after dielectric ionization). If the observed voltage is too low, or if it is too steady, then this is interpreted as an overly conductive gap. These two measurements result in indication of either abnormal and or contamination sparks. The spark generator monitors for a target voltage that varies according to electrode material selected (exact values for individual materials is proprietary). If the resulting voltage observed is consistently too low relative to the expected voltage, a “bad machining” shutdown is initiated. As the work piece material used here, silicon, is not programmed into the machine technical tables, the potential for an inadvertent bad machining

¹⁵ (Kunieda and Ojima)

shutdown is high depending on the electrode-work piece pair selected by the operator during job setup.

Initial attempts to prevent these automatic shutdowns involved removing the top piece of metal from the initial “sandwich” setup described above. This was successful in preventing shutdowns that had been occurring at the start of processing. However, as the electrode was directed to drill to a depth of 0.03” to ensure that each replicate resulted in a complete through-hole of the silicon wafer, the second interface of silicon to metal still resulted in frequent shutdowns. The other issue associated with the use of disparate materials for workpiece support was how to account for different processing speeds for each material, as the metal was generally being cut at a more rapid speed than the silicon during trial runs. Due to machine setup and observable outputs while actually processing, there was no way to exactly verify when processing of silicon ended and when processing of the metal support plate began—which would result in an inherently inaccurate measurement of silicon processing times and therefore measured material removal rates.

Both the processing time and the interface shutdown problems were solved by the use of a second silicon coupon placed underneath the treatment coupon as a sacrificial workpiece. The resulting one-millimeter effective silicon thickness was adequate to prevent workpiece breakage during the initial electrode approach and ensured that the only material processed for each replicate was silicon (thereby ensuring accuracy of measured silicon removal rate). This setup also resulted in a significant and almost complete reduction in automatic machine shutdowns. Analysis of the shutdowns that continued to occur shows that the shutdowns were isolated to the test wafers that were exposed to the higher spark energy. These treatments also exhibited much higher corresponding contamination level in the dielectric during processing, indicating that at higher processing powers supplemental flushing via directed hoses is of much greater importance to keep dielectric contamination in acceptable levels. This higher contamination level is just the condition that would create the overly conductive spark gap that results in these types of shutdowns. The use of supplemental flushing was not employed during any of these experiments, as it would be during normal processing due to the inherent noise that would be introduced to the experiment from any slight variations in flushing flow due to inadvertent changes in nozzle direction and pressure.

settings. Use of supplemental flushing did occur in follow-on work on more complex architectures, and is discussed in the appropriate locations.

3.12 Experimental Design

Spark mode selection again played a significant role in experimental design. Available data concerning spark modes for the die sinker EDM far exceeded that which was available for the WEDM machine, allowing the use of spark mode as a control variable for the roughing experiment. Spark mode M1—used for standard rough cuts and M14—used for micromachining were selected as the roughing spark modes based on the types of cuts being performed. Pilot expert was set to off (1) to prevent any machine initiated input parameter changes and electrode rotation was set to 50 rpm for all experiments.

Table 14: Roboform 350 Die Sinker EDM Controllable Inputs

Parameter	Units	Range	Parameter Description
Spark Mode (M)	N/A	1-28	Determines spark shape
*Voltage (V)	Volts	±80, 120, 160, 200 Volts	No load applied voltage
Peak Current (P)	Amps	0.5 – 128 Amps	Spark current (discrete values, not a continuum)
Pulse On Time (A)	μsec	0.8 – 3200	Duration of spark (discrete values, not a continuum)
*Pulse Off Time (B)	μsec	1.2 - 3200	Time between sparks (discrete values, not a continuum)
*Reference Arc Voltage (RF)	Volts	0, 15-49.5	Voltage maintained during spark discharge
*Machining Time (U)	Seconds	0 – 12.8	Machining time between two pulses of the electrode (discrete values, not a continuum)
*Retraction Time (R)	Seconds	0 – 12.8	Time that electrode is moved away from work piece (discrete values, not a continuum)
*Servo (SV)	%	10-100	Defined as a percent of the total cycle time (A+B+SV)
*Pulsation Speed (VPULS)	inches/min	0 -141.73	Speed of electrode pulsation
Capacitance (C)	nF	Proprietary information	Finishing capacitors
*Pilot Expert	N/A	0,1,2	Optimization setting – allows machine to adjust others settings based on detected response if used
Electrode Rotation	rpm	0-100	Rotational speed of the electrode (if used)

When a roughing mode is selected on the Roboform 350, all of the input parameters of Table 14 are available for operator manipulation either during the job setup (all – based on initial technical table selection) or during the job execution phase (those parameters marked with an asterisk). The range of available adjustment for each parameter is determined by the selection of wire-workpiece material pair.

Fractional factorial experiments were used for the die sinker instead of the previously used Taguchi arrays due to the expected presence of significant interactions as documented in the Roboform 350 machine literature. For the roughing experiment, the decision was made to combine current (P), voltage (V) and on time (A) into a single input variable of Spark Energy (E) as shown in Equation 1, as the literature search and the analysis of the WEDM characterization showed that the spark energy was directly related to MRR and inversely related to the R_a . This decision allowed for a reduction in the number of input parameters and resulted in an experiment where fifteen of the twenty-one of the first-level interactions could be evaluated through the use of a 2^{7-2} 32-level fractional factorial experiment.¹⁶ The control parameters and the selected values for the roughing experiment are included in Table 15. In this particular design, pulsation speed (VPULS) is aliased as the product of parameters P1P2P3 (Spark energy, Mode, and Reference Arc Voltage), and servo (SV) is aliased as the product of parameters P1P2P4P5 (Spark Energy, Mode, Machining Time, and Off Time). Values were selected to be inside the known spectrum of successful machining from literature review but allowed for some buffer from the extreme machine range where practical. Experimental design used for this experiment is shown in Table 16.

For finishing and polishing material processing, the spark circuit in the Roboform 350 is modified to a relaxation-type circuit and varying levels of capacitance become available to the operator. A single spark mode (M4) was selected for the finishing portion of the die sinker experiment even though other polishing spark mode settings were known due to the fact that complete cuts would never be cut in practice with a polishing setting due to the extreme time needed to process with the low powers needed

¹⁶ (Wu and Hamada)

to create a polished surface. When final surface roughness is specifically of interest, the standard practice in EDM processing is to conduct multiple passes in sequence (roughing, finishing, and then polishing). Complete cuts using a polishing setting are unnecessarily time consuming. Additionally, current (P), on time (A), and Reference Arc Voltage (RF) are not selectable parameters after initial set-up and are of very limited P/A combinations for each capacitive selection, making the repeated use of spark energy (E) as a control variable not possible. The selected control parameters for the die sinker finishing experiment and the associated selected values are shown in Table 17. The experimental design used is included in Table 18.

Table 15: Die Sinker EDM Roughing Experiment Settings

	Variable	Low	High
P1	Spark Energy (E)	-768	-3072
P2	Mode	M1	M14
P3	Reference Arc Voltage	0	25
P4	Machining time (U)	0.2	0.4
P5	Off time (B)	6.4	12.8
P6	Pulsation Speed (VPULS)	3	9
P7	Servo (SV)	10	40

Notes:

1. On time (A) was held at 6.4 μ sec for all treatments
2. Current (P) used was 1.5 and 4 amps
3. Voltage used was -80 and -120 volts
4. Retraction time (R) was selected to be paired with the U setting (0.1 and 0.2 sec)
5. Capacitance is zero for non-finishing modes

Table 16: Die Sinker EDM Roughing Experiment Design

	P1	P2	P3	P4	P5	P6	P7
Treatment	E	M	RF	U	B	VPULS	SV
1	-1	-1	-1	-1	-1	-1	1
2	1	-1	-1	-1	-1	1	-1
3	-1	1	-1	-1	-1	1	-1
4	1	1	-1	-1	-1	-1	1
5	-1	-1	1	-1	-1	1	1
6	1	-1	1	-1	-1	-1	-1
7	-1	1	1	-1	-1	-1	-1
8	1	1	1	-1	-1	1	1
9	-1	-1	-1	1	-1	-1	-1
10	1	-1	-1	1	-1	1	1
11	-1	1	-1	1	-1	1	1
12	1	1	-1	1	-1	-1	-1
13	-1	-1	1	1	-1	1	-1
14	1	-1	1	1	-1	-1	1
15	-1	1	1	1	-1	-1	1
16	1	1	1	1	-1	1	-1
17	-1	-1	-1	-1	1	-1	-1
18	1	-1	-1	-1	1	1	1
19	-1	1	-1	-1	1	1	1
20	1	1	-1	-1	1	-1	-1
21	-1	-1	1	-1	1	1	-1
22	1	-1	1	-1	1	-1	1
23	-1	1	1	-1	1	-1	1
24	1	1	1	-1	1	1	-1
25	-1	-1	-1	1	1	-1	1
26	1	-1	-1	1	1	1	-1
27	-1	1	-1	1	1	1	-1
28	1	1	-1	1	1	-1	1
29	-1	-1	1	1	1	1	1
30	1	-1	1	1	1	-1	-1
31	-1	1	1	1	1	-1	-1
32	1	1	1	1	1	1	1

Table 17: Die Sinker EDM Finishing Experiment Settings

	Variable	Low	High
P1	NL Voltage (V)	-80	-120
P2	Off Time (B)	12.8	25
P3	Servo (SV)	55	70
P4	Machining time (U)	0.2	0.4
P5	Pulsation Speed (VPULS)	6	9
P6	Capacitance (C)	C3	C5

Notes for finishing cycle:

1. P and A are calculated by the C setting
2. RF has no influence on this cycle
3. R was selected to be paired with the U setting (0.1 and 0.2)
4. Capacitance settings corresponded to 4.7nF and 22nF and resulted in current settings of 1.0 and 1.5 Amps respectively.
5. On time (A) was constant at 3.2 μ sec for all treatments
6. Spark mode selected was M4 (standard finishing mode)

Table 18: Die Sinker EDM Finishing Experiment Design

	P1	P2	P3	P4	P5	P6
Treatment	V	B	SV	U	VPULS	C
1	-1	-1	-1	-1	-1	-1
2	1	-1	-1	-1	-1	1
3	-1	1	-1	-1	-1	1
4	1	1	-1	-1	-1	-1
5	-1	-1	1	-1	-1	1
6	1	-1	1	-1	-1	-1
7	-1	1	1	-1	-1	-1
8	1	1	1	-1	-1	1
9	-1	-1	-1	1	-1	1
10	1	-1	-1	1	-1	-1
11	-1	1	-1	1	-1	-1
12	1	1	-1	1	-1	1
13	-1	-1	1	1	-1	-1
14	1	-1	1	1	-1	1
15	-1	1	1	1	-1	1
16	1	1	1	1	-1	-1
17	-1	-1	-1	-1	1	1
18	1	-1	-1	-1	1	-1
19	-1	1	-1	-1	1	-1
20	1	1	-1	-1	1	1
21	-1	-1	1	-1	1	-1
22	1	-1	1	-1	1	1
23	-1	1	1	-1	1	1
24	1	1	1	-1	1	-1
25	-1	-1	-1	1	1	-1
26	1	-1	-1	1	1	1
27	-1	1	-1	1	1	1
28	1	1	-1	1	1	-1
29	-1	-1	1	1	1	1
30	1	-1	1	1	1	-1
31	-1	1	1	1	1	-1
32	1	1	1	1	1	1

3.13 Conduct of die sinker experiments

Sample coupons for each experiment were the same size and type as previously used: quartered, four-inch silicon wafer with P-type doping (Boron), <100>-crystal orientation, and between 0.001 and 0.005 ohm-cm resistivity. Each replicate was cut with an individual copper electrode, with each electrode being used on the same replicate of each treatment to preserve consistency and allow for detection of any noise due to replicate order, position or electrode. Electrode wear was measured on a digitally controlled precision lathe following each treatment, and the electrodes were faced square to equal lengths between treatments. Electrode wear was subtracted from machined depth to calculate actual cut depth used in determining the analyzed material removal rates. Machining time for each replicate was recorded as well as all other output data from the machine display following each treatment. Average radius of each cut was measured following ultrasonic cleaning of the test coupon using a six-point best-fit circle measured on a Falcon microscope. Any overcuts resulting from electrode side-sparking or spalling were also measured and noted. All data for the roughing experiment is included in Appendix D – Die Sinker Roughing Experiment Data. Data for the finishing experiment is included in Appendix E – Die Sinker Finishing Experiment Data.

3.14 Analysis of Die Sinker EDM Results

For consistency of analysis between both characterization experiments (WEDM and die sinker), signal-to-noise ratio was used for analysis of the results of the die sinker experiments and was calculated in the same manner as described before. The interactions associated with the die sinker roughing experiment were also analyzed in accordance with techniques described in Wu and Hamada¹⁷. The conditional main effect (ME) is calculated in accordance with Equation 6, where A and B represent generic inputs. Likewise, the overall interaction, $INT(A, B)$, is defined per Equation 7.

¹⁷ (Wu and Hamada)

$$ME(B|A^+) = \bar{u}(B^+|A^+) - \bar{u}(B^-|A^+)$$

Equation 6

$$INT(A, B) = \frac{1}{2} * \{ME(A|B^+) - ME(A|B^-)\}$$

Equation 7

Interaction plots for each interaction significant to at least a 90% confidence interval are included in the following discussion of experimental results.

3.141 Die Sinker Roughing Experiment

Table 19 shows the die sinker EDM roughing experiment results summary for both cut speed and surface roughness (R_a). Standard deviations for each output parameter are also included. Parameter significance for all of the listed data sets was evaluated both by ANOVA analysis using MATLAB and R-value determination calculation as discussed before for the WEDM experiments. R-value results, a visual display of the R-values, and the associated normal probability plots as well as the ANOVA results for each output are included for both experiments.

Cut speed was selected as an output variable in place of MRR as in the WEDM experiments due to the impracticality of accurately measuring removed material for the die sinker experiments and the close relationship of cut speed to MRR on the die sinker EDM. Cut speed analysis by R-Value determination (Table 20, Figure 13 and Figure 14) for the roughing experiment indicates that for maximum cutting speed, inputs $E_2M_2RF_2U_1B_1VPULS_1SV_2$ should represent the input settings for the best output cut speed, with spark energy (E) being the most significant input parameter as expected based on EDM process physics. ANOVA analysis (Figure 15) indicates that spark energy (E), spark mode (M), and machining time (U) are statistically significant to a 90% confidence interval, and verifies that E is the most significant input as expected (based on

F-test). Spark energy also has significant first order interactions with both machining time (U) and off time (B).

Table 19: Die Sinker EDM Roughing Experiment Data Summary

	Mean Cut Speed	Cut Speed S/N	Cut Speed σ	Mean R_a	R_a S/N	$R_a \sigma$
Treatment	(in/min)	(dB)		μ inch	(dB)	
1	0.000201	-74.00	0.000020	81.83	-38.32	11.84
2	0.004055	-48.74	0.001427	114.41	-41.17	1.99
3	0.000202	-74.00	0.000025	80.54	-38.64	35.36
4	0.006151	-44.30	0.000604	112.14	-41.22	31.64
5	0.000334	-69.55	0.000021	78.47	-37.93	8.26
6	0.005902	-44.79	0.000871	120.61	-41.64	8.52
7	0.000176	-75.39	0.000032	107.64	-41.17	47.39
8	0.005829	-45.30	0.001449	158.31	-44.57	72.94
9	0.000152	-76.41	0.000008	73.17	-37.49	19.40
10	0.003427	-49.51	0.000564	160.39	-44.31	43.39
11	0.000138	-77.20	0.000003	68.33	-36.74	8.39
12	0.003561	-50.85	0.001394	93.38	-39.57	22.67
13	0.000177	-75.39	0.000037	84.50	-38.69	19.78
14	0.004156	-47.95	0.000860	118.21	-41.76	39.43
15	0.000146	-76.98	0.000029	100.71	-40.13	15.97
16	0.004959	-48.34	0.002956	90.57	-39.43	28.93
17	0.000478	-66.53	0.000053	79.53	-38.15	17.52
18	0.004150	-47.75	0.000454	76.12	-37.66	7.51
19	0.000727	-62.83	0.000060	87.73	-39.29	34.71
20	0.005159	-46.84	0.001599	93.13	-39.81	36.51
21	0.000532	-65.57	0.000052	103.01	-41.01	54.81
22	0.004976	-46.14	0.000495	121.13	-42.07	46.59
23	0.000489	-66.22	0.000012	86.88	-39.03	25.72
24	0.004920	-48.18	0.002470	88.42	-39.58	43.49
25	0.000578	-64.76	0.000010	79.43	-38.22	22.23
26	0.002752	-51.58	0.000615	81.76	-36.56	14.92
27	0.000331	-69.91	0.000062	81.13	-38.29	15.71
28	0.005004	-47.09	0.001703	65.80	-36.67	21.78
29	0.000586	-64.70	0.000048	90.46	-39.16	9.16
30	0.002869	-52.22	0.000979	113.94	-41.46	38.80
31	0.000239	-74.30	0.000095	70.10	-36.96	8.38
32	0.003785	-49.24	0.001187	105.29	-41.14	53.61

Table 20: Die Sinker Roughing Experiment Mean Cut Speed R-Values

Mean	P1	P2	P3	P4	P5	P6	P7
Cut Speed	E	M	RF	U	B	VPULS	SV
Low	3.43E-04	2.22E-03	2.32E-03	2.77E-03	2.47E-03	2.51E-03	2.28E-03
High	4.48E-03	2.61E-03	2.50E-03	2.05E-03	2.35E-03	2.31E-03	2.54E-03
R-Value	4.14E-03	3.90E-04	1.88E-04	-7.14E-04	-1.24E-04	-2.08E-04	2.63E-04
Effect Rank	1	3	6	2	7	5	4

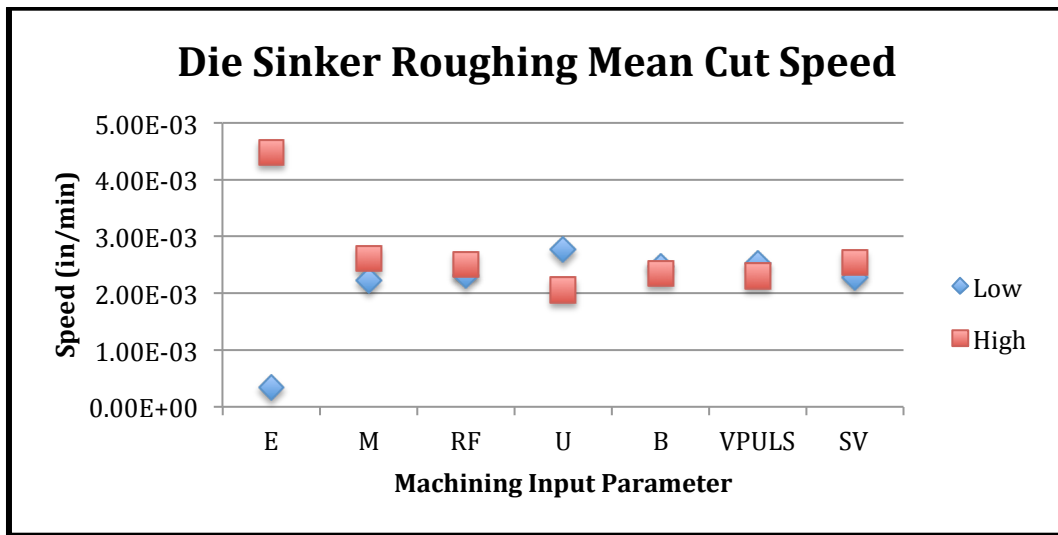


Figure 13: Die Sinker Roughing Mean Cut Speed Input Effects

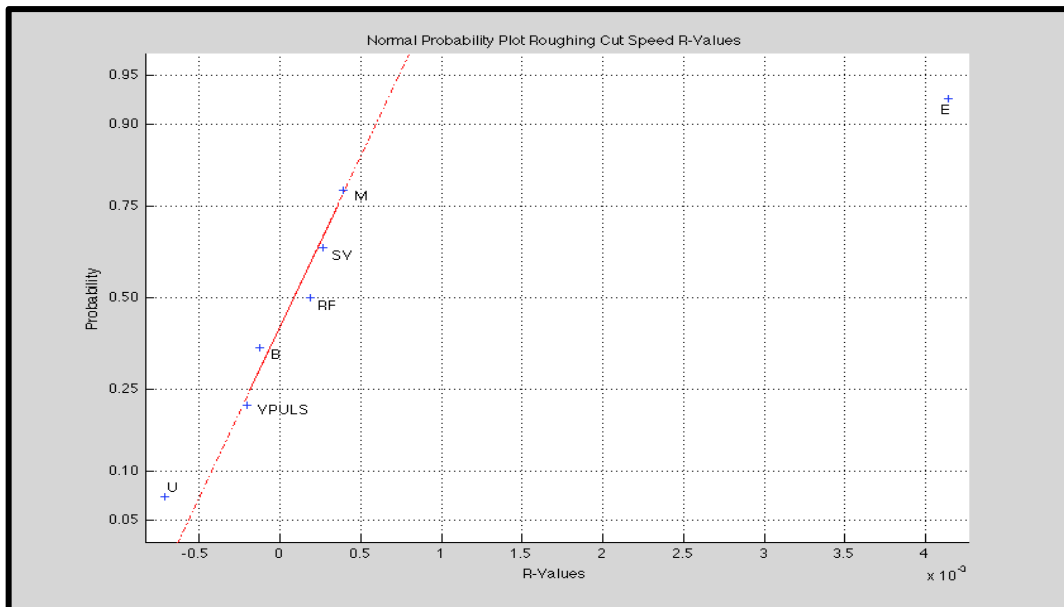


Figure 14: Normal Probability Plot of Die Sinker Roughing Experiment Mean Cut Speed R-Values

Cut Speed Analysis of Variance					
Source	Sum Sq.	d.f.	Mean Sq.	F	Prob>F
E	1.37E-04	1	0.00013682	649.1867	2.41E-07
Mode	1.32E-06	1	1.32E-06	6.2472	0.046564
RF	2.83E-07	1	2.83E-07	1.3425	0.29063
U	4.08E-06	1	4.08E-06	19.3405	0.0045793
B	1.24E-07	1	1.24E-07	0.58776	0.47236
VPULS	3.47E-07	1	3.47E-07	1.6471	0.24669
SV	5.55E-07	1	5.55E-07	2.6317	0.15587
# E*Mode	0	0	0	0	NaN
# E*RF	0	0	0	0	NaN
E*U	3.02E-06	1	3.02E-06	14.3478	0.0090963
E*B	1.47E-06	1	1.47E-06	6.9756	0.038482
# E*VPULS	0	0	0	0	NaN
E*SV	1.78E-07	1	1.78E-07	0.84624	0.3931
# Mode*RF	0	0	0	0	NaN
Mode*U	6.08E-09	1	6.08E-09	0.028836	0.87074
Mode*B	2.97E-08	1	2.97E-08	0.14095	0.72025
# Mode*VPULS	0	0	0	0	NaN
Mode*SV	4.74E-08	1	4.74E-08	0.22469	0.65225
RF*U	3.52E-08	1	3.52E-08	0.16691	0.69705
RF*B	6.54E-07	1	6.54E-07	3.1034	0.1286
# RF*VPULS	0	0	0	0	NaN
RF*SV	3.12E-07	1	3.12E-07	1.4797	0.26951
U*B	2.24E-08	1	2.24E-08	0.10637	0.75539
U*VPULS	1.56E-07	1	1.56E-07	0.73933	0.4229
U*SV	5.67E-08	1	5.67E-08	0.26903	0.62255
B*VPULS	1.47E-08	1	1.47E-08	0.069573	0.80078
B*SV	1.03E-07	1	1.03E-07	0.48952	0.51034
VPULS*SV	1.40E-07	1	1.40E-07	0.66451	0.44612
Error	1.26E-06	6	2.11E-07		
Total	1.54E-04	31			
Constrained (Type III) sums of squares. Terms marked with # are not full rank.					

Figure 15: Die Sinker Roughing Mean Cut Speed ANOVA

Evaluation of the interaction plots for mean cut speed analysis (Figure 16) indicates that the best cut speeds are achieved if the spark energy (E) is low for a given machining time (U) or machining time low for a given spark energy. This indicates that based on

this interaction, that the lower machining time should be selected when using a higher spark energy. It is critical to note that this is contrary to what might be expected physically – where more machining time would improve MRR. This can be explained by examining the secondary impact that machining time has on dielectric renewal and recovery. As machining time increases, the electrode spends more time closer to the workpiece, increasing the MRR, and thus the amount of material introduced into the dielectric. At some point, this removed material will interfere with the sparking process and begin to reduce MRR. It seems likely that at the spark energy-machining time combinations examined in this experiment that this could be occurring.

Cut speed is improved with higher spark energy for either value of off time (B), but the effect of off time on cut speed depends on the spark energy level selected. It is interesting to note that the interaction between spark energy and off time is antagonistic in the range analyzed, as indicated by the opposite signs of the conditional main effects. This is most easily seen by the opposing slopes depicted in the chart of the E to B interaction (bottom left of Figure 16). This situation indicates that the underlying response surface for the E to B interaction is relatively complicated and may merit a more thorough investigation if optimum settings are needed or desired for some reason.

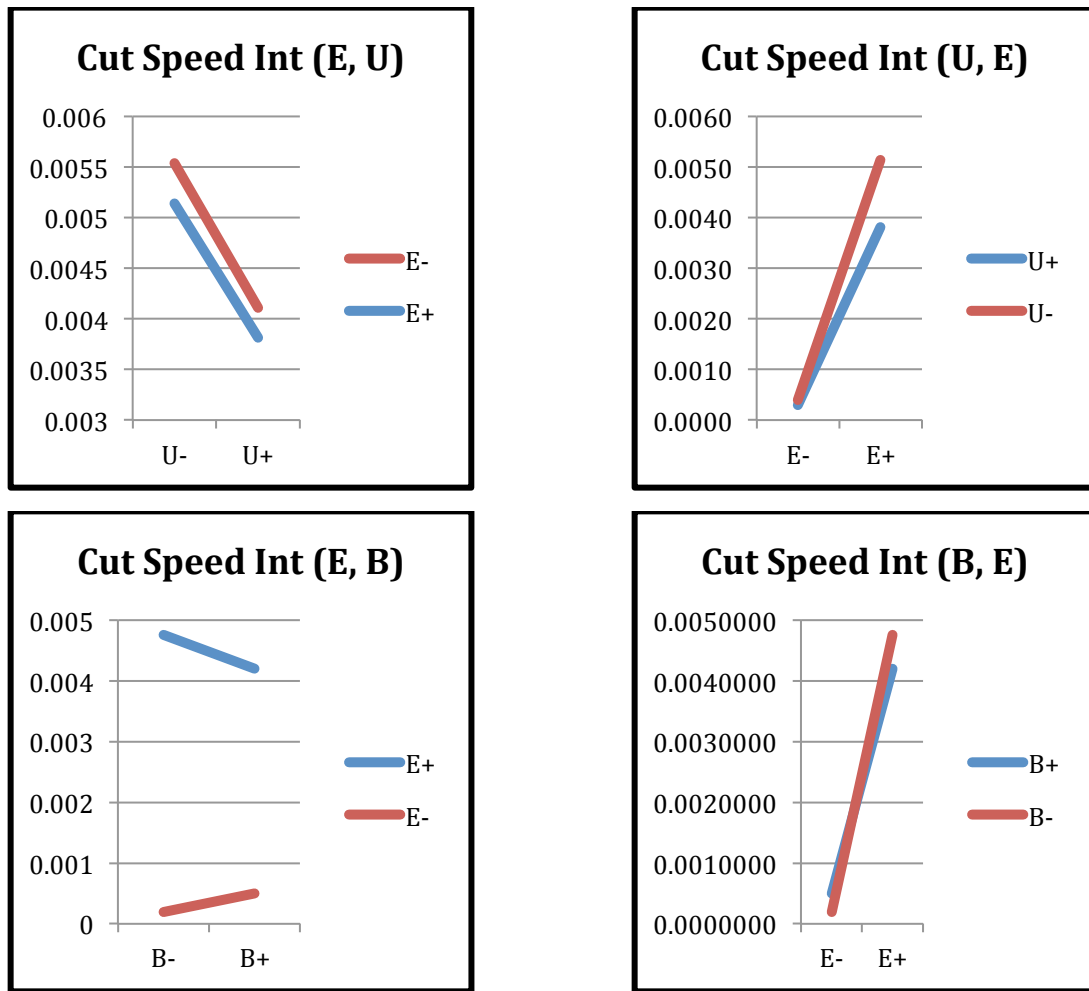


Figure 16: Interaction Plots for Die Sinker Roughing Mean Cut Speed
For Spark Energy (E) and Off Time (B)

Analysis was also conducted on die sinker roughing cut speed S/N ratio and demonstrates some differences from the pervious analysis of die sinker mean cut speed. Best cut speed S/N ratio for die sinker roughing is achieved by $E_2M_2RF_2U_1B_2VPULS_2SV_2$ (different from cut speed in that off time and pulsation speed are indicated to be better at the high value), and the effect rank of the R-values indicates that off time may have a more significant impact on cut speed than previously indicated by the mean cut speed ANOVA analysis. This indication also coincides with the operators' experience in using the Roboform 350, hardware literature and the previously mentioned research. ANOVA analysis of the die sinker cut speed S/N ratio also indicates that spark energy, machining time, off time, and servo are the statistically significant

inputs to cut speed S/N to a 90% confidence interval. Significant interactions are implied between spark energy and off time, reference arc voltage and off time, and between servo and off time. Calculated R-values are given in Table 21 and depicted graphically in Figure 17 and Figure 18. ANOVA results are included in Figure 19.

Table 21: Die Sinker Roughing Experiment Cut Speed S/N R-Values

Cut Speed	P1	P2	P3	P4	P5	P6	P7
S/N	E	M	RF	U	B	VPULS	SV
Low	-70.86	-59.07	-59.52	-57.88	-61.17	-59.67	-60.57
High	-48.05	-59.81	-59.39	-61.03	-57.74	-59.24	-58.34
R-Value	22.81	-0.74	0.13	-3.14	3.43	0.44	2.22
Effect Rank	1	5	7	3	2	6	4

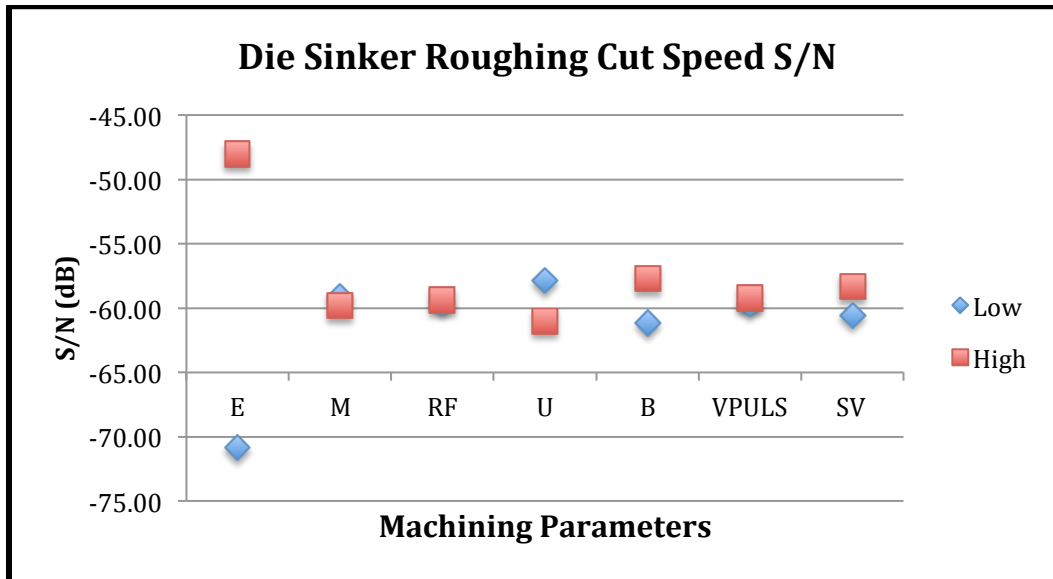


Figure 17: Die Sinker Roughing Cut Speed S/N Input Effects

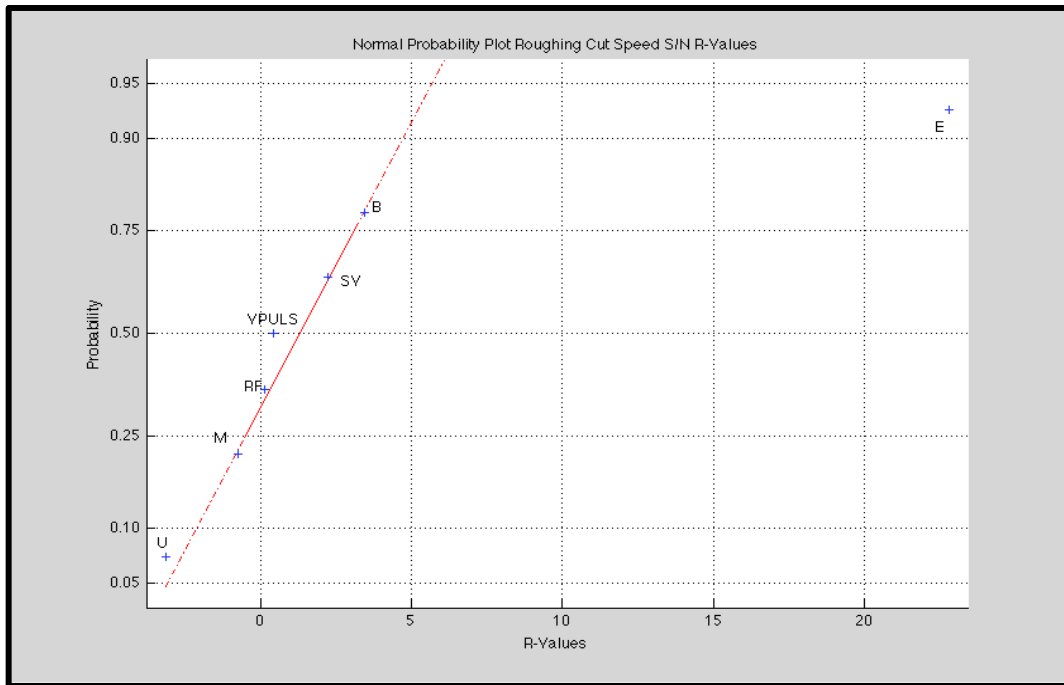


Figure 18: Normal Probability Plot of Die Sinker Cut Speed S/N R-Values

Analysis of the statistically significant interactions (Figure 20) for cut speed S/N ratio reinforces the previous analysis that the response surface for the spark energy (E) to off time (B) interaction may merit further future analysis. Additionally, it can be seen that the reference arc voltage (RF) to off time (B) interaction is similarly complex, although less significant to the process based on the ANOVA of Figure 19. Servo to off time interaction performed as expected based on the documentation included with the die sinker by the manufacturer.

Cut Speed S/N Analysis of Variance					
Source	Sum Sq.	d.f.	Mean Sq.	F	Prob>F
E	4161.4564	1	4161.4564	2936.2939	2.65E-09
Mode	4.047	1	4.047	2.8555	0.14202
RF	0.13005	1	0.13005	0.091762	0.77218
U	79.0653	1	79.0653	55.7879	0.00029722
B	93.9821	1	93.9821	66.3131	0.00018435
VPULS	1.5225	1	1.5225	1.0743	0.33994
SV	39.4272	1	39.4272	27.8196	0.0018752
# E*Mode	0	0	0	0	NaN
# E*RF	0	0	0	0	NaN
E*U	0.021013	1	0.021013	0.014826	0.90706
E*B	168.1778	1	168.1778	118.6651	3.55E-05
# E*VPULS	0	0	0	0	NaN
E*SV	1.5312	1	1.5312	1.0804	0.33866
# Mode*RF	0	0	0	0	NaN
Mode*U	4.0612	1	4.0612	2.8656	0.14144
Mode*B	0.013612	1	0.013612	0.0096049	0.92512
# Mode*VPULS	0	0	0	0	NaN
Mode*SV	0.099013	1	0.099013	0.069863	0.80038
RF*U	1.0011	1	1.0011	0.70638	0.43286
RF*B	13.2613	1	13.2613	9.357	0.022256
# RF*VPULS	0	0	0	0	NaN
RF*SV	0.01445	1	0.01445	0.010196	0.92286
U*B	0.24851	1	0.24851	0.17535	0.68998
U*VPULS	0.18	1	0.18	0.12701	0.73375
U*SV	1.8145	1	1.8145	1.2803	0.30103
B*VPULS	0.090313	1	0.090313	0.063724	0.80913
B*SV	9.3312	1	9.3312	6.584	0.042567
VPULS*SV	0.56711	1	0.56711	0.40015	0.55034
Error	8.5035	6	1.4172		
Total	4633.2222	31			
Constrained (Type III) sums of squares. Terms marked with # are not full rank.					

Figure 19: Die Sinker Roughing Experiment Cut Speed S/N ANOVA

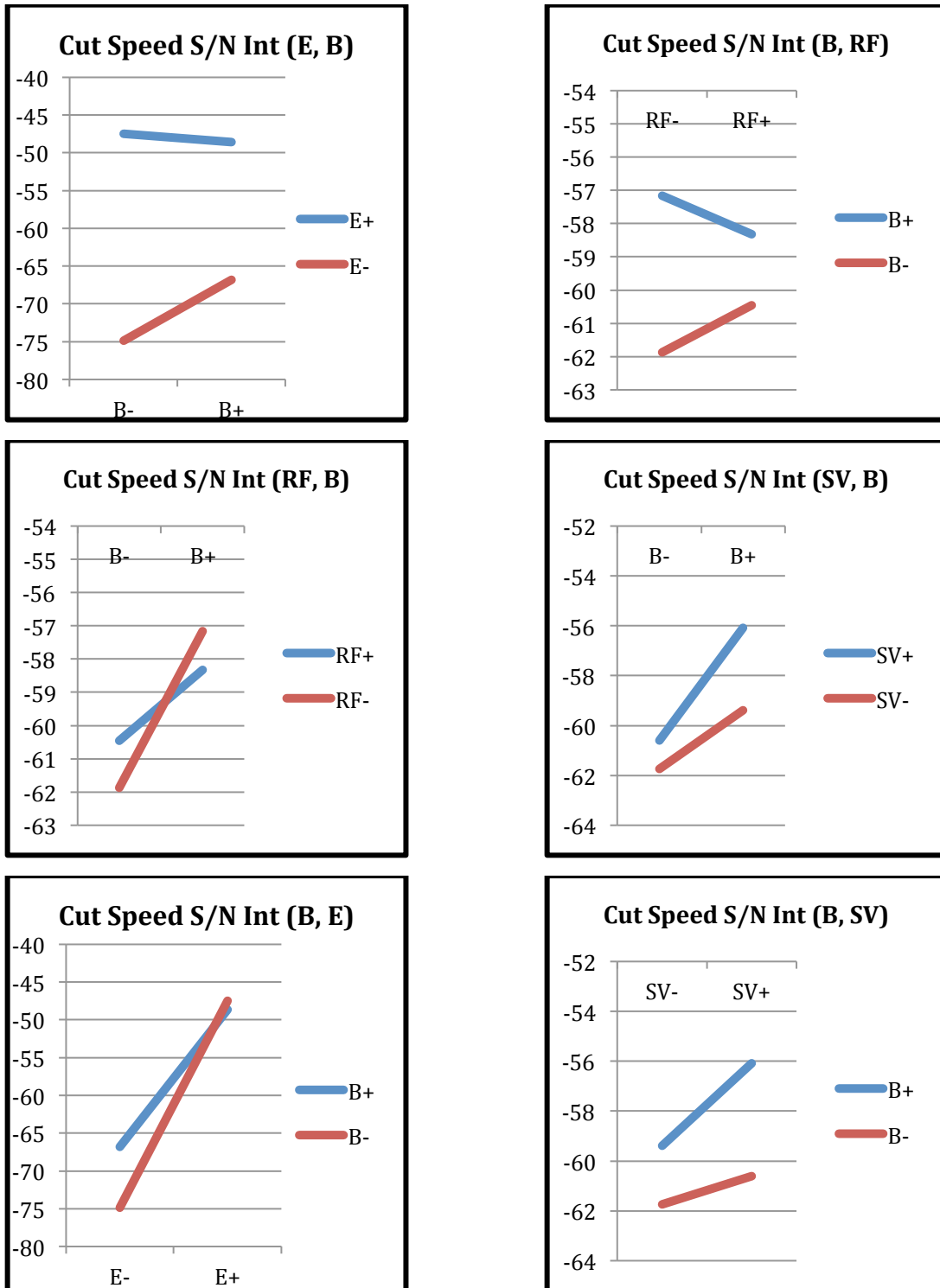


Figure 20: Die Sinker Cut Speed S/N Interaction Plots

For Spark Energy (E), Off Time (B), Reference Arc Voltage (RF), and Servo (SV)

For the roughing settings, cut speed variability is significantly affected by the choice of spark energy (E), spark mode (M), and servo (SV) setting based on ANOVA analysis (Figure 24). The best settings for the most reproducible speed results based on the range of inputs evaluated are $E_1M_1RF_1U_1B_2VPULS_1SV_2$. Calculated R-values, graphical depiction of response based on choice of input, and ANOVA analysis of the cut speed deviation are included in Table 22, Figure 21, Figure 22 and Figure 24 respectively. There is only one statistically significant interaction when evaluating to a 90% confidence interval, that between spark energy (E) and servo setting (E), and the interaction plots are included in Figure 23. The interaction plots indicate that regardless of servo selection, lower spark energy selection results in less variability in cut speed.

Table 22: Die Sinker Roughing Experiment Cut Speed Standard Deviation R-Values

Cut Speed	P1	P2	P3	P4	P5	P6	P7
Std Dev	E	M	RF	U	B	VPULS	SV
Low	3.54E-05	3.91E-04	5.38E-04	6.03E-04	6.47E-04	5.48E-04	7.92E-04
High	1.23E-03	8.55E-04	7.25E-04	6.59E-04	6.18E-04	7.14E-04	4.70E-04
R-Value	1.19E-03	4.64E-04	1.87E-04	5.65E-05	-2.87E-05	1.67E-04	-3.22E-04
Effect Rank	1	2	4	6	7	5	3

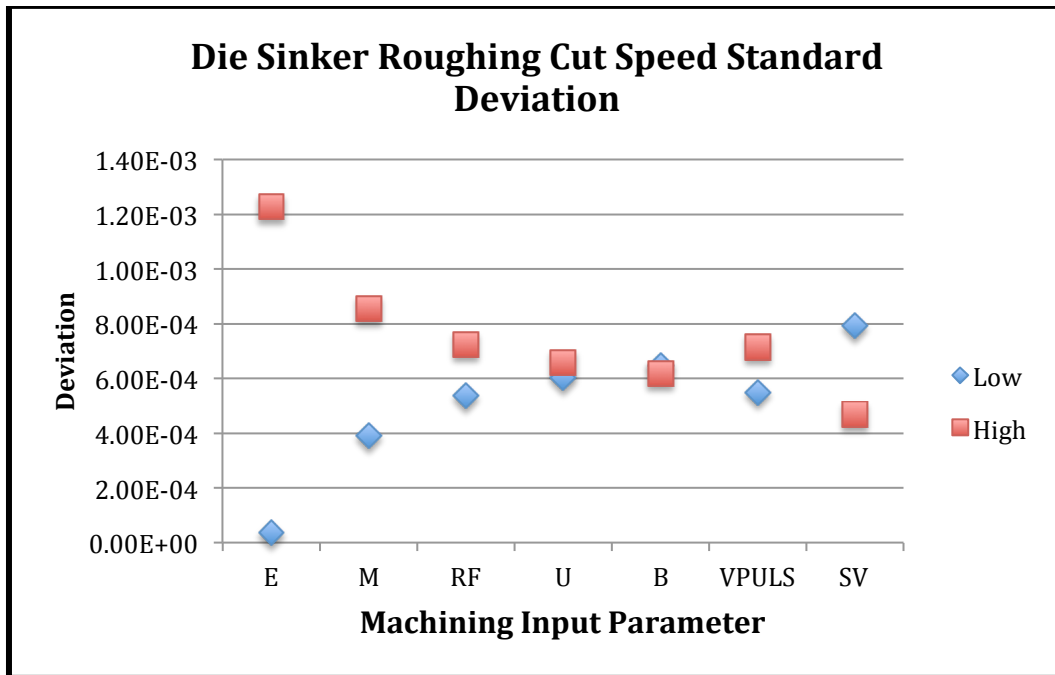


Figure 21: Die Sinker Roughing Experiment Cut Speed Standard Deviation Input Effects

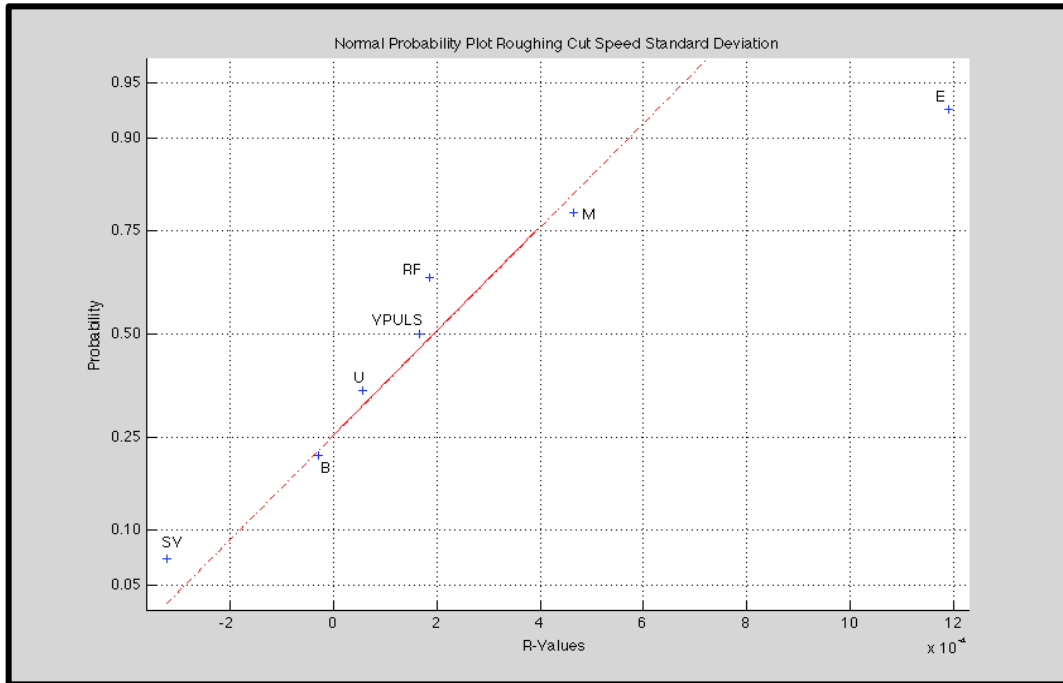


Figure 22: Normal Probability Plot of Cut Speed S/N Standard Deviation R-Values

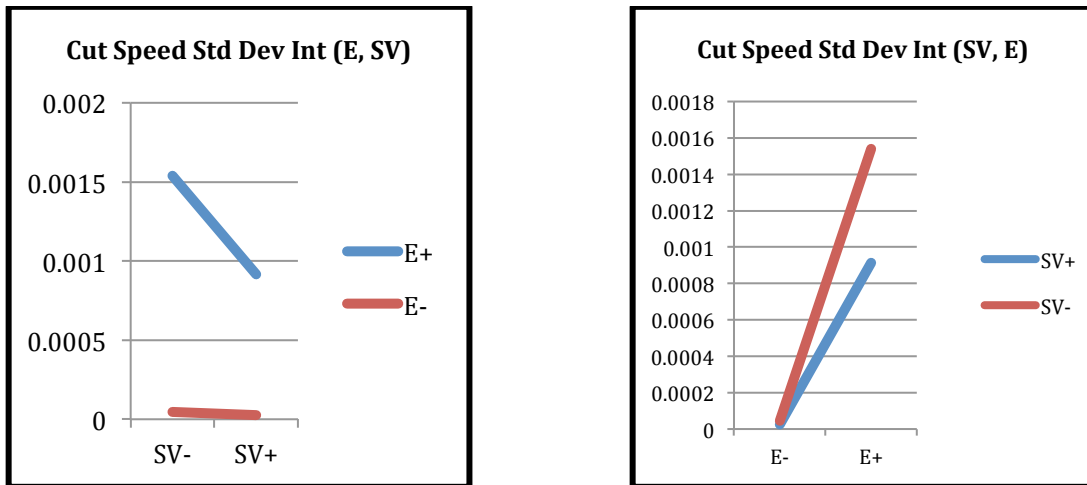


Figure 23: Die Sinker Roughing Experiment Cut Speed Standard Deviation Interaction Plots For Spark Energy (E) and Servo (SV)

Cut Speed Std Dev Analysis of Variance					
Source	Sum Sq.	d.f.	Mean Sq.	F	Prob>F
E	1.14E-05	1	1.14E-05	96.711	6.37E-05
Mode	1.60E-06	1	1.60E-06	13.6705	0.01012
RF	2.80E-07	1	2.80E-07	2.3832	0.1736
U	2.57E-08	1	2.57E-08	0.21852	0.65667
B	5.15E-09	1	5.15E-09	0.043882	0.84101
VPULS	2.22E-07	1	2.22E-07	1.8921	0.21811
SV	8.31E-07	1	8.31E-07	7.0771	0.03751
# E*Mode	0	0	0	0	NaN
# E*RF	0	0	0	0	NaN
E*U	2.38E-08	1	2.38E-08	0.20242	0.66857
E*B	2.21E-08	1	2.21E-08	0.18784	0.67987
# E*VPULS	0	0	0	0	NaN
E*SV	7.30E-07	1	7.30E-07	6.2208	0.046898
# Mode*RF	0	0	0	0	NaN
Mode*U	6.57E-08	1	6.57E-08	0.55971	0.48266
Mode*B	1.01E-07	1	1.01E-07	0.86062	0.38936
# Mode*VPULS	0	0	0	0	NaN
Mode*SV	1.27E-07	1	1.27E-07	1.082	0.33835
RF*U	1.41E-08	1	1.41E-08	0.12022	0.74063
RF*B	6.37E-08	1	6.37E-08	0.54286	0.48905
# RF*VPULS	0	0	0	0	NaN
RF*SV	8.26E-08	1	8.26E-08	0.70384	0.43364
U*B	1.13E-07	1	1.13E-07	0.95901	0.36526
U*VPULS	1.10E-07	1	1.10E-07	0.9389	0.36998
U*SV	8.74E-08	1	8.74E-08	0.74422	0.42145
B*VPULS	2.21E-07	1	2.21E-07	1.8865	0.21871
B*SV	4.84E-08	1	4.84E-08	0.41197	0.54469
VPULS*SV	2.05E-07	1	2.05E-07	1.7447	0.23469
Error	7.04E-07	6	1.17E-07		
Total	1.90E-05	31			
Constrained (Type III) sums of squares. Terms marked with # are not full rank.					

Figure 24: Die Sinker Roughing Experiment Cut Speed Standard Deviation ANOVA

Die sinker surface roughness using the roughing settings resulted in fairly extreme roughness. Evidence of plasma tunneling (a persistent spark channel) existed on all but the first high spark energy setting (treatment #2). This tunneling resulted in local areas of

visibly significant overcut outside of the radius of the main cut and loss of feature accuracy for each of these treatments. Based on this result, lower voltage (below $\pm 120\text{V}$), and thus spark energy, would be recommended for any processing where feature accuracy is of specific concern and low resistivity material is being utilized. This voltage choice may still be acceptable for rough cutting where the cut edge is sufficiently removed from feature boundaries, and where a multi-pass technique will be used as it did generally provide for a faster cut speed than the lower voltage choice. Some care must be taken to ensure that the pitting resulting from a rough cut is shallow enough that subsequent finishing and or polishing results in the desired surface roughness (see Section 4.4 Hemisphere Negatives using Die Sinker EDM for additional discussion on this topic). As can be seen from the analysis of the data, spark energy is the only parameter of statistical significance for this output (90% confidence interval). There are no interactions of significance present in the data. Analytical results for R_a are given in Table 23, Figure 25, Figure 26 and Figure 27. Additionally, the results of evaluation of the R_a S/N are in complete agreement with the Mean R_a analysis and also show no significant interactions. Analytical results for R_a S/N are presented in Table 24, Figure 28, Figure 29 and Figure 30.

Table 23: Die Sinker Roughing Experiment Mean R_a R-Values

Mean	P1	P2	P3	P4	P5	P6	P7
R_a	E	M	RF	U	B	VPULS	SV
Low	84.59	98.03	89.30	99.37	107.67	94.85	92.24
High	107.10	93.13	102.39	92.32	88.99	96.84	99.45
R-Value	22.51	-4.90	13.09	-7.04	-18.68	1.99	7.21
Effect Rank	1	6	3	5	2	7	4

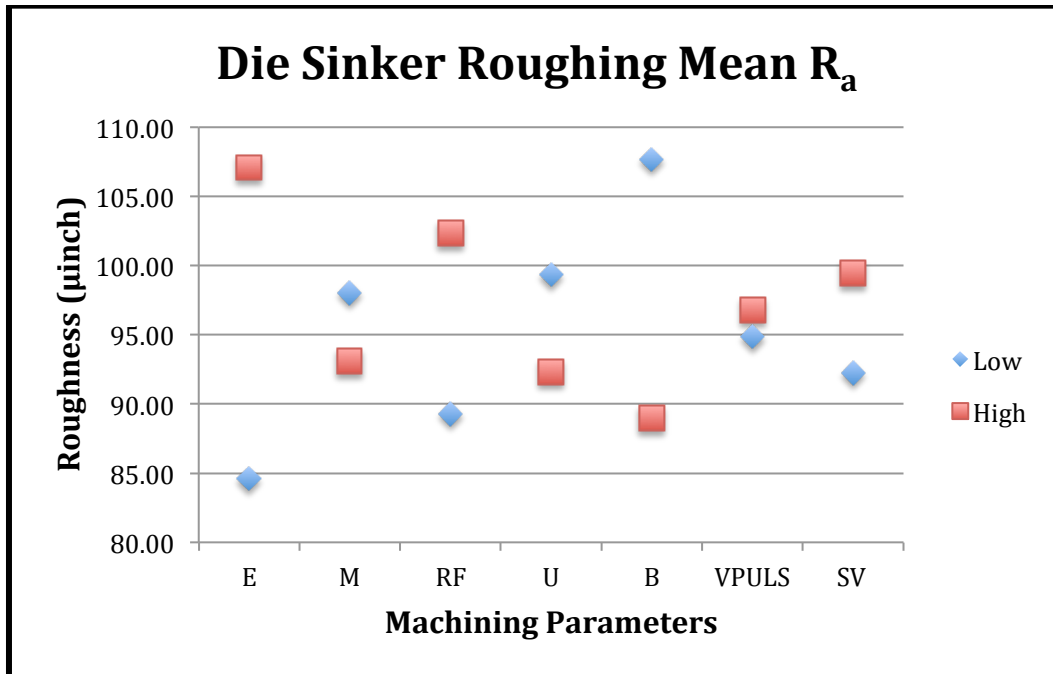


Figure 25: Die Sinker Roughing Experiment Mean R_a Input Effects

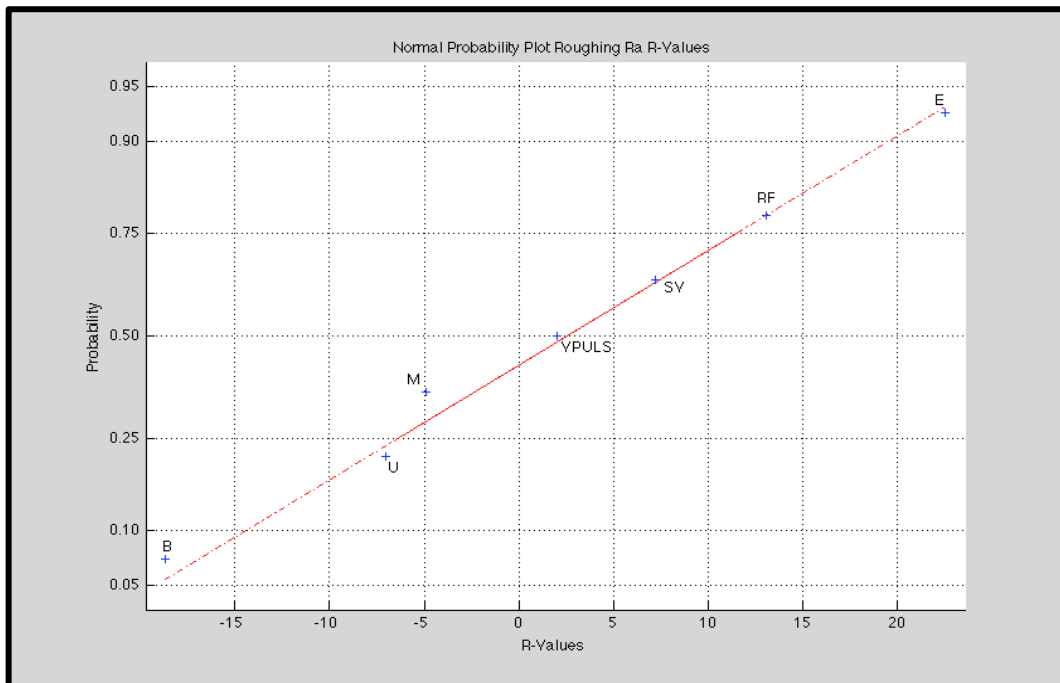


Figure 26: Normal Probability Plot of Die Sinker Roughing Experiment Mean R_a R-Values

Mean R _a Analysis of Variance					
Source	Sum Sq.	d.f.	Mean Sq.	F	Prob>F
E	4053.3757	1	4053.3757	7.0007	0.038239
Mode	235.8249	1	235.8249	0.4073	0.54691
RF	1370.6539	1	1370.6539	2.3673	0.17482
U	397.1267	1	397.1267	0.68589	0.43926
B	1503.5757	1	1503.5757	2.5969	0.1582
VPULS	31.6211	1	31.6211	0.054614	0.82299
SV	416.0891	1	416.0891	0.71864	0.42911
# E*Mode	0	0	0	0	NaN
# E*RF	0	0	0	0	NaN
E*U	0.2574	1	0.2574	0.00044457	0.98386
E*B	1589.2113	1	1589.2113	2.7448	0.14865
# E*VPULS	0	0	0	0	NaN
E*SV	503.6345	1	503.6345	0.86984	0.38699
# Mode*RF	0	0	0	0	NaN
Mode*U	863.5129	1	863.5129	1.4914	0.26781
Mode*B	68.8258	1	68.8258	0.11887	0.74203
# Mode*VPULS	0	0	0	0	NaN
Mode*SV	63.7603	1	63.7603	0.11012	0.75129
RF*U	147.2757	1	147.2757	0.25436	0.632
RF*B	111.6392	1	111.6392	0.19281	0.67596
# RF*VPULS	0	0	0	0	NaN
RF*SV	65.9813	1	65.9813	0.11396	0.74718
U*B	8.6632	1	8.6632	0.014962	0.90664
U*VPULS	126.2858	1	126.2858	0.21811	0.65696
U*SV	224.4551	1	224.4551	0.38766	0.55644
B*VPULS	17.7757	1	17.7757	0.030701	0.86667
B*SV	390.252	1	390.252	0.67401	0.44305
VPULS*SV	231.8243	1	231.8243	0.40039	0.55023
Error	3473.9846	6	578.9974		
Total	16370.9664	31			
Constrained (Type III) sums of squares. Terms marked with # are not full rank.					

Figure 27: Die Sinker Roughing Experiment R_a ANOVA

Table 24: Die Sinker Roughing Experiment R_a S/N R-Values

Ra S/N	P1	P2	P3	P4	P5	P6	P7
	E	M	RF	U	B	VPULS	SV
Low	-38.70	-39.70	-38.88	-40.08	-42.56	-39.60	-39.35
High	-40.54	-39.51	-40.36	-39.16	-39.07	-39.64	-39.89
R-Value	-1.84	0.18	-1.48	0.92	3.49	-0.03	-0.54
Effect Rank	2	6	3	4	1	7	5

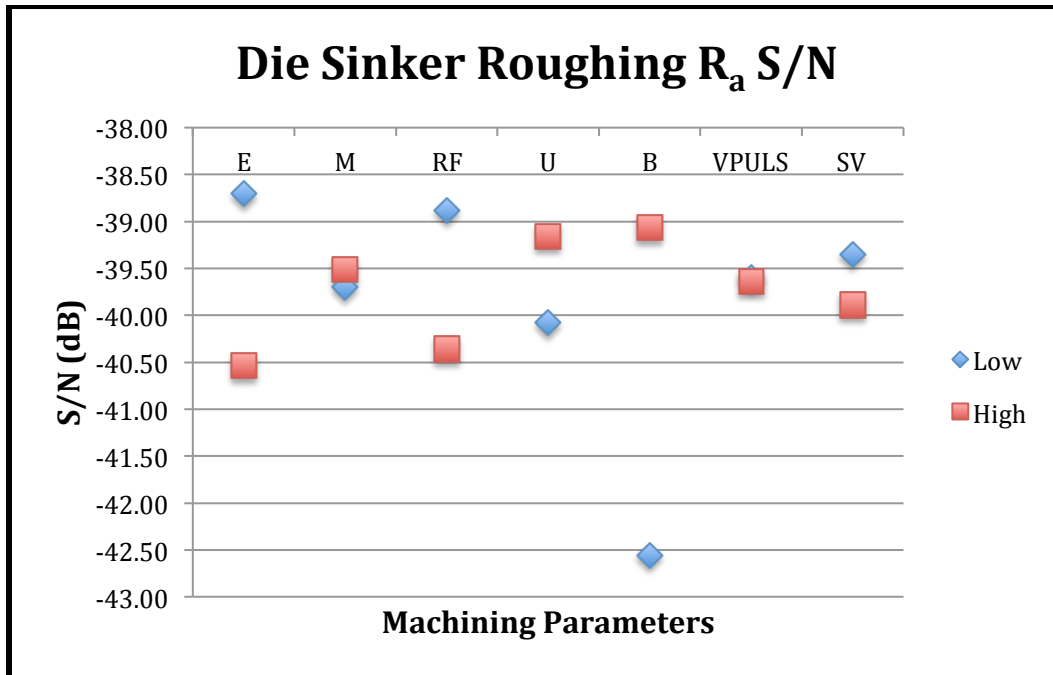


Figure 28: Die Sinker Roughing Experiment R_a S/N R-Values

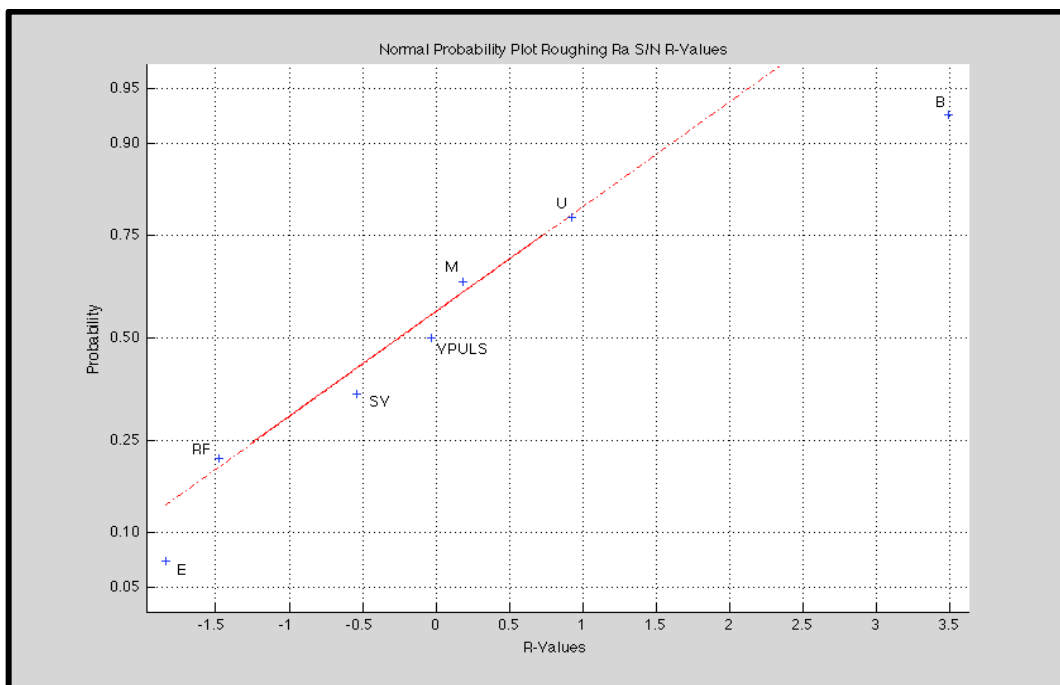


Figure 29: Normal Probability Plot for Die Sinker Roughing Experiment R_a S/N R-Values

Ra S/N Analysis of Variance					
Source	Sum Sq.	d.f.	Mean Sq.	F	Prob>F
E	27.0113	1	27.0113	4.8443	0.070009
Mode	0.3528	1	0.3528	0.063272	0.80979
RF	17.4345	1	17.4345	3.1267	0.12743
U	6.7344	1	6.7344	1.2078	0.3139
B	9.8124	1	9.8124	1.7598	0.23291
VPULS	0.0078125	1	0.0078125	0.0014011	0.97136
SV	2.3113	1	2.3113	0.4145	0.5435
# E*Mode	0	0	0	0	NaN
# E*RF	0	0	0	0	NaN
E*U	0.0338	1	0.0338	0.0060618	0.94047
E*B	12.1525	1	12.1525	2.1794	0.19032
# E*VPULS	0	0	0	0	NaN
E*SV	4.3218	1	4.3218	0.77508	0.41252
# Mode*RF	0	0	0	0	NaN
Mode*U	6.1952	1	6.1952	1.1111	0.33244
Mode*B	0.4232	1	0.4232	0.075898	0.79218
# Mode*VPULS	0	0	0	0	NaN
Mode*SV	0.1352	1	0.1352	0.024247	0.88136
RF*U	0.10811	1	0.10811	0.019389	0.89381
RF*B	1.9503	1	1.9503	0.34977	0.57583
# RF*VPULS	0	0	0	0	NaN
RF*SV	0.30031	1	0.30031	0.053859	0.82419
U*B	0.08	1	0.08	0.014347	0.90857
U*VPULS	0.40951	1	0.40951	0.073443	0.79547
U*SV	3.6181	1	3.6181	0.64887	0.45125
B*VPULS	0.0006125	1	0.0006125	0.00010985	0.99198
B*SV	1.0368	1	1.0368	0.18594	0.68138
VPULS*SV	1.2246	1	1.2246	0.21962	0.65587
Error	33.4556	6	5.5759		
Total	131.235	31			
Constrained (Type III) sums of squares. Terms marked with # are not full rank.					

Figure 30: Die Sinker Roughing Experiment R_a S/N ANOVA

Die sinker surface roughness variability is significantly dependent on selected spark energy and selected reference arc voltage to an 85% confidence interval only. Low values of all settings except machining/retraction time pair resulted in the lowest

variability in surface roughness for this experiment. Based on the Effect Heredity Principal in Wu and Hamada's text¹⁸, "for an interaction to be considered significant, at least one main effect involved in the interaction must also be significant." As such, no interactions meet significance requirements, and the marginal *INT* (*E*, *SV*) and *INT* (*M*, *U*) indicated in the ANOVA of Figure 32 can be disregarded.

Table 25: Die Sinker Roughing Experiment R_a Standard Deviation R-Values

Ra	P1	P2	P3	P4	P5	P6	P7
Std Dev	E	M	RF	U	B	VPULS	SV
Low	22.16	24.20	21.60	30.30	27.09	25.90	25.89
High	32.04	31.45	32.61	23.91	28.22	28.31	28.32
R-Value	9.88	7.25	11.01	-6.39	1.13	2.41	2.44
Effect Rank	2	3	1	4	7	6	5

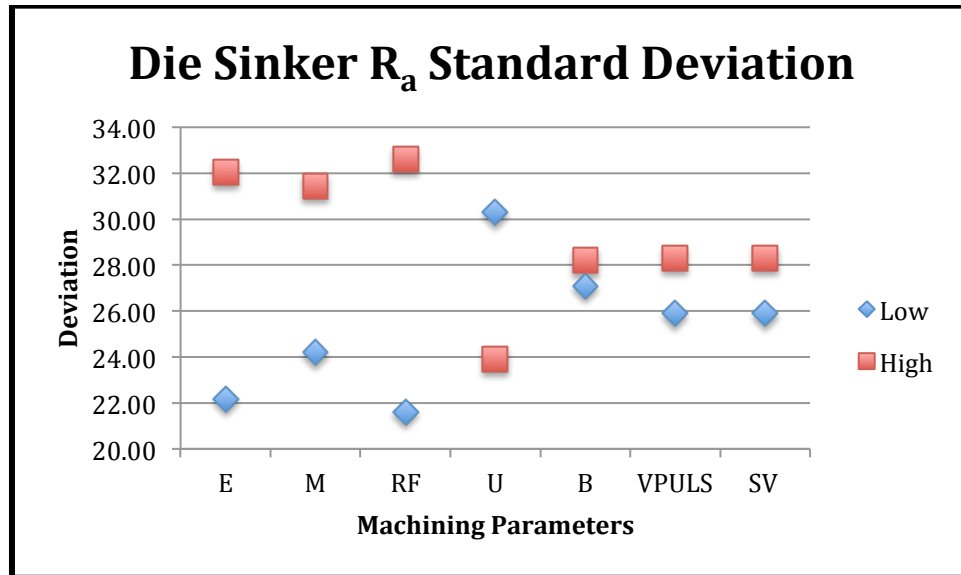


Figure 31: Die Sinker Roughing Experiment R_a Standard Deviation R-Values

¹⁸ (Wu and Hamada)

Ra Standard Deviation Analysis of Variance					
Source	Sum Sq.	d.f.	Mean Sq.	F	Prob>F
E	781.014	1	781.014	2.9308	0.13775
Mode	604.2157	1	604.2157	2.2674	0.18283
RF	970.3114	1	970.3114	3.6412	0.10497
U	326.7207	1	326.7207	1.226	0.31058
B	39.4938	1	39.4938	0.1482	0.71353
VPULS	46.4889	1	46.4889	0.17445	0.69072
SV	47.5069	1	47.5069	0.17827	0.68757
# E*Mode	0	0	0	0	NaN
# E*RF	0	0	0	0	NaN
E*U	535.7083	1	535.7083	2.0103	0.20602
E*B	2.0757	1	2.0757	0.0077892	0.93254
# E*VPULS	0	0	0	0	NaN
E*SV	1289.4312	1	1289.4312	4.8387	0.070131
# Mode*RF	0	0	0	0	NaN
Mode*U	1280.0535	1	1280.0535	4.8035	0.070909
Mode*B	211.7168	1	211.7168	0.79448	0.40707
# Mode*VPULS	0	0	0	0	NaN
Mode*SV	5.8226	1	5.8226	0.02185	0.88733
RF*U	226.1533	1	226.1533	0.84866	0.39247
RF*B	58.1312	1	58.1312	0.21814	0.65694
# RF*VPULS	0	0	0	0	NaN
RF*SV	0.5434	1	0.5434	0.0020392	0.96545
U*B	121.2514	1	121.2514	0.45501	0.52509
U*VPULS	24.6929	1	24.6929	0.092662	0.7711
U*SV	83.6895	1	83.6895	0.31405	0.59549
B*VPULS	1.0476	1	1.0476	0.0039313	0.95204
B*SV	100.2882	1	100.2882	0.37634	0.56209
VPULS*SV	1.5182	1	1.5182	0.005697	0.94229
Error	1598.8989	6	266.4831		
Total	9074.8514	31			
Constrained (Type III) sums of squares. Terms marked with # are not full rank.					

Figure 32: Die Sinker Roughing Experiment R_a Standard Deviation ANOVA

3.142 Die Sinker Finishing Experiment

Conduct of the die sinker finishing experiment was identical to the roughing experiment with the following exceptions. First, as the Roboform 350 uses a capacitive

circuit for finishing and polishing spark modes, capacitance (C) was introduced as an input parameter. Due to machine setup and design, this resulted in no operator control over current (P), on-time (A), and reference arc voltage (RF) for each individual capacitance setting once selected. This effectively removed spark energy (E) as a selectable input variable, but introduced no load voltage (V) in its place and a 2^{6-1} experimental design (Table 18: Die Sinker EDM Finishing Experiment Design) resulted. In this design, capacitance (C) was aliased as a product of the first five input parameters. Finally, based on the results of the roughing experiment, higher off times, pulsation speeds, and servo settings were selected for this experiment (Table 17: Die Sinker EDM Finishing Experiment Settings). Additionally, an error in machine programming introduced an additional treatment to this experiment that allowed for sufficient degrees of freedom for complete first level interaction analysis. Summary results for the entire finishing experiment are included in Table 27. Complete data for the finishing experiment is included in Appendix E – Die Sinker Finishing Experiment Data.

Die sinker mean cut speed during the finishing experiment was on average about half as fast as that achieved during the roughing experiment. Cut speed analysis indicates that maximum cutting speed should be achieved when inputs of $V_2B_1SV_1U_1VPULS_2C_2$ are used based on calculated R-Values (Table 26, Figure 33, and Figure 34). In using the capacitive circuitry, the magnitude of capacitance is the most significant input, and the only input parameter of statistical significance as indicated by ANOVA analysis (Figure 35). Cut speed and cut speed S/N analyses are in agreement for this experiment as well, with some minor variation in the ranking in the R-values calculated for the inputs of least significance. There are no statistically significant interactions for either output parameter.

Table 26: Die Sinker Finishing Experiment Mean Cut Speed R-Values

Mean	P1	P2	P3	P4	P5	P6
Cut Speed	V	B	SV	U	VPULS	C
Low	1.15E-03	1.39E-03	1.37E-03	1.46E-03	1.27E-03	5.29E-04
High	1.41E-03	1.17E-03	1.20E-03	1.08E-03	1.29E-03	1.98E-03
R-Value	2.61E-04	-2.18E-04	-1.70E-04	-3.80E-04	2.44E-05	1.45E-03
Effect Rank	3	5	6	2	4	1

Table 27: Die Sinker EDM Finishing Experiment Data Summary

	Mean	S/N	Cut Speed	Mean	S/N	
	Cut Speed	Speed	σ	Ra	Ra	Ra σ
Treatment	(in/min)	dB	inch/min	μ inch	dB	μ inch
1	0.000488	-66.30	0.000040	45.34	-33.14	2.30
2	0.003446	-49.29	0.000227	60.03	-35.58	3.10
3	0.002173	-53.27	0.000074	60.88	-35.70	3.06
4	0.000902	-60.89	0.000014	47.02	-33.48	5.21
5	0.000385	-68.31	0.000014	52.88	-34.51	6.75
6	0.000698	-63.16	0.000039	52.67	-34.49	7.60
7	0.000256	-71.85	0.000008	36.08	-31.15	0.83
8	0.001686	-55.46	0.000023	69.96	-37.14	20.75
9	0.001888	-54.75	0.000321	65.75	-36.49	14.18
10	0.000778	-62.21	0.000051	52.62	-34.50	8.72
11	0.000244	-72.27	0.000007	65.39	-36.64	22.43
12	0.002262	-52.91	0.000031	73.19	-37.32	8.21
13	0.000466	-66.65	0.000019	50.31	-34.15	10.31
14	0.002454	-52.21	0.000076	69.43	-36.83	0.87
15	0.001596	-55.94	0.000021	74.03	-37.39	2.63
16	0.000529	-65.54	0.000009	47.18	-33.50	4.15
17	0.003043	-50.38	0.000205	67.80	-36.64	4.82
18	0.000884	-61.08	0.000032	50.14	-34.06	6.97
19	0.000316	-70.06	0.000024	52.96	-34.53	6.98
20	0.002399	-52.40	0.000011	66.70	-36.63	15.13
21	0.000401	-67.95	0.000017	49.11	-33.87	6.35
22	0.002780	-51.13	0.000072	80.82	-38.16	4.27
23	0.001748	-55.15	0.000036	77.25	-37.86	14.44
24	0.000555	-65.12	0.000013	56.02	-35.01	6.70
25	0.000411	-67.73	0.000009	48.65	-33.79	6.45
26	0.000411	-67.73	0.000009	84.62	-38.65	15.74
27	0.001577	-56.05	0.000045	69.81	-36.89	5.33
28	0.000632	-63.99	0.000002	59.78	-35.65	12.16
29	0.001585	-56.02	0.000080	61.19	-35.74	3.83
30	0.000608	-64.32	0.000008	52.83	-34.46	0.80
31	0.000299	-70.54	0.000025	45.31	-33.13	2.51
32	0.001580	-56.03	0.000040	74.05	-37.39	1.88
33	0.002700	-51.42	0.000197	74.71	-37.53	10.82

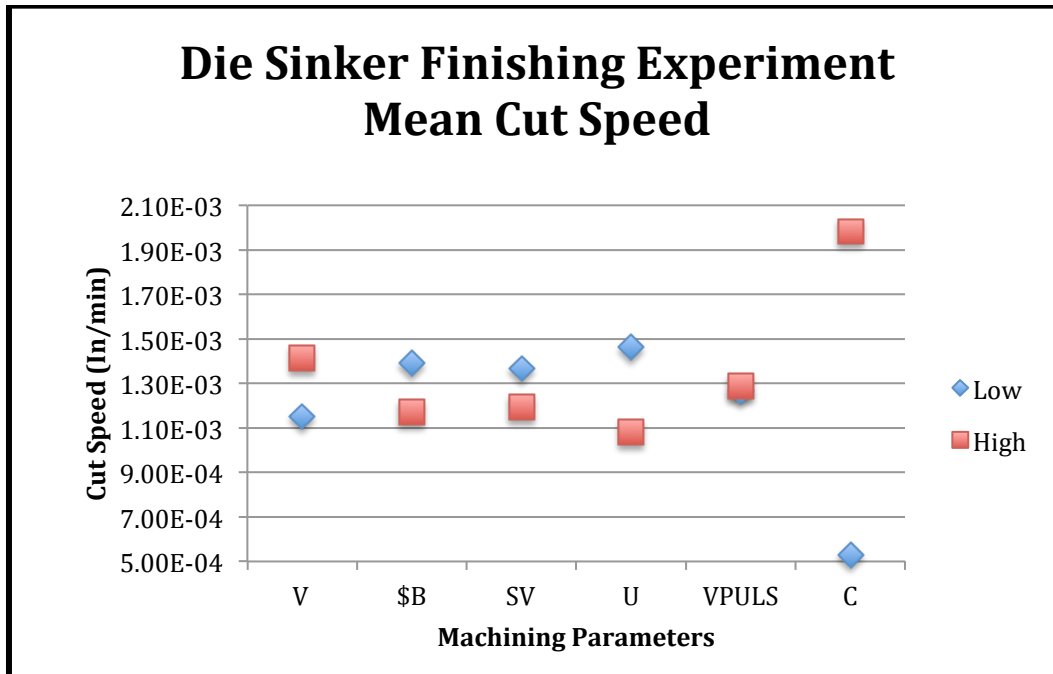


Figure 33: Die Sinker Finishing Cut Speed Input Effects

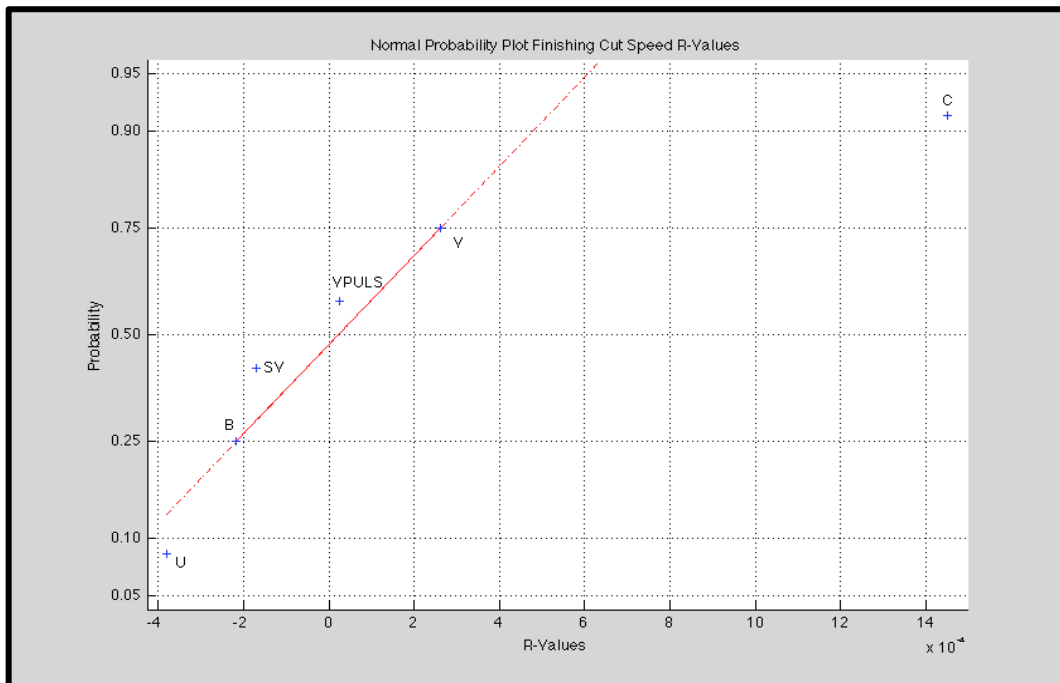


Figure 34: Normal Probability Plot of Die Sinker Finishing Experiment Mean Cut Speed R-Values

Cut Speed Analysis of Variance					
Source	Sum Sq.	d.f.	Mean Sq.	F	Prob>F
V	8.85E-07	1	8.85E-07	2.3631	0.15248
B	1.88E-07	1	1.88E-07	0.50172	0.49348
SV	4.53E-07	1	4.53E-07	1.2096	0.29491
U	8.93E-07	1	8.93E-07	2.3862	0.15068
VPULS	1.02E-08	1	1.02E-08	0.027168	0.87207
C	1.68E-05	1	1.68E-05	45.0023	3.34E-05
V*B	1.14E-08	1	1.14E-08	0.030535	0.86446
V*SV	1.44E-07	1	1.44E-07	0.3834	0.5484
V*U	2.67E-07	1	2.67E-07	0.7129	0.41647
V*VPULS	8.77E-07	1	8.77E-07	2.3413	0.15422
V*C	6.14E-10	1	6.14E-10	0.0016389	0.96843
B*SV	1.75E-08	1	1.75E-08	0.046676	0.83291
B*U	2.26E-07	1	2.26E-07	0.60396	0.45346
B*VPULS	8.57E-09	1	8.57E-09	0.022893	0.88248
B*C	5.80E-09	1	5.80E-09	0.015494	0.90319
SV*U	9.98E-07	1	9.98E-07	2.6664	0.13076
SV*VPULS	6.31E-07	1	6.31E-07	1.6848	0.22084
SV*C	1.38E-07	1	1.38E-07	0.3698	0.55546
U*VPULS	1.02E-06	1	1.02E-06	2.7273	0.12687
U*C	5.70E-07	1	5.70E-07	1.5224	0.24297
VPULS*C	9.70E-11	1	9.70E-11	0.0002590	0.98745
Error	4.12E-06	11	3.74E-07		
Total	2.88E-05	32			
Constrained (Type III) sums of squares.					

Figure 35: Die Sinker Finishing Experiment Cut Speed ANOVA

Table 28: Die Sinker Finishing Experiment Cut Speed S/N R-Values

Cut Speed	P1	P2	P3	P4	P5	P6
S/N	V	B	SV	U	VPULS	C
Low	-62.04	-59.90	-60.08	-59.60	-60.69	-66.23
High	-58.97	-61.09	-60.99	-61.56	-60.42	-55.20
R-Value	3.07	-1.19	-0.91	-1.96	0.27	11.03
Effect Rank	2	4	5	3	6	1

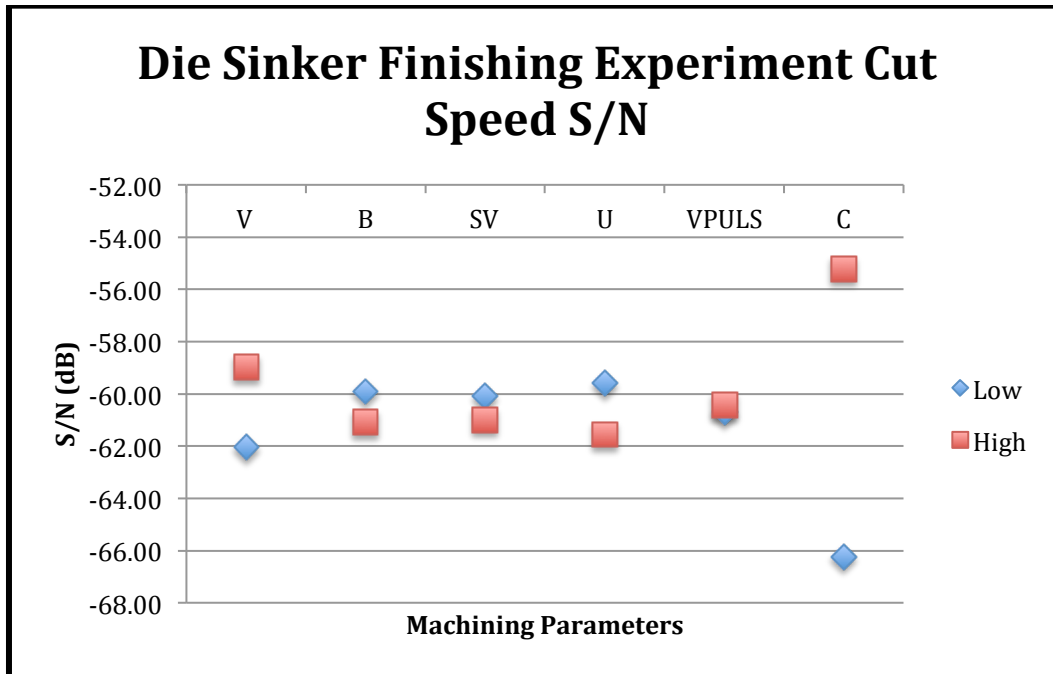


Figure 36: Die Sinker Finishing Experiment Cut Speed S/N Input Effects

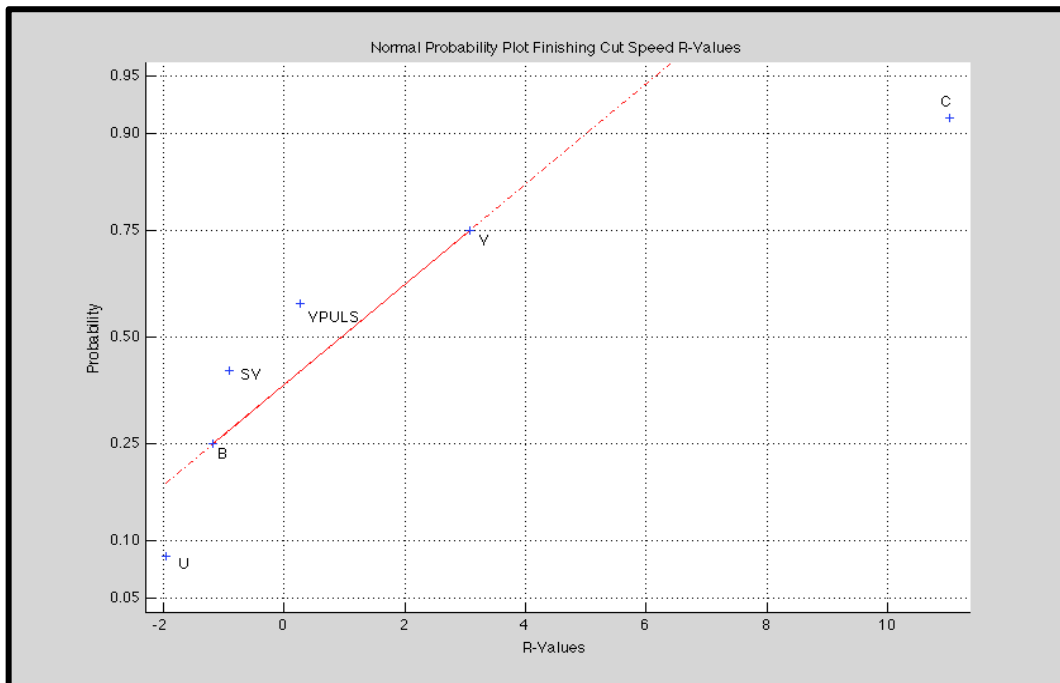


Figure 37: Normal Probability Plot of Die Sinker Cut Speed S/N R-Values

Cut Speed S/N Analysis of Variance					
Source	Sum Sq.	d.f.	Mean Sq.	F	Prob>F
V	102.6955	1	102.6955	5.4222	0.039971
B	3.9992	1	3.9992	0.21115	0.65481
SV	14.1922	1	14.1922	0.74933	0.40517
U	21.6021	1	21.6021	1.1406	0.30841
VPULS	0.093385	1	0.093385	0.0049306	0.94528
C	981.6454	1	981.6454	51.8293	1.75E-05
V*B	2.4586	1	2.4586	0.12981	0.72545
V*SV	8.3277	1	8.3277	0.43969	0.52092
V*U	22.8217	1	22.8217	1.205	0.29578
V*VPULS	47.3106	1	47.3106	2.4979	0.1423
V*C	44.2682	1	44.2682	2.3373	0.15454
B*SV	1.3318	1	1.3318	0.070315	0.79578
B*U	1.9908	1	1.9908	0.10511	0.75186
B*VPULS	0.015933	1	0.015933	0.0008412	0.97738
B*C	29.6433	1	29.6433	1.5651	0.23687
SV*U	55.8782	1	55.8782	2.9503	0.11385
SV*VPULS	35.4072	1	35.4072	1.8694	0.19883
SV*C	0.000243	1	0.0002432	1.28E-05	0.9972
U*VPULS	46.3338	1	46.3338	2.4464	0.14609
U*C	4.87	1	4.87	0.25713	0.62211
VPULS*C	0.1441	1	0.1441	0.0076083	0.93206
Error	208.3397	11	18.94		
Total	1646.256	32			
Constrained (Type III) sums of squares.					

Figure 38: Die Sinker Finishing Experiment Cut Speed S/N ANOVA

Cut speed variability for the die sinker in finishing mode was also evaluated. The lowest variability was introduced when $V_2B_2SV_2U_2VPULS_2C_1$ were the selected inputs (Table 29). This is visually depicted in Figure 39. Capacitance (C) and off time (B) are the statistically significant input parameters, and also result in a significant interaction effect. The normal probability plot indicates that voltage (V) and machining time (U) may also have some impact not due to system noise, but it is not statistically significant as tested. The interaction of servo to pulsation speed indicated in the ANOVA analysis (Figure 41) is ignored due to the previously discussed heredity principle.

Table 29: Die Sinker Finishing Experiment Cut Speed Standard Deviation R-Values

Cut Speed	P1	P2	P3	P4	P5	P6
Std Dev	V	B	SV	U	VPULS	C
Low	6.71E-05	8.17E-05	6.89E-05	6.15E-05	6.09E-05	1.98E-05
High	4.10E-05	2.40E-05	4.09E-05	4.70E-05	4.84E-05	8.71E-05
R-Value	-2.61E-05	-5.77E-05	-2.80E-05	-1.45E-05	-1.24E-05	6.73E-05
Effect Rank	4	2	3	5	6	1

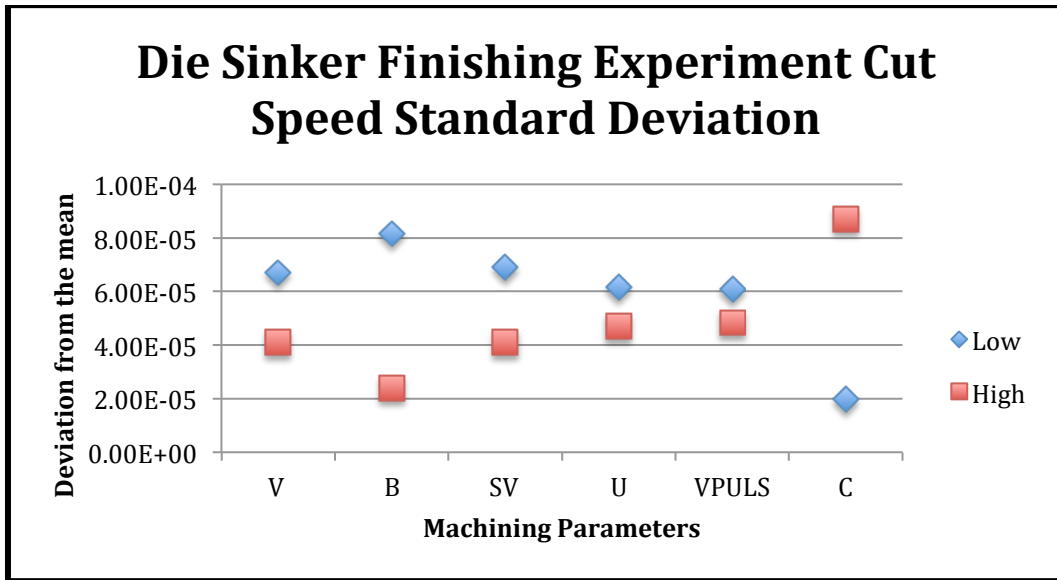


Figure 39: Die Sinker Finishing Experiment Cut Speed Standard Deviation Input Effects

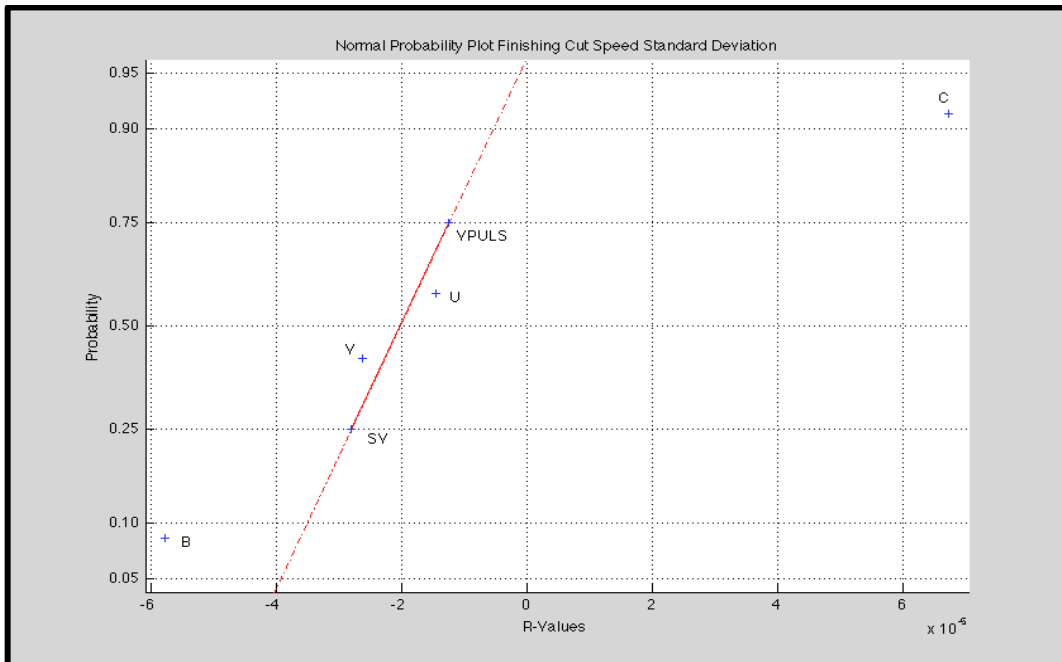
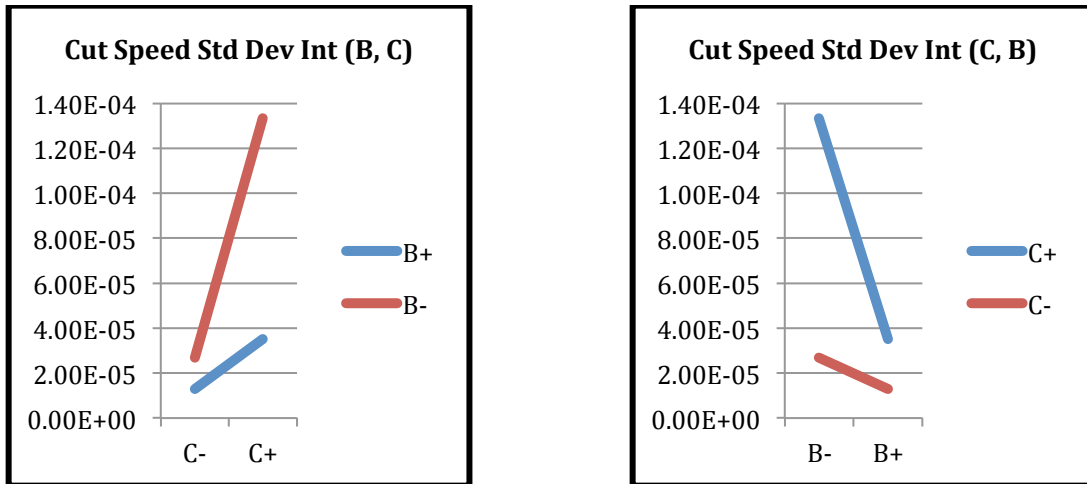


Figure 40: Normal Probability Plot of Die Sinker Finishing Experiment Cut Speed Standard Deviation R-Values

Cut Speed Std Dev Analysis of Variance					
Source	Sum Sq.	d.f.	Mean Sq.	F	Prob>F
V	4.16E-09	1	4.16E-09	1.293	0.27965
B	2.63E-08	1	2.63E-08	8.1872	0.01548
SV	8.90E-09	1	8.90E-09	2.7661	0.12448
U	9.14E-10	1	9.14E-10	0.28411	0.60462
VPULS	2.37E-09	1	2.37E-09	0.73561	0.40937
C	3.45E-08	1	3.45E-08	10.7365	0.0073775
V*B	8.92E-10	1	8.92E-10	0.27744	0.60884
V*SV	3.56E-09	1	3.56E-09	1.1083	0.31503
V*U	1.84E-09	1	1.84E-09	0.57304	0.46496
V*VPULS	2.74E-09	1	2.74E-09	0.85224	0.37573
V*C	5.08E-09	1	5.08E-09	1.5793	0.2349
B*SV	6.81E-09	1	6.81E-09	2.1184	0.17347
B*U	4.85E-10	1	4.85E-10	0.15077	0.70521
B*VPULS	2.69E-09	1	2.69E-09	0.83597	0.38016
B*C	1.49E-08	1	1.49E-08	4.6236	0.054623
SV*U	5.77E-10	1	5.77E-10	0.17933	0.68011
SV*VPULS	1.08E-08	1	1.08E-08	3.3695	0.093571
SV*C	6.35E-09	1	6.35E-09	1.9744	0.18758
U*VPULS	4.16E-09	1	4.16E-09	1.293	0.27965
U*C	9.77E-11	1	9.77E-11	0.030392	0.86477
VPULS*C	8.01E-10	1	8.01E-10	0.24899	0.62761
Error	3.54E-08	11	3.22E-09		
Total	1.77E-07	32			
Constrained (Type III) sums of squares.					

Figure 41: Die Sinker Finishing Experiment Cut Speed Standard Deviation ANOVA

The single significant cut speed standard deviation interaction, *INT* (B, C), shows that as capacitance increases, that higher off time produces less variability in processing speed. This is physically logical in that the increased off time allows for better dielectric recovery and impurity removal in the face of increased spark energy and resultant increased material removal rate resulting from increased capacitance.



**Figure 42: Die Sinker Finishing Experiment Cut Speed Standard Deviation Interaction Plots
For Off Time (B) and Capacitance (C)**

Mean surface roughness for the die sinker finishing experiment is best for input settings of $V_1B_1SV_2U_1VPULS_1C_1$, with capacitance, pulsation speed and no load voltage having the greatest impact (Table 30). Relative input parameter effect is depicted graphically in Figure 43. ANOVA analysis (Figure 45) indicates that input parameters no load voltage, pulsation speed and capacitance are statistically significant, and that there is a significant interaction, $INT(VPULS, U)$. R_a S/N analysis also shows analytical results similar to the mean R_a analysis (Table 31, Figure 47, and Figure 49).

Table 30: Die Sinker Finishing Experiment Mean R_a R-Values

Mean	P1	P2	P3	P4	P5	P6
R_a	V	B	SV	U	VPULS	C
Low	58.67	59.60	60.67	58.85	57.67	50.71
High	62.32	60.97	60.22	62.13	63.04	69.59
R-Value	3.64	1.37	-0.44	3.29	5.37	18.88
Effect Rank	3	5	6	4	2	1

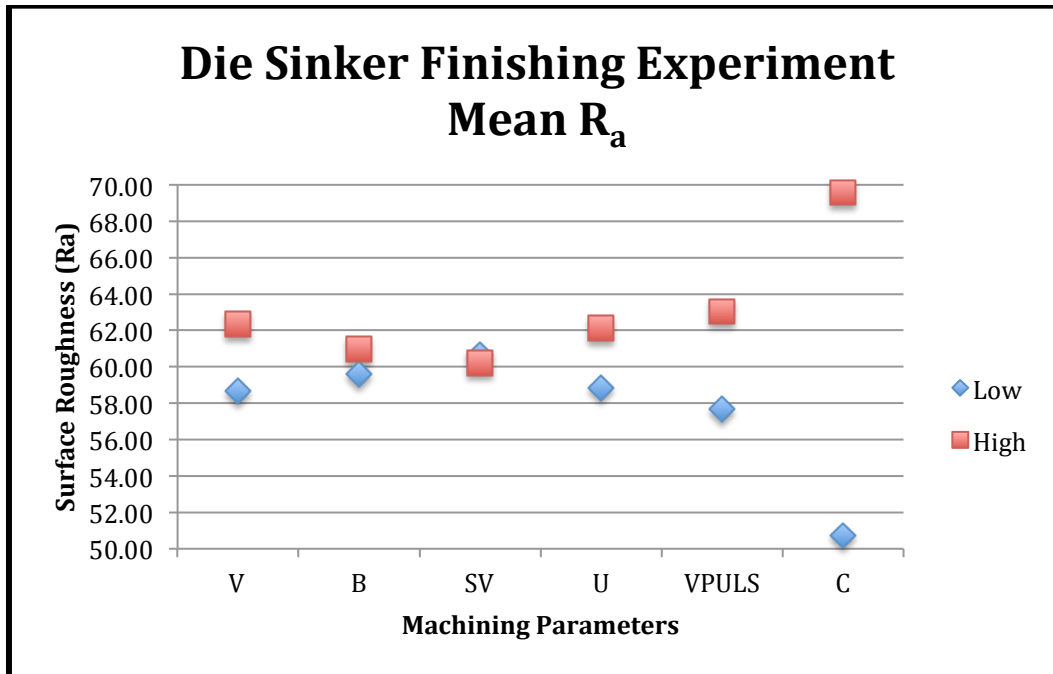


Figure 43: Die Sinker Finishing Experiment Mean R_a Input Effects

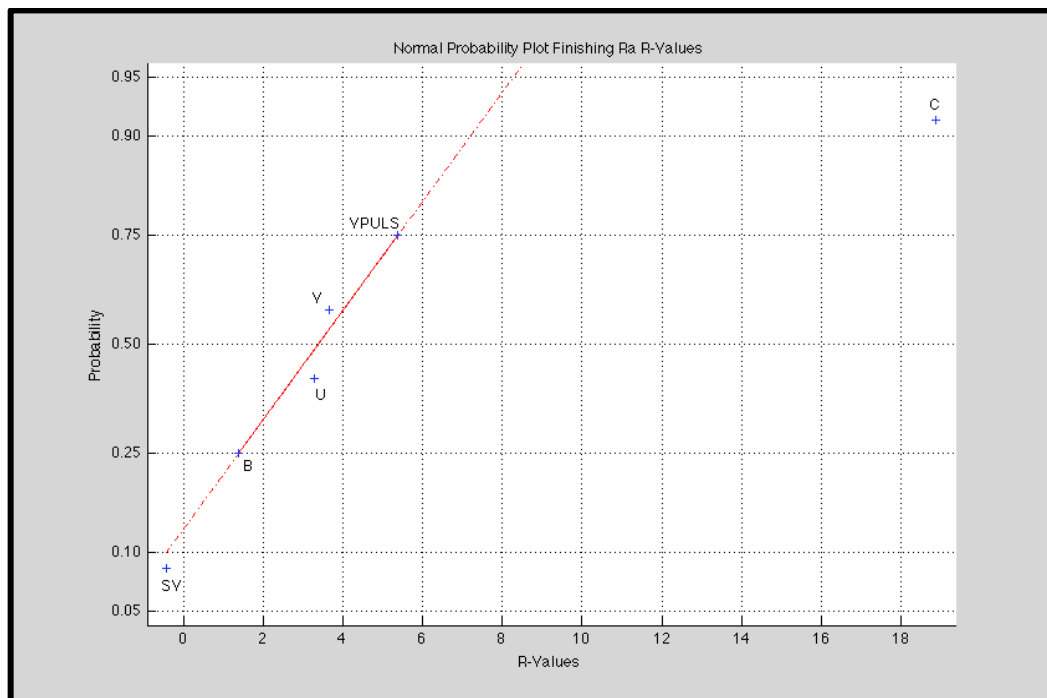


Figure 44: Normal Probability Plot of Die Sinker Finishing Experiment Mean R_a R-Values

R _a Analysis of Variance					
Source	Sum Sq.	d.f.	Mean Sq.	F	Prob>F
V	160.3596	1	160.3596	3.6562	0.082245
B	25.0839	1	25.0839	0.57191	0.46539
SV	10.556	1	10.556	0.24068	0.63336
U	135.0534	1	135.0534	3.0792	0.10707
VPULS	191.888	1	191.888	4.3751	0.060466
C	2871.9092	1	2871.9092	65.4796	5.86E-06
V*B	69.1065	1	69.1065	1.5756	0.2354
V*SV	41.0996	1	41.0996	0.93707	0.35383
V*U	0.62998	1	0.62998	0.014364	0.90676
V*VPULS	25.1197	1	25.1197	0.57273	0.46508
V*C	13.7065	1	13.7065	0.31251	0.58735
B*SV	5.7958	1	5.7958	0.13214	0.72311
B*U	11.0293	1	11.0293	0.25147	0.62593
B*VPULS	14.4886	1	14.4886	0.33034	0.57703
B*C	4.5302	1	4.5302	0.10329	0.75394
SV*U	168.5218	1	168.5218	3.8423	0.075791
SV*VPULS	9.3668	1	9.3668	0.21356	0.653
SV*C	69.0581	1	69.0581	1.5745	0.23556
U*VPULS	208.6515	1	208.6515	4.7573	0.051764
U*C	0.0035064	1	0.0035064	7.99E-05	0.99303
VPULS*C	54.182	1	54.182	1.2354	0.29007
Error	482.4554	11	43.8596		
Total	4619.7897	32			
Constrained (Type III) sums of squares.					

Figure 45: Die Sinker Finishing Experiment R_a ANOVA

Figure 46 depicts the significant interaction for pulsation speed and machining time when R_a is analyzed for the finishing mode on the die sinker. The plots show an antagonistic interaction, where better R_a was observed for combinations of low pulsation speed and low machining time or high pulsation speed and high machining time. The impact is much more significant at the lower settings. The heredity principle made the indicated servo to machining time interaction insignificant for mean R_a analysis. This interaction was also statistically insignificant when R_a S/N is analyzed, reinforcing the

conclusion of the previous analysis. The interaction for R_a S/N ($INT(VPULS, U)$ - Figure 50) shows the same general characteristics as for mean R_a as well.

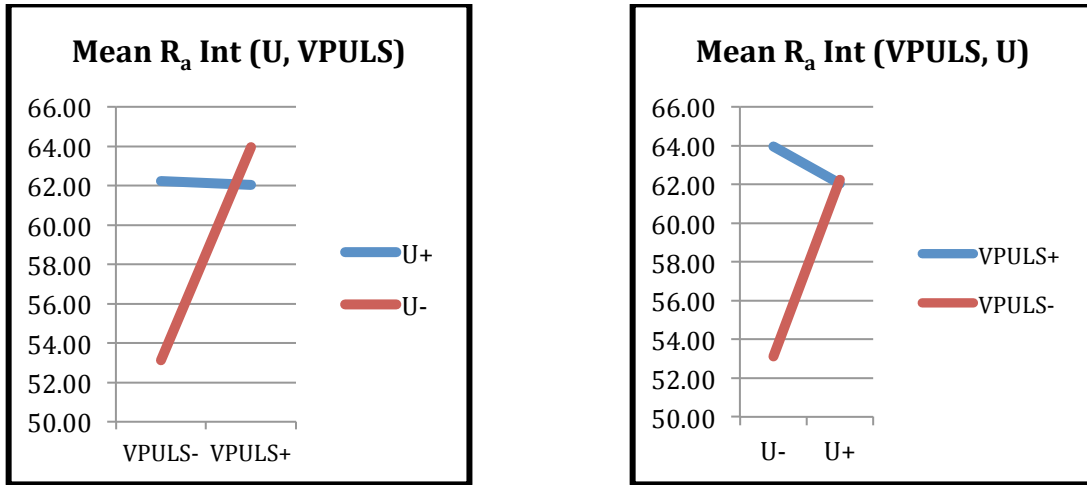


Figure 46: Die Sinker Finishing Experiment R_a Interaction Plots
For Machining Time (U) and Pulsation Speed (VPULS)

Table 31: Die Sinker Finishing Experiment R_a S/N R-Values

Ra S/N	P1	P2	P3	P4	P5	P6
	V	B	SV	U	VPULS	C
Low	-35.24	-35.39	-35.61	-35.26	-35.13	-34.10
High	-35.80	-35.59	-35.43	-35.78	-35.88	-36.85
R-Value	-0.56	-0.20	0.17	-0.52	-0.76	-2.75
Effect Rank	3	5	6	4	2	1

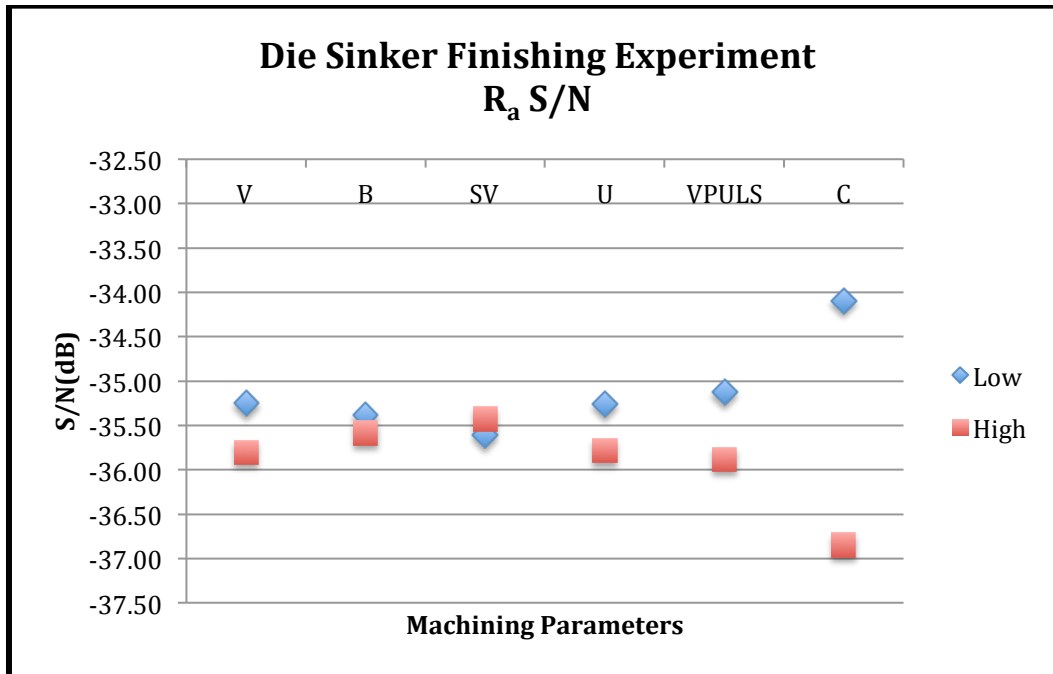


Figure 47: Die Sinker Finishing Experiment R_a S/N Input Effects

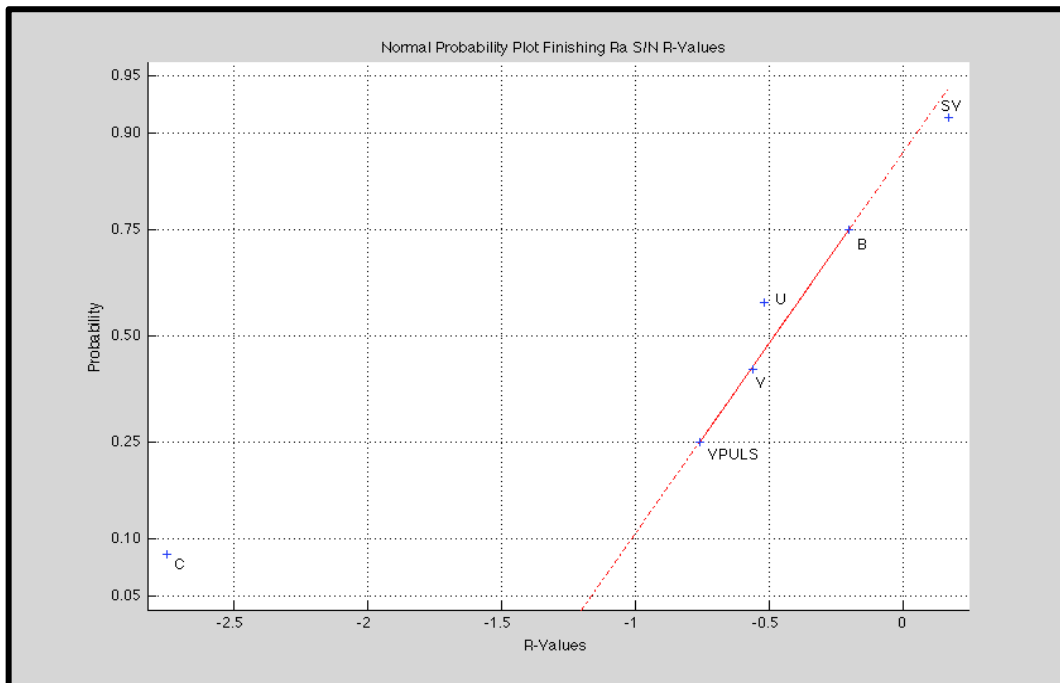


Figure 48: Normal Probability Plot of Die Sinker Finishing Experiment R_a S/N R-Values

Ra S/N Analysis of Variance					
Source	Sum Sq.	d.f.	Mean Sq.	F	Prob>F
V	3.7016	1	3.7016	3.3844	0.092935
B	0.48483	1	0.48483	0.44329	0.51926
SV	0.63397	1	0.63397	0.57965	0.46246
U	3.2623	1	3.2623	2.9828	0.11209
VPULS	3.7813	1	3.7813	3.4573	0.089906
C	61.132	1	61.132	55.8943	1.24E-05
V*B	0.83538	1	0.83538	0.76381	0.40082
V*SV	1.4217	1	1.4217	1.2999	0.27845
V*U	0.21893	1	0.21893	0.20017	0.66326
V*VPULS	0.37726	1	0.37726	0.34494	0.56885
V*C	0.052347	1	0.052347	0.047862	0.83083
B*SV	0.52944	1	0.52944	0.48408	0.50102
B*U	0.23173	1	0.23173	0.21187	0.65427
B*VPULS	0.058698	1	0.058698	0.053669	0.82105
B*C	0.22228	1	0.22228	0.20324	0.66088
SV*U	3.3242	1	3.3242	3.0393	0.10911
SV*VPULS	0.27106	1	0.27106	0.24784	0.6284
SV*C	1.838	1	1.838	1.6805	0.22139
U*VPULS	5.4956	1	5.4956	5.0247	0.046572
U*C	0.13482	1	0.13482	0.12327	0.73214
VPULS*C	0.50887	1	0.50887	0.46527	0.50928
Error	12.0308	11	1.0937		
Total	101.4402	32			
Constrained (Type III) sums of squares.					

Figure 49: Die Sinker Finishing Experiment R_a S/N ANOVA

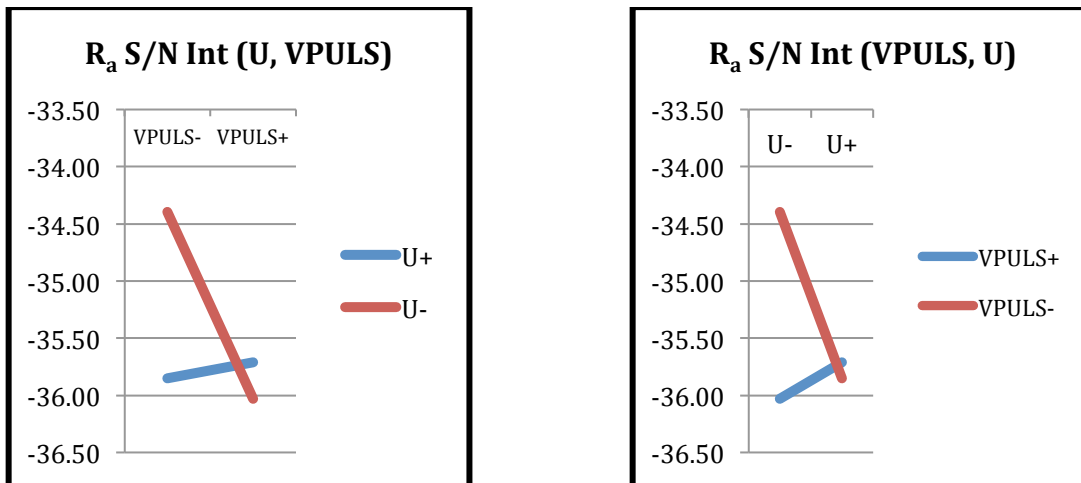


Figure 50: Die Sinker Finishing Experiment R_a S/N Interaction Plots

Variability in R_a was evaluated for the finishing experiment as well. The least variability was observed with selected settings at $V_1B_1SV_2U_1VPULS_2C_1$, with off time, servo, and capacitance contributing the most experimental variability (Table 32, Figure 51, and Figure 53). Again, this is explainable when the introduction of material to the dielectric during the material removal process is considered with the effect that these parameters have on the average concentration of foreign material in the dielectric. The spark energy level and dielectric flushing both have an impact on contamination and therefore have an observable impact on the machining process and spark quality when viewing both the roughing and finishing experiment data sets for the die sinker.

Table 32: Die Sinker Finishing Experiment R_a Standard Deviation R-Values

Ra	P1	P2	P3	P4	P5	P6
Std Dev	V	B	SV	U	VPULS	C
Low	7.30	6.56	8.80	7.42	7.57	6.90
High	7.64	8.27	6.20	7.51	7.36	7.99
R-Value	0.34	1.72	-2.59	0.10	-0.21	1.08
Effect Rank	4	2	1	6	5	3

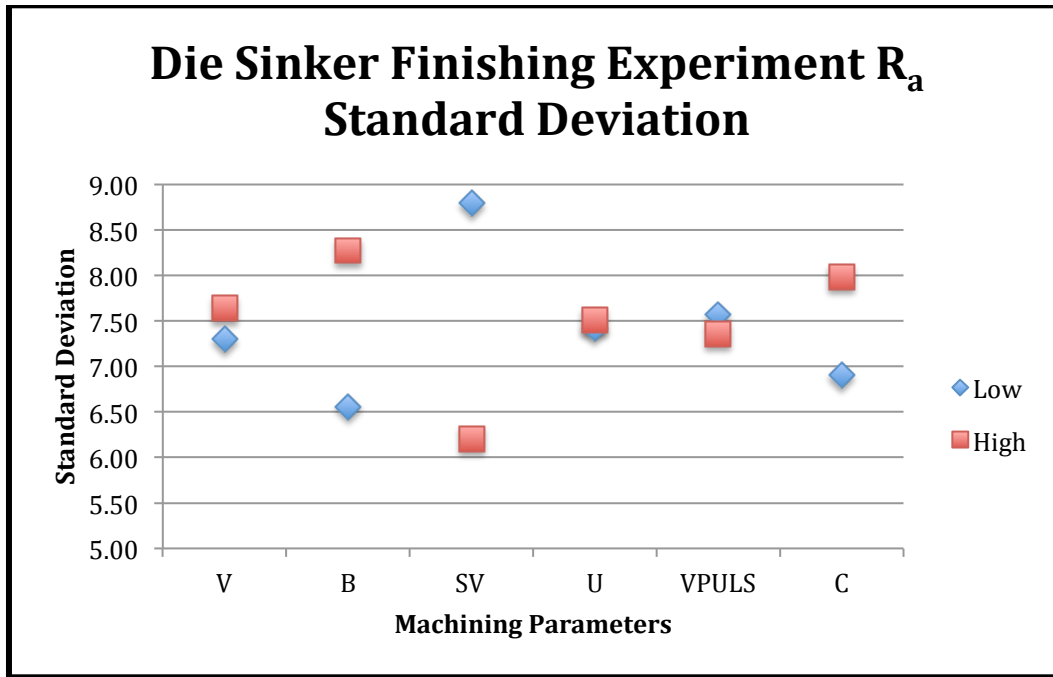


Figure 51: Die Sinker Finishing Experiment R_a Standard Deviation Input Effects

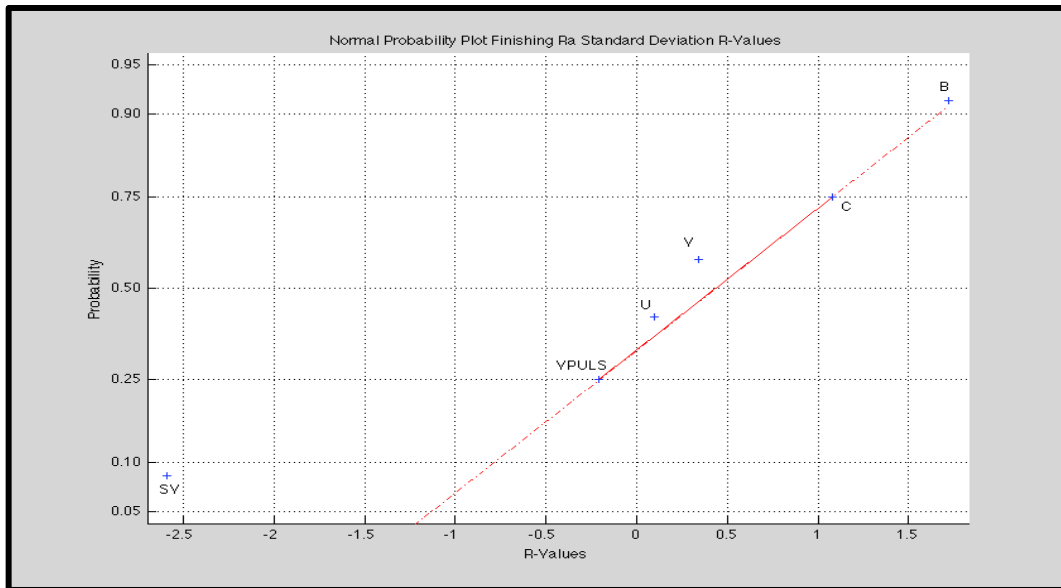


Figure 52: Normal Probability Plot of Die Sinker Finishing Experiment Standard Deviation R-Values

Ra Std Dev Analysis of Variance					
Source	Sum Sq.	d.f.	Mean Sq.	F	Prob>F
V	1.7568	1	1.7568	0.050189	0.82684
B	24.4446	1	24.4446	0.69833	0.42112
SV	63.0168	1	63.0168	1.8003	0.20672
U	0.34845	1	0.34845	0.0099545	0.92232
VPULS	0.8308	1	0.8308	0.023734	0.88035
C	8.3064	1	8.3064	0.2373	0.63573
V*B	19.1615	1	19.1615	0.54741	0.47487
V*SV	4.5482	1	4.5482	0.12993	0.72533
V*U	45.2729	1	45.2729	1.2934	0.2796
V*VPULS	7.3448	1	7.3448	0.20983	0.65582
V*C	11.6497	1	11.6497	0.33281	0.57563
B*SV	0.71894	1	0.71894	0.020539	0.88863
B*U	30.4168	1	30.4168	0.86895	0.37125
B*VPULS	0.021837	1	0.021837	0.00062383	0.98052
B*C	0.72388	1	0.72388	0.02068	0.88826
SV*U	246.5204	1	246.5204	7.0426	0.022434
SV*VPULS	10.1427	1	10.1427	0.28976	0.6011
SV*C	12.0473	1	12.0473	0.34417	0.56928
U*VPULS	52.2039	1	52.2039	1.4914	0.24753
U*C	66.9978	1	66.9978	1.914	0.19395
VPULS*C	12.93	1	12.93	0.36938	0.55568
Error	385.0457	11	35.0042		
Total	996.0487	32			
Constrained (Type III) sums of squares.					

Figure 53: Die Sinker Finishing Experiment R_a Standard Deviation ANOVA

3.15 Confirmation of Experiment Results

Confirmation runs similar to those conducted for the WEDM, and using the same replicate pattern and material setups were conducted for the die sinker following analysis of the characterization results.

3.151 Die Sinker Roughing Experiment

The cut speed confirmation run achieved a Cut speed of 6.3×10^{-3} inches/min with a S/N of -44.02 dB. This was a slight improvement over the best treatment conducted during the characterization (treatment #4, 6.15×10^{-3} inches/min, -44.3 dB).

The R_a confirmation run for the roughing experiments achieved a R_a of 53 μ inches with a S/N of -34.5 dB. This was a 2 dB improvement over the best treatment (treatment #26, 81.76 μ inches, -36.56 dB).

3.152 Die Sinker Finishing Experiment

The cut speed confirmation for the finishing settings for the die sinker (-49.29 dB, 3.44×10^{-3} inches/min) only equaled the speed achieved during the characterization (treatment #2). The only difference in the settings for these two treatments was pulsation speed, where the confirmation run used 9 inches/min and the treatment used 6 inches/min, a relatively small difference over the range of machining and retraction times, which in this case were the same for both treatments.

The R_a confirmation run for the finishing treatments achieved a R_a of 30.34 μ inches with a S/N of -29.64 dB. This was a 1.5 dB improvement over treatment #7, which had achieved a surface roughness of 36.08 μ inches with a S/N of -31.15 dB.

4.0 Processing Testing and Production Examples

4.1 Effect of Doping Type in Die Sinker Processing

Literature concerning EDM of silicon substrate discusses the use of different dopants (P-type versus N-type material). Discussion is limited largely to polarity of the electrode used during processing—negative when processing P-type material (as was done during the characterization experiments of Section 2.0) and positive when machining N-type material¹⁹. Kunieda et al found that when P-type material when attempted to be machined with a positive polarity electrode, experiences no sparking²⁰. This research also experienced that the rectifying contact set up is sufficient such that even at low resistivity ($\sim 10^{-2}$ ohm-cm), no sparking will occur. In fact, the Roboform 350 will break most workpieces in this situation, and could be damaged if proper care is not taken to prevent initiation of machining with incorrect voltage settings either during job setup or during the machining process, when inadvertent machine adjustment could result in a voltage polarity shift, as the machine will can change directly from (-)80 volts to (+)80 volts with the tap of a touch screen.

Following completion of the die sinker characterization and confirmation runs, a repeat of the finishing experiment speed confirmation run was conducted with N-type material of identical crystal orientation and 1.87×10^{-2} ohm-cm resistivity in order to observe the impact of dopant type on processing time. Machine setup and conduct of the experiment were identical to the characterization experiments conducted on the die sinker.

Where the speed confirmation run using P-type material had taken, on average, 8.22 minutes to complete the directed cuts using the settings of Table 33 with negative voltage settings, an identical run, using the N-type material discussed above, completed the same cuts in 5.92 minutes on average—72% of the time required for the P-type material. It is important to note that the electrode wear for the N-type test was significantly greater than that for the P-type (0.003” for N-type versus 0.0017” for P-type). To account for this, difference, average processing speed was also calculated. For

¹⁹ (Kunieda and Ojima 2000)

²⁰ (Kunieda and Ojima 2000)

the P-type confirmation run, average processing speed was 3.43×10^{-3} inches/min. The N-type dopant test achieved speed of 4.56×10^{-3} inches/min, a 33% improvement in processing speed.

Table 33: Dopant Test Input Parameter Settings

P	A	B	SV	R	U	VPULS	M	C	V	RF
1.5	3.2	12.8	55	0.1	0.2	9.0	4	5	± 120	25

4.2 Effect of Resistivity on Die Sinker Processing

Reynaerts²¹ states that a modern EDM should be able to process silicon substrate up to 50 ohm-cm resistivity without any of the enhancements to surface discussed in Kunieda's work²² provided that the spark generator can achieve no-load voltage of 200V or greater.

As the Roboform 350 has a maximum magnitude voltage of 200 volts, it was determined appropriate to evaluate the effect of resistivity on processing speed. Using the N-type material and data achieved from the polarity test, additional wafers of higher order resistivity that were procured for this test were also cut using the identical experimental set up as the characterization experiments. Resistivity of the test pieces and average processing times are contained in Table 34 and depicted with a second-order polynomial trend line in Figure 54. As can be seen, processing time increases significantly once resistivity increases above one ohm-cm. As such, unless specifically necessary for the application selected, highly doped, low resistivity material is suggested for use on both the WEDM and the die sinker machines.

Table 34: Resistivity Test Data

Resistivity (Ohm- cm)	Average Processing Time (Minutes)
0.01871	5.92
0.02584	6.16
0.6683	23.8
1.597	132

²¹ (Reynaerts, Heeren and Van Brussel 1997)

²² (Kunieda and Ojima 2000)

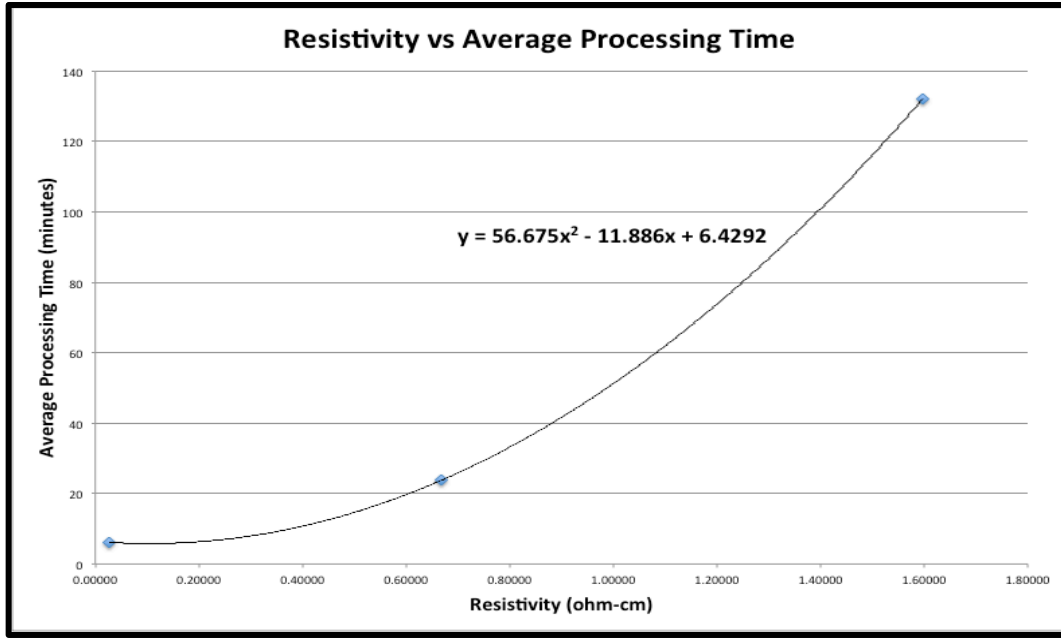


Figure 54: Effect of Silicon Resistivity on Processing Time

4.3 Cantilever Beam Width Using the Roboform 240 WEDM

One-centimeter long cantilever beams of decreasing beam width were cut in 500- μm thick silicon wafer (10^{-3} ohm-cm, $\langle 100 \rangle$ crystal orientation, P-type (B) doping) to determine minimum accurate feature size achievable for this type of feature on the Roboform 240 WEDM. Settings used for the smallest beams successfully cut are included in Table 35.

Table 35: Cantilever Beam Settings

Mode	Voltage	Current	On time	Off Time	Injection	Wire Speed	Servo
M7	-80 Volts	4 Amps	0.3 μsec	3.75 μsec	Off	8	0.4

Roughing settings were used (M1) initially and were used to successfully cut beam widths down to 0.0323" (791 μm). A minimum beam width of 0.0071" (174 μm) with a cut kerf of 0.0103" (252 μm) was achieved using the finishing settings above (Figure 55, Figure 56). A loss of some feature accuracy (approximately 50 μm) was incurred at this width due to some minor flexing of the beam during processing. The

subsequent loss of consistent beam width from the second cut is not apparent to the naked eye, but can be seen under sufficient magnification. Slightly smaller beam dimensions may be possible by either shortening beam length or reducing overall spark energy (and subsequent servo processing speed) or a combination of these adjustments. It is expected that flexure beams of similar length would exhibit less loss of feature accuracy/straightness due to increased mechanical stiffness and that a finer minimum structural width would also be achieved.

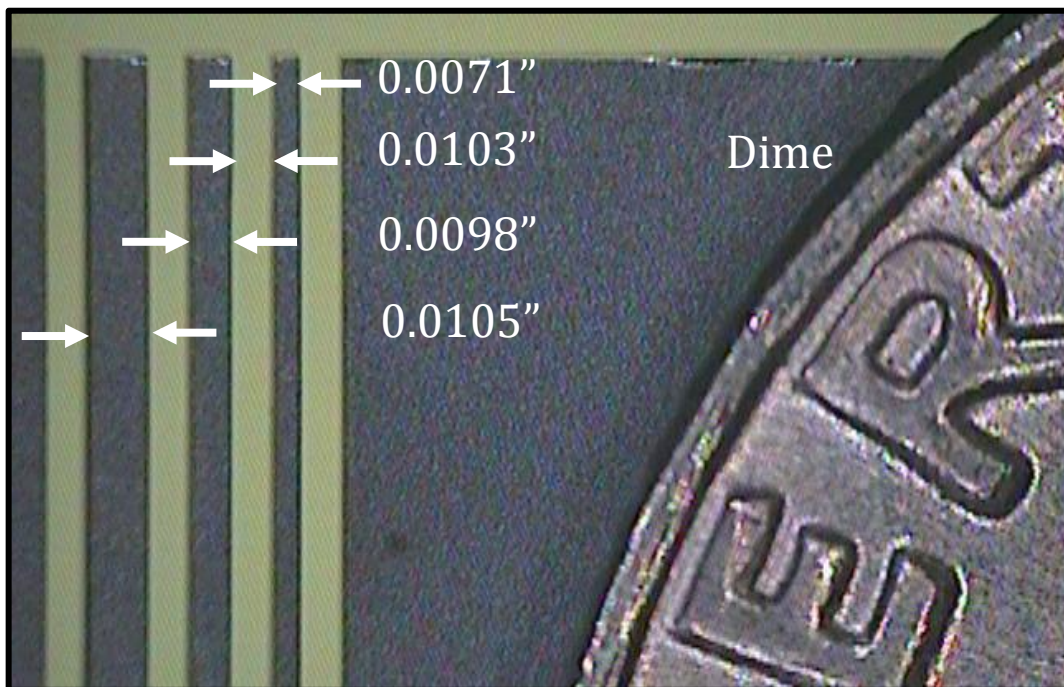


Figure 55: Cantilever beams in Silicon

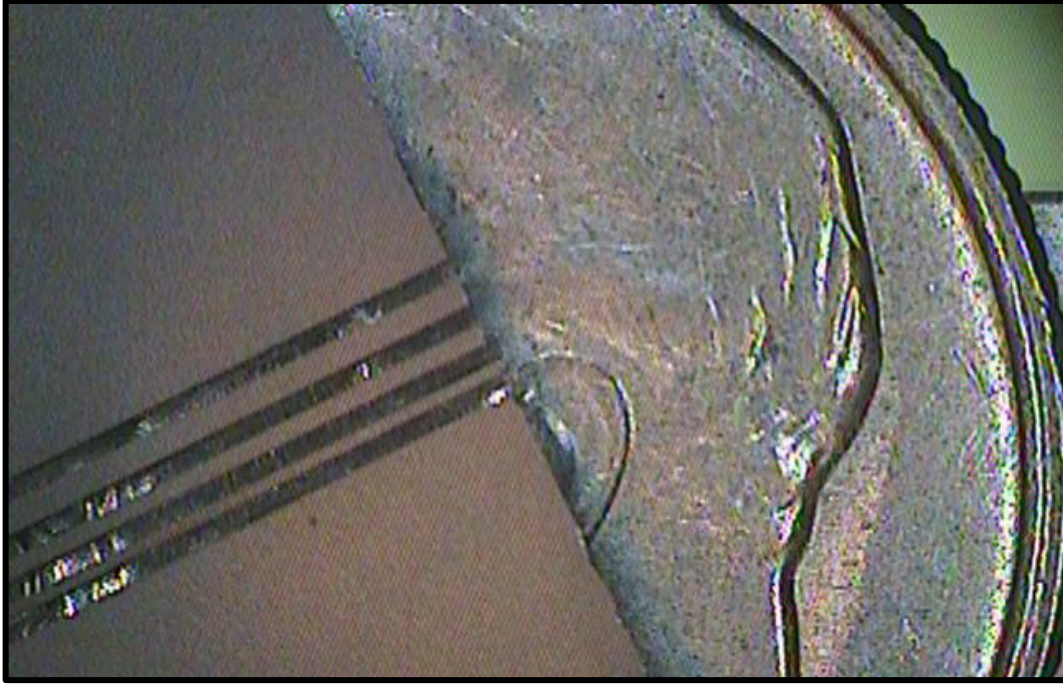


Figure 56: Cantilever Beams, reduced magnification

4.4 Hemisphere Negatives using Die Sinker EDM

Hemispherical negatives were cut into various samples of silicon substrate. In the first attempt, a 0.015-inch radius hemisphere was cut into the same batch of 500- μm silicon wafers as used in the characterization experiments previously discussed. Three individual electrodes with increasingly larger diameters (0.022", 0.025", and 0.0299") were fabricated using copper stock on a high-accuracy lathe. The electrodes were directed to cut to depths of 0.01", 0.012" and 0.015" respectively. The electrodes were used for roughing, finishing and polishing passes respectively. The resulting hemispherical cut had an average radius of 0.0157" based on a six-point best-fit measurement at the top of the cut (flat surface). Two of the electrodes (after use) and the resulting hemisphere (focused on the bottom (top right) and top) are shown in Figure 57. Settings used and processing times for this hemisphere are given in Table 36. Due to size of the hemisphere, surface roughness was not measurable on available equipment.

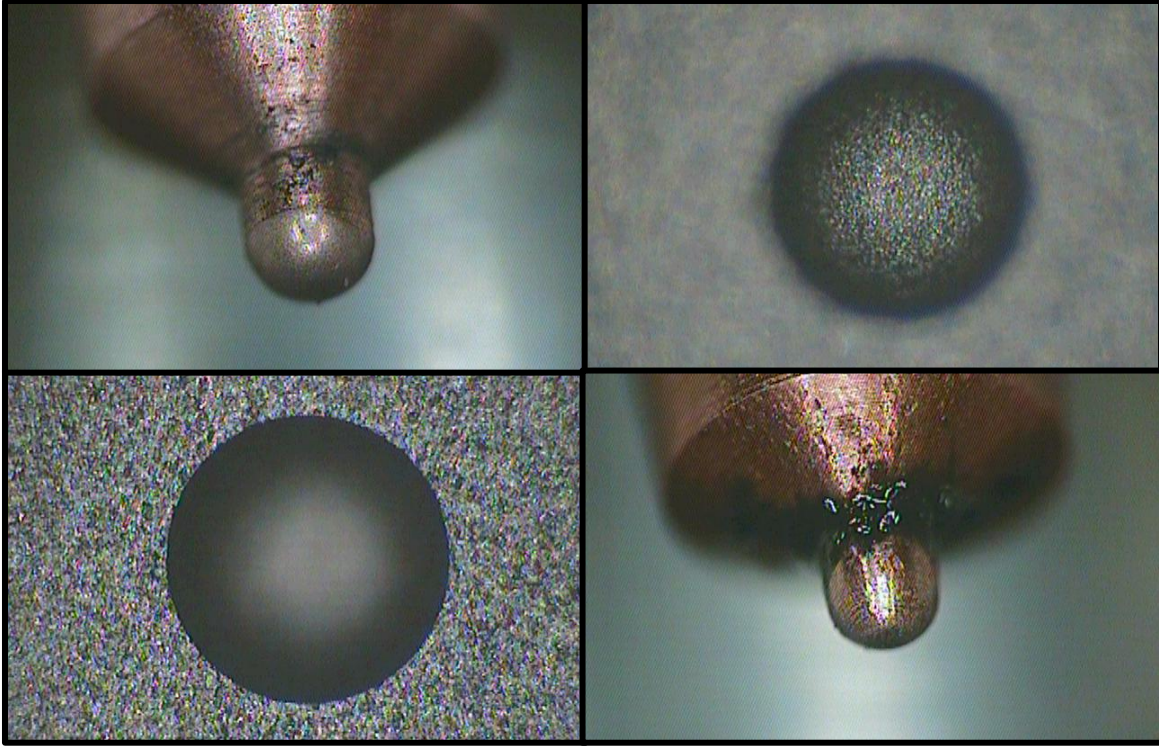


Figure 57: 0.015" Radius Hemispherical Cut and Electrodes

Table 36: 0.015" Radius Hemisphere Settings

Electrode	P	A	B	SV	R	U	VPULS	M	C	V	RF	Time
1	1.0	3.2	25	55	0.1	0.2	9.0	4	5	-120	25	0:45
2	0.5	1.6	25	55	0.2	0.4	9.0	4	3	-80	25	1:19
3	0.5	1.6	25	55	0.4	1.6	9.0	6	3	-80	25	6:38

Additional hemispheres of 3-mm diameter were cut into 3000- μm thick silicon wafers using a similar technique with three processing electrodes. For these larger hemispheres, the third electrode was manufactured from a copper-tungsten alloy to minimize wear to the electrode and then polished with diamond compound to allow a better resulting surface finish to the work piece than that achieved in the 1.5 mm trial. Initial stock silicon used for these 3-mm diameter hemispheres (hemispheres #1 through 4) was limited to higher resistivity values of between 1 and 10 ohm-cm based on availability and resulted in much slower processing times on the order of five hours per replicate. Additionally, due to the higher resistivity, higher voltages were used for the first four replicates to achieve reasonable processing speeds.

Lower resistivity material was also processed (0.016 ohm-cm, <557> crystal orientation). Reduced spark energies were utilized to minimize depth of pitting during the roughing process to ensure best resulting surface roughness following the finishing and polishing passes. Several adjustments were made during the processing, as well as a comparison of processing times for various settings. Surface roughness of 10.5 μ inches was achieved with a processing time of approximately 180 minutes, the bulk of which (2.75 hours) was for the polishing pass. Features with slightly reduced surface roughness of 25-40 μ inches were achieved in just over an hour. It was noted that this crystal orientation exhibited a greater propensity for chipping, as several hemispheres had surface edge chips evident immediately after processing and before handling (See Figure 60). Settings utilized and resulting processing data is enclosed in Appendix F – Hemispherical Geometry Data. Scanning electron microscope and traditional microscopic pictures of these features are included below.

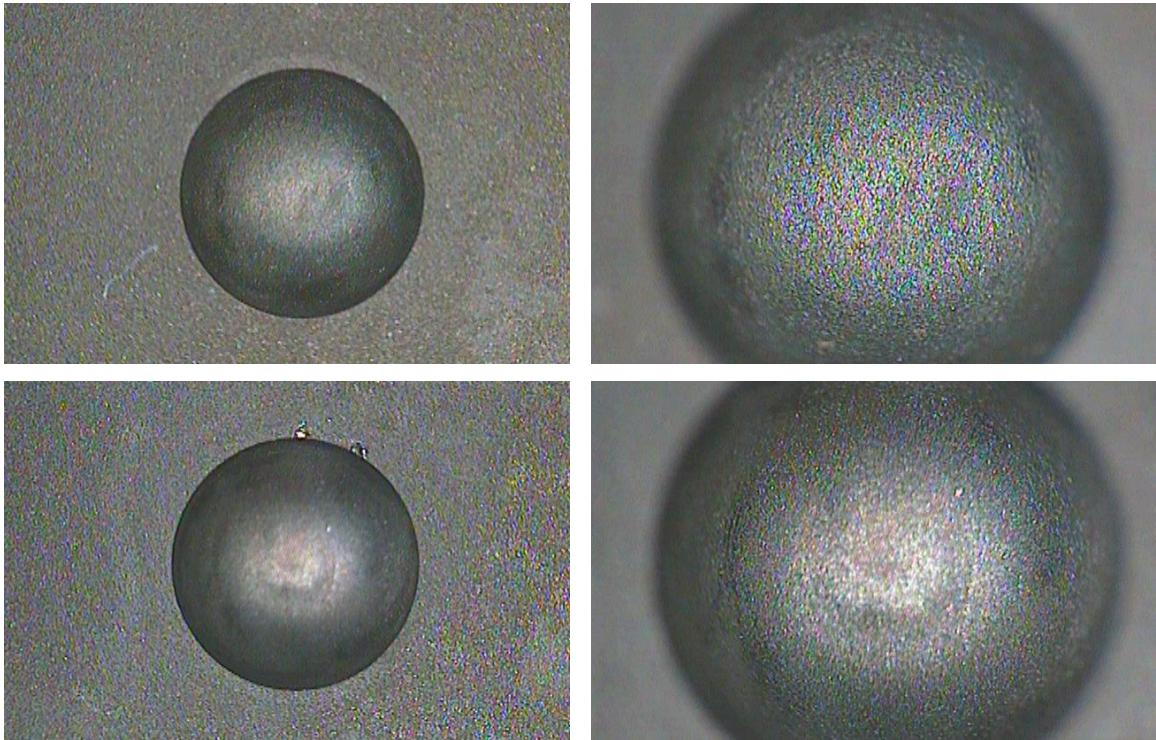


Figure 58: Hemisphere #8, $R_a = 21.4 \mu$ inches (top), and #9, $R_a = 13.6 \mu$ inches (bottom)

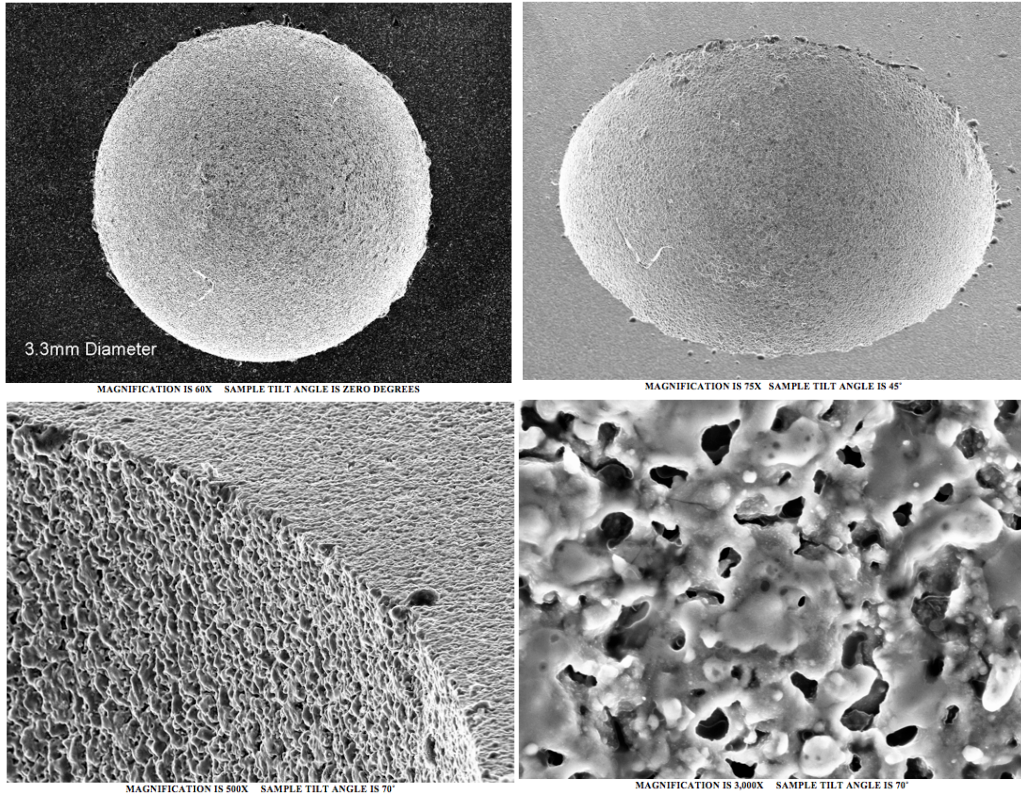


Figure 59: SEM photos of Hemisphere #4, no R_a taken, but estimated at 90-120 μ inches

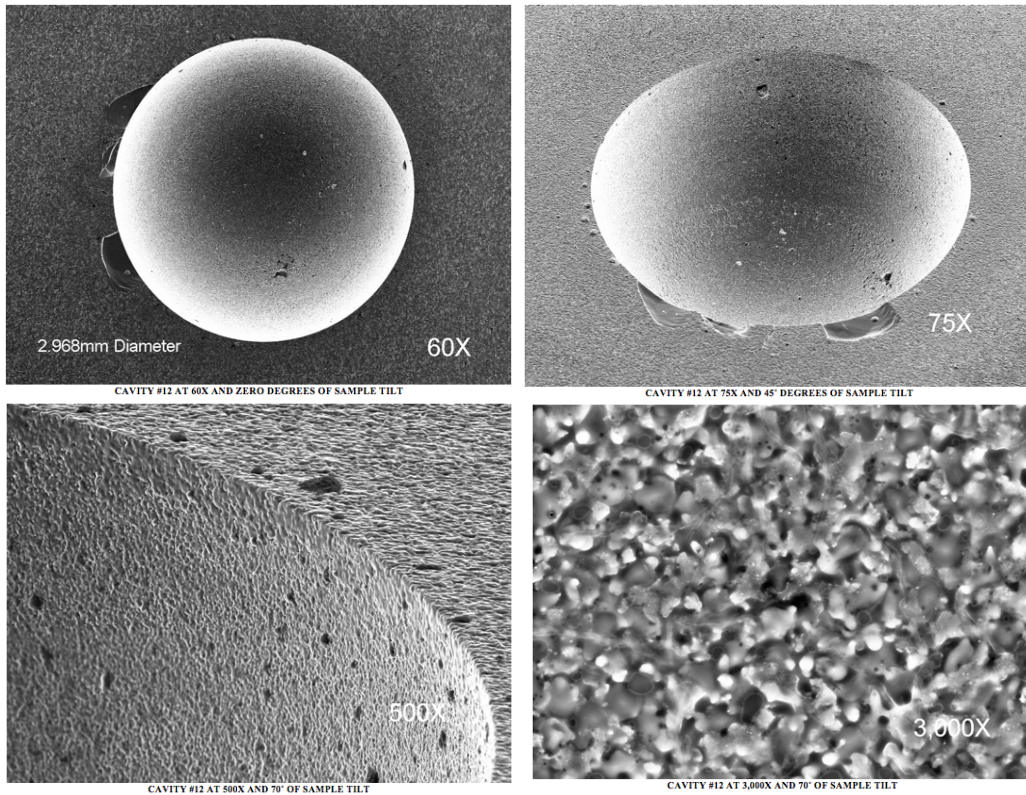
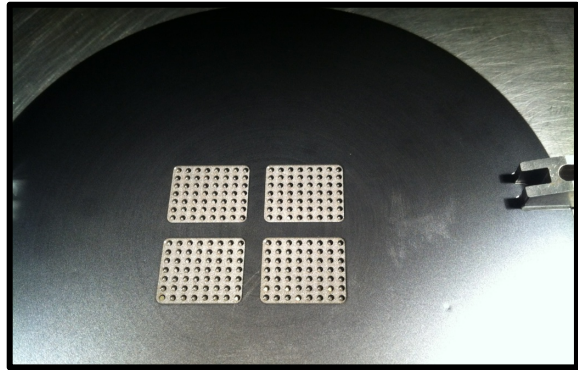
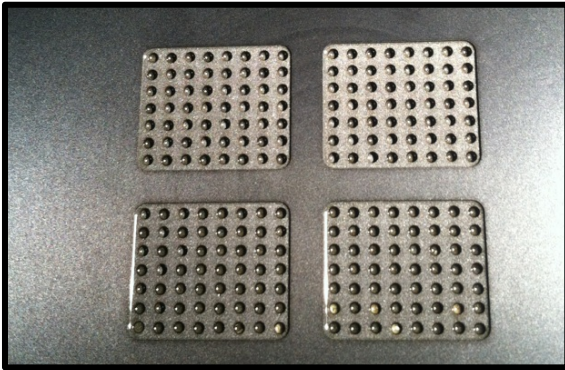


Figure 60: SEM of Hemisphere #12, avg R_a 10.5 μ inches. Note the chipping around feature edge.

4.5 A Complex Processing Example

During the course of the thesis work, as it became evident that processing of silicon substrate was possible, demand for customer processing began to come into the shop. An example of the types of more complex geometries cut, with double sided depth cuts and through holes, using the knowledge developed from the preceding characterizations is shown in the following photos.



(THIS PAGE INTENTIONALLY LEFT BLANK)

5.0 Machinist's Guidance and Lessons Learned

The purpose of this section is to provide a machinist's ready-reference handbook of lessons learned for the EDM of silicon on the Roboform 240 and Roboform 350.

5.1 General guidelines

- Resist the urge to “tweak” settings too much. Make small adjustments based on knowledge, and observe system response.
- For spark mode, if settings data is known, use the choice that makes the best sense based on desires (electrode wear vs. processing time)
- Use capacitive settings where possible, they tend to be relatively faster for silicon.
- Increases in spark energy result in increased MRR => I, V, and A higher (or V and C for relaxation circuits)
 - For increased material wear, supplemental flushing becomes more important as MRR increases. There's only so much material you can put into the dielectric at a time.
 - Increases in spark energy also tend to increase surface roughness and potential for material damage.
- Keep interactions in mind when making adjustments. See Section 3.14 Analysis of Die Sinker EDM Results for details.
- Increases in off time will slow processing, but will generally reduce the risk to the process (breakage and other damage).
 - For the die sinker, increases in B result in fewer observed abnormal discharges and contamination.
- Servo increases have a similar effect as increasing off time. They also tend to result in improvements in surface finishing.
- Increased resistivity requires increases in the magnitude of voltage.
 - Use $\pm 200\text{V}$ for any resistivity over $1.0\ \Omega\text{-cm}$ for rough cuts or if final surface roughness is not of concern.

5.2 WEDM specific information

- Start with slower control speeds than estimated as possible, and adjust up until observable spark is “steady” if there is any doubt or concern about wire breakage or the ability to process a work piece.
- Observing the spark pattern at the start of processing is valuable. High resistivity pieces frequently spark initially, then short and stop processing due to wire procession being too fast.
- Thicker material will have lower MRR. Maximum possible control speed will be reduced in a direct fashion.
- Do not use automatic wire breaks in pieces where feature accuracy is important as the tension in the wire will be released and the subsequent movement of the wire will likely cause damage to the work piece.

5.3 RAM EDM specific pointers

Capacitive settings:

- Lower C numbers correspond to lower removal rates and better surface finish. The effects of C numbers over 5 are largely untested in this paper, and may be worth evaluating.
- Ensure you are looking closely at the current setting (P) and on time (A) that results from a capacitive selection in M4 or M6. Frequently there is more than one available for a given capacitance.
 - In addition, if a specific P/A/C setting is desired, but not available in the desired M code, the M code can be changed from 4 to 6 once the technical table is selected.

5.4 Fixturing and Handling

- Based on silicon's brittle nature, care should be taken when cleaning processed material, as the slightest abrasion may result in chipping of machined surfaces
- Ensure fixtures are sufficiently separated from processing locations to ensure maximum possible flushing.

(THIS PAGE INTENTIONALLY LEFT BLANK)

6.0 Conclusions and Future Work

6.1 General Conclusions

The foregoing chapters detailed the characterization of EDM for both the Roboform 240 WEDM and the Roboform 350 Die Sinker EDM and some of their potential applications. Results indicate that this processing technology can be readily employed in the area of rapid prototyping of silicon-based MEMs.

6.2 Areas for Future Study

While conducting this thesis, several observations and outcomes presented themselves as appropriate areas of further study. These areas of potential study have been categorized either by machine type or general in nature.

6.2.1 WEDM

- The results of the characterization of WEDM R_a for both roughing and finishing settings should be re-examined. Based on analysis of the physics of the process, it seems likely that for the roughing experiment that there was some issue either with measurement or an unexpected interaction. For the finishing experiment, lower spark energy parameters are likely to be more appropriate for the desired lower R_a .

6.2.2 Die Sinker EDM

- With the presence of excessive “side-sparking” on the higher voltage of the roughing experiment causing a loss of feature accuracy, it would be appropriate to assess the voltage or spark energy where this phenomenon takes place. Based on the observed changes in spark quality with workpiece resistivity, this evaluation should take workpiece resistivity into account.

- During processing of the die sinker replicates, it was observed that the exit path for the electrode had a variable tendency to result in chipping along the circumference of the feature. Brief examination of the physics of the process seems to indicate that hydraulic forces are the likely cause of the chipping, as the brittle nature of the workpiece becomes more of an issue as it gets thinner, and so any amount of hydraulic force will likely cause chipping unless relieved in some manner. Determining a “best” processing method to eliminate or minimize the occurrence of this chipping would be valuable. It was also evident during hemisphere processing that the crystal orientation has an impact on chipping and merits further study.
- The replicates for the die sinker characterization had a tendency towards much higher variability (measured as a ratio of standard deviation of either MRR or R_a to the mean MRR or R_a) than the WEDM. Understanding the reasons for this high variability will better allow the machine operator to predict cost to produce specific workpieces.
- The spark energy to off time interaction in the die sinker EDM indicated the possibility of a more complex response surface than expected, and may merit further study.

6.2.3 General Areas

- Application of these results to μ EDM machines appears to be possible. Closer evaluation and study to allow for certainty in this appraisal would be appropriate and would allow machine operators to create silicon MEMS of significantly smaller minimum dimension sizes.
- Optimization of this process for either speed or surface roughness are potential areas that could make use of this theses data to simplify that process. Utility for the machine operator for any particular type of workpiece other than something mass-produced is debatable however.

- The impact of electrode type was not evaluated in this study and appears to be of significant potential as it has been shown for specific metals that electrodes of different types have different impacts on processing.
- Study of contact improvement²³ for high resistivity workpieces using various plating methods may also be of value for this type of application.

²³ (Kunieda and Ojima 2000)

(THIS PAGE INTENTIONALLY LEFT BLANK)

Bibliography

Depraz, J. M. *EDM Wire Cutting Reference Manual*. Geneva: Charmilles.

DiBitonto, Daryl D, Philip T. Eubank, Mukund R. Patel, and Maria A. Barrufet. "Theoretical models of the electrical discharge machining process. I. A simple cathode erosion model." *Journal of Applied Physics*, 1989: 4095-4103.

Fraley, Stephanie, Mike Oom, Ben Terrien, and John Zalewski. *Design of experiments via taguchi methods: orthogonal arrays*. November 27, 2007. https://controls.engin.umich.edu/wiki/index.php/Design_of_experiments_via_taguchi_methods:_orthogonal_arrays (accessed July 23, 2011).

Guitrau, E. P. *The EDM Handbook*. Cincinnati, OH: Hanser Gardner Publications, 1997.

Heeren, Paul-Henri's, Dominiek Reynaerts, Hendrik Van Brussel, Cynthia Beuret, Olle Larsson, and Axel Bertholds. "Microstructuring of silicon by electro-discharge machining (EDM) - part II: applications." *Sensors and Actuators* (Elsevier), 1997: 379-386.

Kunieda, Masanori, and Satoyuki Ojima. "Improvement of EDM efficiency of silicon single crystal through ohmic contact." *Journal of the International Societies for Precision Engineering and Nanotechnology*, 2000: 185-190.

Lin, Yan-Cherng, Chao-Hsu Cheng, Bo-Lin Su, and Lih-Ren Hwang. "Machining Characteristics and Optimization of Machining Parameters of SKH 57 High-Speed Steel Using Electrical Discharge Machining Based on Taguchi Method ." *Materials and Manufacturing Processes*, 2006: 922-929.

Reynaerts, Dominiek, Paul-Henri's Heeren, and Hendrik Van Brussel. "Microstructuring of silicon by electro-discharge machining (EDM) - part 1: Theory." *Sensors and Actuators*, 1997: 212-218.

Shabgard, M R, M R Farahmand, and A Ivanov. "Mathematical modelling and comparative study of the machining characteristics in ultrasonic-assisted electrical discharge machining of cemented tungsten carbide (WC-10%Co)." *Journal of Engineering Manufacture*, 2009: 1115-1126.

Wu, C. F. Jeff, and Michael Hamada. *Experiments: Planning, Analysis, and Parameter Design Optimization*. New York, NY: John Wiley & Sons, INC, 2000.

(THIS PAGE INTENTIONALLY LEFT BLANK)

Appendix A – Literature Search Summation

Author	Title	Process	Material	Parameters of interest	Ranges	Notes
Heeren	Microstructuring of Si by EDM pt2	RAM	Si (n)	Dielectric	DI water	rotating electrode
				Electrode	W-Cu Wire	started with 150 um electrode and reduced diameter using sacrificial wire
				Resistivity	50, 4	
				Holes:		
				75 um	40 um electrode	not very good for data presentation, although method description is adequate
				660 um	620 um electrode	
Song	A Study of microcracks in sparked silicon surface	RAM	Si(p- B)	Electrode	W (0.15mm)	low spark energy (1.8 uJ) did not show cracks
			<100>	Dielectric	DI Water	good data on crack propagation dependence on crystal orientation
			<110>	RC relaxation ckt		post=processing etch discussed as potential technique to remove recast layer/cracks
			650 um wafer	NL Volt	60, 80, 100, 160 V	
				Capacitance	1000 pF	
				Spark Energy (result)	1.8, 3.2, 5, 16 uJ	
Ming-Huo	Study of EDM of BaTiO3	RAM	BaTiO3	Cu Electrode	Positive polarity	Taguchi method & genetic algorithm to model surface roughness
				Conductivity	1.00E-02	
				Electrode rpm	75-200 rpm	
				Pulse on time	75-1200usec	
				Discharge voltage	30-50V	

Puertas	Modeling of surface roughness in the EDM reaction bonded silicon carbide	RAM	SiSiC	pulse time	30/70 usec	DOE & ANOVA analysis
				duty cycle	0.4/0.6	CU electrodes
				NL Voltage	-120/-200 Volts	Advance/return speed (1mm/s), 2m/s)
				flush pressure	20/40 KPA	5 factors most widespread
				intensity	2/6 amps	evaluation length of 6.4mm
						2^(5-1) design
Uno	High efficiency boring of monocrystalline silicon ingot by EDM	RAM	Si (P-type)	conductivity	0.01 ohm-cm	1mm Cu pipe electrode, rotating at 90 rpm
			<100>	thickness	5mm	copper plate (1mm) used to enhance contact
				Polarity	positive	Found relationships for MRR vs pulse on time at different currents
				Intensity	2, 6, 15A	electrode wear vs pulse on at different currents
				pulse on	4,8,12,20,28 usec	Ra vs pulse on at different current
				Duty factor	50%	method improvement by plating(1mm Cu) to prevent tip cracking
				Capacitance	380 pF	bored 200mm ingot, roughly linear MRR
				dielectric	"non-flammable"	
Kunieda	Improvement of EDM efficiency of silicon single crystal through ohmic contact	RAM	Si (P-Type)	thickness	0.75 mm	CVD of Al (P-Type) or Au-Sb(N-type)
			Si (N-Type)	resistivity	354(p) 8.3(n) ohm-cm	
				NL: Volt	280	
				Intensity	3.5 Amps	
				Pulse on	30 us	
				Pulse interval	200 us	
				electrode	Cu	
				Dielectric	EDM oil	
				polarity	negative (p, Al)	
					positive (n, Sb-Au)	

Weng	Fabrication of micro components to Si wafer using EDM process	RAM	Si (n- Sb)	electrode	W-C, Cu, Graphite-Cu	W-C (30 um) - through hole in 13sec, W-C (50um) - through 18sec
			<110>	wafer	4", 0.5mm thick	
			0.005-0.002 ohm-c,	Voltage	45V	
			.5mm	Intensity	0.3A	
				pulse on	15 usec	
				pulse off	600 usec	
				electrode	Cu	
				same wafer		
				Voltage	45V	
				Intensity	0.25A	
				same on/off times		
				electrode	Cu	slot cut 50um
				NL	45 V	
				Intensity	.3 A	
				on time	50 us	
				off time	1200 us	
Reynaerts	Microstructuring of Si by EDM - theory	RAM				process discussion and examples of work done thru 1997
		WEDM				Discusses contacts in RAM and measures to take:
						1) polarity (to forward bias surface contact)
						2) plating with a conductor
						Has good material properties of Silicon vs Steel (0.8 % C)
						n-type found to be slightly easier to machine (wrt speed)

Davila	Microstructure and microchemistry of silicon particles formed during EDM	RAM	Si	thickness	5mm	sandwiched between Ag plates for contact
				electrodes	silver (1mm OD), hollow	
				intensity	2-15 A	
				pulse on	4 - 29 us	
Dhar	Mathematical modeling of EDM of ...	RAM	composites	current		effect on MRR, TWR, Over cut
				pulse on		3 factor, 3 level full factorial design with ANOVA
				air gap voltage		
Song	Investigation of MEDM for SI microstructure fabrication	MEDM	Si (p)	resistivity	0.02 ohm-cm	cut 250x50x5000 um slots
		RAM		electrode	tungsten wire (150 um)	
				rotating speed	1500-2500rpm	
				Applied Voltage	60-250V	60, 80, 100, 120, 150, 160, 180, 250 V
				polarity	negative	
				Intensity	0.8 A	
				pulse on	1 us	
				pulse off	18-32 us	
				Capacitance	lowest 2 settings available	
						Microbeam structure cutting
						- discusses two different machining paths (cut and mill and multipass)
				Voltage	100V	cut beams from 650 um thick wafer
				small capacitor	energy 5 uJ	25, 30, 35 and 55 um width. Length - 4mm
				pulse on	0.1 us	25 um beam unsuccessful, 30 and 35 um beam had 3-4 um cracks
						reduced voltage to 60 V (1.8uJ) - produced all beams down to 25um
						achieved Ra~ 3um
				off time	18-32 us	helps process stability and cutting speed

						Most important parameters are voltage, capacitance and off time
Izquierdo	Inverse Determination of discharge properties...	RAM	Steel			only one interesting point about off time being sufficient to allow complete collapse
						of the plasma channel to ensure sparking is distributed. This implies that off time may be related to
Zhang Yong	Research of micro-EDM and its applications	MEDM	Si (N-type)	Ag-W Electrode		multiple processes examined in this paper
				kerosene		
				Open Voltage	100V, 150V, 80V	
				(+) polarity		
				rotating spindle	3000 rpm	
				Capacitance	1000 pF	
Dhanink	Modeling f single resistance capacitance...	MEDM				modeling of process
Chung	Surface finishing of MEDM holes in DI water	MEDM	304 SS	voltage	80 V	
				tool rotation	1200 rom	
Song	Experimental Study of MEDM machining performance on Silicon Wafer	MEDM	Si (p - Boron)	electrode	tungsten wire (150um)	tests revealed that E<5uJ removal dominated by melt/evap (no spalling)
			<100>	rotation speed	1500-2500 rpm	evaluated MRR for different cutting depths at 3 NL voltages
				conductivity	0.02 ohm-cm	showed MRR for Si was higher than for SS
				capacitance	1000pF (fixed)	compared Ra for the two materials - Ra increases as V increases
				NL Voltage	60-250 V (steps)	no cracks < 1.8uJ
				spark energy (result)	1.8-32 uJ	

Tosello	High AR micro tooling	MEDM	Si	Conductivity		Had some draft angles in smaller channels(flushing)
				8" wafer 1mm thick		
				Ti/Au coating via PVD		
		WEDM	Si	W-C electrode	15, 45, 68 um	channels of 20,50, 75 and 90 um (nominal)
Manna	Taguchi and gauss elimination method	WEDM	SiC (Al reinforced)	Brass electrode	250um	L18 experiment (2 ¹ x3 ⁷ experiment)
				NL voltage	100, 75 V	Good method for calculating MRR
				pulse on	0.7, 0.6, 0.5 us	
				pulse off	14, 15, 16 us	
				intensity	120, 100, 80 A	
				wire feed rate	5,6,7 m/min	
				wire tension	1140, 1020, 900 gms	
				gap voltage	20, 25, 30 V	
Luo	Investigation of Si wafering by WEDM	WEDM	Si (N-type)	pulse on time	1-256 usec	
				pulse interval	2-512 usec	
				peak current	0.1-20 A	
				NL Voltage	10-180 V	
				disch current rise time	0-40 usec	
Stauffert		WEDM	Si (n)	spring element	0.3-0.5 mm thickness	
	Behavior of a silicon spring fabricated by WEDM		<100>	RC generator		
				Capacitance	500-10000 pF	
Uno	WEDM Slicing of monocrystalline Si ingot	WEDM	Si (p)	resistivity	0.01 ohm-cm	MRR vs on time, Ra vs on time (both for all intensities)
			40 mm thick	electrode	Molybdenum (180um)	cut a 6 inch ingot after - took 140 minutes

				polarity	negative	
				dielectric	DI water	
				gap voltage	100V	
				Intensity	3, 12, 22 A	
				on time	5, 10, 20, 40, 75 us	
				DF	15%	
				feed rate	10 m/s	
				tension	0.6 kgf	
Reynaerts	Machining of 3D microstructures in Si by EDM	???	Si (polycrystalline)	Cu electrode	dice	24 different test structures
			350 um thick wafer	Tungsten wire electrode	accelerator (50um)	holes, gears, dice, resonant beam accelerator
						double beam structure (50um beams with 61.5 um separation)
Dhanik	Evolution of EDM process....					modeling of EDM process physics
DiBitonto	Theoretical Models of EDM process p1					cathode and anode erosion models

Appendix B – WEDM Roughing Experiment Data

Treatment	Run	Wafer #	Replicate	Cut length (in)	kerf size (in)	time to cut (sec)	MRR (mm ³ /min)	Mean MRR (mm ³ /min)	Mean Squared	MRR Std Dev	Sample Variance	$\eta = \ln(\mu^2/s^2)$	Ra (uin)	Mean Ra	Mean squared	Ra Std Dev	$\eta = \ln(\mu^2/s^2)$
1	5	6-3	1	0.4548	0.0112	315	0.00329	0.00337	1.136E-05	0.00007	4.432E-09	7.85	93.446	93.21	8689.1	1.340	8.78
			2	0.4555	0.0117	314	0.00345						94.343				
			3	0.4557	0.0114	313	0.00337						93.788				
			4	0.4572	0.0115	317	0.00337						91.284				
2	8	7-2	1	0.4599	0.0119	31	0.03588	0.03414	1.165E-03	0.00123	1.523E-06	6.64	89.408	88.12	7765.0	1.701	8.43
			2	0.4594	0.0118	33	0.03338						88.856				
			3	0.4579	0.0114	32	0.03315						85.619				
			4	0.4568	0.0114	31	0.03414						88.595				
3	9	7-3	1	0.4553	0.0122	32	0.03528	0.03534	1.249E-03	0.00081	6.637E-07	7.54	142.634	148.7	22134.6	8.133	7.91
			2	0.456	0.0121	32	0.03504						154.295				
			3	0.456	0.0122	31	0.03647						157.154				
			4	0.4572	0.0119	32	0.03455						141.025				
4	7	7-1	1	0.4549	0.0122	315	0.00358	0.00355	1.258E-05	0.00003	1.036E-09	9.40	129.937	134.4	18067.4	6.673	7.90
			2	0.4542	0.012	315	0.00352						142.169				
			3	0.4535	N/A	315	N/A						127.876				
			4	0.4539	0.0121	315	0.00354						137.678				
5	10	7-4	1	0.4189	0.0116	315	0.00313	0.00328	1.074E-05	0.00010	9.216E-09	7.06	96.789	92.16	8494.2	6.121	7.24
			2	0.4403	0.0114	307	0.00332						89.618				
			3	0.4383	0.0113	304	0.00331						97.541				
			4	0.4371	0.0114	303	0.00334						84.707				
6	3	6-1	1	0.4478	0.012	310	0.00352	0.00350	1.226E-05	0.00005	2.700E-09	8.42	138.681	136.7	18706.5	5.660	8.10
			2	0.4593	0.0119	312	0.00356						132.354				
			3	0.4515	0.0118	311	0.00348						132.118				
			4	0.4557	0.0117	315	0.00344						143.934				
7	6	6-4	1	0.4539	0.0122	30	0.03751	0.03560	1.268E-03	0.00144	2.081E-06	6.41	106.12	112.6	12694.0	5.249	7.79
			2	0.4528	0.0119	31	0.03532						111.086				
			3	0.4521	0.012	31	0.03557						115.276				
			4	0.4501	0.0119	32	0.03402						118.189				
8	12	9-2	1	0.4544	0.0125	316	0.00365	0.00353	1.247E-05	0.00011	1.187E-08	6.96	107.499	105.6	11157.0	7.875	7.26
			2	0.4535	0.0118	316	0.00344						104.666				
			3	0.4537	0.012	316	0.00350						114.689				
			4	0.4543	N/A	316	N/A						95.653				
9	11	9-1	1	0.4579	0.012	32	0.03490	0.03484	1.213E-03	0.00011	1.111E-08	11.60	152.943	159.1	25342.7	11.33	7.71
			2	0.4555	0.012	32	0.03471						146.671				
			3	0.4538	N/A	32	N/A						166.031				
			4	0.4511	0.0118	31	0.03490						171.131				

10	2	4-4	1	0.4661	0.0118	34	0.03287	0.03394	1.152E-03	0.00108	1.174E-06	6.89	113.074	104.9	11020.7	10.18	6.99
			2	0.4623	N/A	32	N/A						99.485				
			3	0.4598	0.012	32	0.03504						113.98				
			4	0.4578	0.0113	31	0.03391						93.379				
11	4	6-2	1	0.4591	0.0115	319	0.00336	0.00343	1.177E-05	0.00005	2.530E-09	8.44	103.04	106.7	11403.6	5.761	7.59
			2	0.4554	0.0119	316	0.00349						102.262				
			3	0.4515	0.0117	312	0.00344						106.998				
			4	0.4474	0.0117	310	0.00343						114.85				
12	1	4-3	1	0.4526	0.0117	31	0.03471	0.03373	1.138E-03	0.00070	4.872E-07	7.76	168.609	168.4	28379.9	14.39	7.59
			2	0.454	0.0115	32	0.03316						167.39				
			3	0.4563	0.0115	32	0.03333						151.317				
			4	0.4578	0.0116	32	0.03373						186.537				
N/A	Conf	56-3	1	0.4019	0.0116	11	0.08613	0.08485	7.200E-03	0.00990	9.794E-05	4.30		#DIV/	#DIV/0!	#DIV/	#DIV/
	MR		2	0.4024	0.0115	10	0.09404										
			3	0.4032	0.0118	13	0.07438										
			4	0.4035	N/A	11	N/A										
N/A	Conf	56-4	1	0.4045	0.0121	282	0.00353	0.00349	1.220E-05	0.00003	9.159E-10	9.50	109.84	104.1	10846.2	7.764	7.24
	Ra		2	0.4045	0.0119	282	0.00347						93.14				
			3	0.4043	0.012	283	0.00348						104.23				
			4	0.4038	0.012	282	0.00349						109.37				

Appendix C – WEDM Finishing Experiment Data

Run #	Treatment	Wafer #	Replicate	length of cut (in)	kerf size (in)	time to cut (sec)	MRR (mm ³ /min)	Mean MRR	Mean Squared	MRR Std Dev	Sample Variance	$\eta = \ln(\mu^2/s^2)$	Ra (uin)	Mean Ra	Ra Std Dev	$\eta = \ln(\mu^2/s^2)$
2	1	10-1	1	0.453	0.0105	942	0.00103	0.00104	1.077E-06	0.00001	6.443E-11	9.72	23.108	24.164	2.405	5.49
			2	0.4531	0.0107	943	0.00104						26.403			
			3	0.4422	0.0106	917	0.00104						25.865			
			4	0.4357	0.0106	902	0.00104						21.278			
1	2	9-3	1	0.4528	0.0109	235	0.00427	0.00415	1.721E-05	0.00012	1.482E-08	7.06	28.508	31.818	3.288	5.73
			2	0.4535	0.0107	236	0.00418						35.927			
			3	0.4544	0.0107	237	0.00417						32.881			
			4	0.4549	0.0102	237	0.00398						29.957			
7	3	11-2	1	0.2599	0.0107	136	0.00416	0.00421	1.776E-05	0.00007	4.559E-09	8.27	36.784	34.974	2.734	6.10
			2	0.4548	0.0108	237	0.00421						36.32			
			3	0.4552	0.0109	234	0.00431						35.883			
			4	0.4555	0.0107	237	0.00418						30.91			
5	4	10-4	1	0.4511	0.0116	937	0.00113	0.00113	1.283E-06	0.00001	6.333E-11	9.92	46.306	40.953	4.432	5.94
			2	0.4513	0.0115	939	0.00112						36.892			
			3	0.4522	0.0116	943	0.00113						37.761			
			4	0.453	0.0117	943	0.00114						42.851			
8	5	11-3	1	0.4525	0.0105	236	0.00409	0.00414	1.712E-05	0.00003	1.208E-09	9.56	33.813	32.359	3.918	5.59
			2	0.453	0.0106	235	0.00415						36.647			
			3	0.4529	0.0106	236	0.00413						31.617			
			4	0.4529	0.0107	236	0.00417						27.36			
6	6	11-1	1	0.4517	0.0105	941	0.00102	0.00106	1.131E-06	0.00003	9.291E-10	7.10	24.612	24.859	0.949	6.48
			2	0.4537	0.0109	945	0.00106						26.193			
			3	0.4552	0.0112	943	0.00110						24.684			
			4	0.457	0.0109	949	0.00107						23.948			
4	7	10-3	1	0.4552	0.0117	947	0.00114	0.00112	1.257E-06	0.00002	2.672E-10	8.46	36.112	36.721	0.785	7.45
			2	0.455	0.0115	947	0.00112						37.783			
			3	0.4542	0.0114	945	0.00111						36.142			
			4	0.4532	0.0113	942	0.00110						36.846			
3	8	10-2	1	0.4527	0.0109	237	0.00423	0.00420	1.761E-05	0.00004	1.884E-09	9.14	29.967	29.806	1.923	6.14
			2	0.4527	0.0108	236	0.00421						32.11			
			3	0.4529	0.0108	236	0.00421						29.738			
			4	0.4528	0.0106	236	0.00413						27.407			
Conf MRR	N/A	57-1	1	0.4052	0.0105	57	0.01517	0.01511	2.284E-04	0.00017	2.992E-08	8.94		#DIV/0	#DIV/	#DIV/0!
			2	0.4057	0.0105	58	0.01493									
			3	0.4055	0.0106	57	0.01532									
			4	0.4047	0.0106	58	0.01503									
Conf Ra	N/A	57-2	1			900	0.00000	0.00000	0.000E+0	0.00000	0.000E+0	#DIV/0!	43.77	38.100	3.935	5.91
			2			844	0.00000						37.62			
			3			845	0.00000						36.05			
			4			846	0.00000						34.96			

Appendix D – Die Sinker Roughing Experiment Data

Run	Replicat e	Shutdowns			Time	Electrode Wear inches	6-pt best fit Radius	Max Diameter of Cut inches	Overcut inches	Actual Depth inches	Speed in/min	Mean Speed	Speed Std Dev	Speed S/N	Ra	Mean Ra	Ra Std Dev	S/N MRR
		start	mid	end														
1	1	0	0	0	2:06:56	0.0016	0.0461	0.0922	0.0011	0.02836	2.23E-04	2.013E-04	1.966E-05	-74.00	80.98	81.83	1.18E+01	-38.32
	2	0	0	0	2:31:29	0.0018	0.0462	0.0924	0.0012	0.02816	1.86E-04				94.07			
	3	0	0	0	2:25:48	0.0016	0.0460	0.0920	0.0010	0.02836	1.95E-04				70.44			
2	1	0	0	0	0:05:08	0.0008	0.0462	0.0924	0.0012	0.02916	5.68E-03	4.055E-03	1.427E-03	-48.74	116.16	114.41	1.99E+00	-41.17
	2	0	0	0	0:09:42	0.0008	0.0477	0.0954	0.0027	0.02916	3.01E-03				114.84			
	3	0	0	0	0:08:23	0.0008	0.0477	0.0954	0.0027	0.02916	3.48E-03				112.24			
3	1	0	0	0	2:39:01	0.0018	0.0461	0.0922	0.0011	0.02816	1.77E-04	2.024E-04	2.451E-05	-74.00	118.2	80.54	3.54E+01	-38.64
	2	0	0	0	2:05:02	0.0017	0.0458	0.0916	0.0008	0.02826	2.26E-04				75.36			
	3	0	0	0	2:17:53	0.0018	0.0458	0.0916	0.0008	0.02816	2.04E-04				48.05			
4	1	0	0	0	0:04:58	0.0007	0.0458	0.0916	0.0008	0.02926	5.89E-03	6.151E-03	6.036E-04	-44.30	133.53	112.14	3.16E+01	-41.22
	2	0	0	0	0:05:10	0.0004	0.0461	0.0922	0.0011	0.02956	5.72E-03				127.09			
	3	0	0	0	0:04:21	0.0002	N/A	N/A	N/A	0.02976	6.84E-03				75.79			
5	1	0	0	0	1:19:31	0.0021	0.0456	0.0912	0.0006	0.02786	3.50E-04	3.343E-04	2.096E-05	-69.55	71.66	78.47	8.26E+00	-37.93
	2	0	0	0	1:29:23	0.0022	0.0460	0.0920	0.0010	0.02776	3.11E-04				76.09			
	3	0	0	0	1:22:22	0.0018	0.0456	0.0912	0.0006	0.02816	3.42E-04				87.65			
6	1	0	0	0	0:04:34	0.0004	0.0462	0.0962	0.0031	0.02956	6.47E-03	5.902E-03	8.712E-04	-44.79	129.27	120.61	8.52E+00	-41.64
	2	0	0	0	0:04:40	0.0004	0.0462	0.1026	0.0063	0.02956	6.33E-03				112.24			
	3	0	0	0	0:06:02	0.0004	0.0461	0.0963	0.0032	0.02956	4.90E-03				120.31			
7	1	0	0	0	2:48:43	0.0014	0.0460	0.0920	0.0010	0.02856	1.69E-04	1.755E-04	3.226E-05	-75.39	161.75	107.64	4.74E+01	-41.17
	2	0	0	0	3:14:30	0.0014	0.0460	0.0920	0.0010	0.02856	1.47E-04				87.67			
	3	0	0	1	2:15:43	0.0014	0.0461	0.0922	0.0011	0.02856	2.10E-04				73.51			
8	1	0	0	0	0:06:53	0.0006	0.0471	0.0991	0.0046	0.02936	4.27E-03	5.829E-03	1.449E-03	-45.30	241.16	158.31	7.29E+01	-44.57
	2	0	0	0	0:04:08	0.0005	0.0466	0.0995	0.0048	0.02946	7.13E-03				103.76			
	3	0	0	0	0:04:49	0.0006	0.0468	0.1010	0.0055	0.02936	6.10E-03				130.01			
9	1	4	2	0	3:08:24	0.0019	0.0462	0.0924	0.0012	0.02806	1.49E-04	1.516E-04	8.132E-06	-76.41	86.96	73.17	1.94E+01	-37.49
	2	4	1	0	2:55:11	0.0018	0.0462	0.0924	0.0012	0.02816	1.61E-04				81.56			
	3	3	0	1	3:14:00	0.0018	0.0462	0.0924	0.0012	0.02816	1.45E-04				50.99			
X	1	3	0	0	0:07:09	0.0008	0.0466	0.1025	0.0063	0.02916	4.08E-03	3.427E-03	5.640E-04	-49.51	133.23	160.39	4.34E+01	-44.31
	2	3	0	0	0:09:27	0.0008	0.0463	0.1011	0.0056	0.02916	3.09E-03				210.44			
	3	4	0	0	0:09:25	0.0006	0.0471	0.0991	0.0046	0.02936	3.12E-03				137.51			

11	1	0	0	0	3:21:08	0.0016	0.0462	0.0924	0.0012	0.02836	1.41E-04	1.382E-04	2.644E-06	-77.20	60.7	68.33	8.39E+00	-36.74
	2	0	0	0	3:30:21	0.0014	0.0461	0.0922	0.0011	0.02856	1.36E-04				77.32			
	3	0	0	0	3:27:25	0.0014	0.0462	0.0924	0.0012	0.02856	1.38E-04				66.96			
12	1	0	0	0	0:06:30	0.0004	0.0460	0.0968	0.0034	0.02956	4.55E-03	3.561E-03	1.394E-03	-50.85	74.57	93.38	2.27E+01	-39.57
	2	0	0	0	0:14:50	0.0008	0.0464	0.0928	0.0014	0.02916	1.97E-03				118.55			
	3	0	0	1	0:07:04	0.0005	0.0464	0.0928	0.0014	0.02946	4.17E-03				87.02			
13	1	0	0	0	2:09:33	0.0016	0.0462	0.0924	0.0012	0.02836	2.19E-04	1.767E-04	3.703E-05	-75.39	83.71	84.50	1.98E+01	-38.69
	2	0	3	0	3:08:14	0.0018	0.0461	0.0922	0.0011	0.02816	1.50E-04				104.66			
	3	0	0	0	2:55:26	0.0016	0.0459	0.0918	0.0009	0.02836	1.62E-04				65.12			
14	1	0	0	0	0:05:41	0.0007	0.0466	0.1002	0.0051	0.02926	5.15E-03	4.156E-03	8.601E-04	-47.95	110.8	118.21	3.94E+01	-41.76
	2	0	0	0	0:08:02	0.0008	0.0466	0.0932	0.0016	0.02916	3.63E-03				83.02			
	3	0	0	0	0:07:51	0.001	0.0469	0.0967	0.0034	0.02896	3.69E-03				160.82			
15	1	0	0	0	3:28:26	0.0017	0.0461	0.0922	0.0011	0.02826	1.36E-04	1.465E-04	2.854E-05	-76.98	97.27	100.71	1.60E+01	-40.13
	2	1	0	0	3:46:59	0.0016	0.0460	0.0920	0.0010	0.02836	1.25E-04				118.12			
	3	0	0	0	2:39:42	0.0014	0.0460	0.0920	0.0010	0.02856	1.79E-04				86.75			
16	1	0	0	0	0:09:30	0.0008	0.0482	0.0964	0.0032	0.02916	3.07E-03	4.959E-03	2.956E-03	-48.34	84.49	90.57	2.89E+01	-39.43
	2	0	0	0	0:03:32	0.0004	0.0469	0.0978	0.0039	0.02956	8.37E-03				122.06			
	3	0	0	0	0:08:30	0.0007	0.0480	0.0960	0.0030	0.02926	3.44E-03				65.17			
17	1	0	0	0	1:07:02	0.002	0.0459	0.0918	0.0009	0.02796	4.17E-04	4.781E-04	5.341E-05	-66.53	95.27	79.53	1.75E+01	-38.15
	2	1	0	0	0:56:16	0.0018	0.0459	0.0918	0.0009	0.02816	5.00E-04				60.65			
	3	0	0	0	0:54:42	0.0017	0.0458	0.0916	0.0008	0.02826	5.17E-04				82.67			
18	1	0	0	0	0:08:00	0.0009	0.0468	0.0975	0.0038	0.02906	3.63E-03	4.150E-03	4.545E-04	-47.75	68.12	76.12	7.51E+00	-37.66
	2	0	0	0	0:06:49	0.0004	0.0471	0.0975	0.0038	0.02956	4.34E-03				77.21			
	3	0	0	0	0:06:33	0.0006	0.0463	0.0987	0.0044	0.02936	4.48E-03				83.02			
19	1	0	0	0	0:39:48	0.0012	0.0452	0.0904	0.0002	0.02876	7.23E-04	7.269E-04	6.039E-05	-62.83	116.93	87.73	3.47E+01	-39.29
	2	0	0	0	0:36:26	0.0012	0.0451	0.0902	0.0001	0.02876	7.89E-04				96.91			
	3	0	0	0	0:43:00	0.0012	0.0454	0.0908	0.0004	0.02876	6.69E-04				49.36			
20	1	0	0	0	0:04:43	0.0006	0.0465	0.0930	0.0015	0.02936	6.22E-03	5.159E-03	1.599E-03	-46.84	51.02	93.13	3.65E+01	-39.81
	2	0	0	0	0:08:47	0.0008	0.0461	0.0922	0.0011	0.02916	3.32E-03				112.6			
	3	0	0	0	0:04:57	0.0006	0.0464	0.0977	0.0039	0.02936	5.93E-03				115.78			
21	1	0	0	0	0:48:37	0.002	0.0459	0.0918	0.0009	0.02796	5.75E-04	5.318E-04	5.239E-05	-65.57	47.89	103.01	5.48E+01	-41.01
	2	0	3	0	0:51:30	0.0018	0.0458	0.0916	0.0008	0.02816	5.47E-04				103.63			
	3	0	0	0	0:59:15	0.0019	0.0458	0.0916	0.0008	0.02806	4.74E-04				157.5			

22	1	0	0	0	0:05:15	0.0009	0.0464	0.0992	0.0046	0.02906	5.54E-03	4.976E-03	4.951E-04	-46.14	152.82	121.13	4.66E+01	-42.07
	2	0	0	0	0:06:17	0.0011	0.0468	0.1044	0.0072	0.02886	4.59E-03				67.64			
	3	0	0	0	0:06:07	0.0006	0.0466	0.0932	0.0016	0.02936	4.80E-03				142.93			
23	1	0	0	0	0:56:09	0.0018	0.0454	0.0908	0.0004	0.02816	5.02E-04	4.890E-04	1.163E-05	-66.22	77.31	86.88	2.57E+01	-39.03
	2	0	0	0	0:58:14	0.0016	0.0459	0.0918	0.0009	0.02836	4.87E-04				67.32			
	3	0	0	0	0:59:16	0.0016	0.0456	0.0912	0.0006	0.02836	4.79E-04				116.02			
24	1	0	0	0	0:10:08	0.0014	0.0469	0.0938	0.0019	0.02856	2.82E-03	4.920E-03	2.470E-03	-48.18	114.29	88.42	4.35E+01	-39.58
	2	0	0	0	0:03:49	0.0008	0.0464	0.0971	0.0036	0.02916	7.64E-03				38.21			
	3	0	0	0	0:06:44	0.001	0.0472	0.0989	0.0045	0.02896	4.30E-03				112.75			
25	1	0	0	0	0:47:44	0.002	0.0463	0.0926	0.0013	0.02796	5.86E-04	5.781E-04	1.022E-05	-64.76	102.39	79.43	2.22E+01	-38.22
	2	0	0	0	0:47:21	0.0024	0.0461	0.0922	0.0011	0.02756	5.82E-04				58			
	3	0	0	0	0:48:39	0.0024	0.0462	0.0924	0.0012	0.02756	5.66E-04				77.9			
26	1	0	0	0	0:08:26	0.0008	0.0470	0.1047	0.0074	0.02916	3.46E-03	2.752E-03	6.145E-04	-51.58	71.21	81.76	1.49E+01	-36.56
	2	0	0	0	0:11:40	0.0012	0.0468	0.0998	0.0049	0.02876	2.47E-03				N/A			
	3	0	0	0	0:12:22	0.0011	0.0470	0.0940	0.0020	0.02886	2.33E-03				92.31			
27	1	0	0	0	1:34:03	0.00496	0.0459	0.0918	0.0009	0.025	2.66E-04	3.315E-04	6.162E-05	-69.91	63.03	81.13	1.57E+01	-38.29
	2	0	0	0	1:07:00	0.00396	0.0460	0.0920	0.0010	0.026	3.88E-04				89.04			
	3	0	0	0	1:16:21	0.00396	0.0457	0.0914	0.0007	0.026	3.41E-04				91.31			
28	1	0	0	0	0:05:52	0.0008	0.0464	0.1017	0.0059	0.02916	4.97E-03	5.004E-03	1.703E-03	-47.09	49.01	65.80	2.18E+01	-36.67
	2	0	0	0	0:04:22	0.0006	0.0467	0.0969	0.0035	0.02936	6.72E-03				57.99			
	3	0	0	0	0:08:51	0.0006	0.0461	0.0922	0.0011	0.02936	3.32E-03				90.41			
29	1	0	0	0	0:44:10	0.0016	0.0462	0.0924	0.0012	0.02836	6.42E-04	5.862E-04	4.843E-05	-64.70	101.04	90.46	9.16E+00	-39.16
	2	0	0	0	0:50:27	0.0018	0.0459	0.0918	0.0009	0.02816	5.58E-04				85.27			
	3	0	0	0	0:50:05	0.002	0.0460	0.0920	0.0010	0.02796	5.58E-04				85.08			
30	1	0	0	0	0:08:27	0.0004	0.0465	0.0930	0.0015	0.02956	3.50E-03	2.869E-03	9.791E-04	-52.22	85.78	113.94	3.88E+01	-41.46
	2	0	0	0	0:08:43	0.0006	0.0462	0.0969	0.0035	0.02936	3.37E-03				158.2			
	3	0	0	0	0:16:38	0.001	0.0456	0.0912	0.0006	0.02896	1.74E-03				97.85			
31	1	0	0	0	3:30:59	0.002	0.0461	0.0922	0.0011	0.02796	1.33E-04	2.393E-04	9.488E-05	-74.30	60.58	70.10	8.38E+00	-36.96
	2	2	0	0	1:41:53	0.0023	0.0456	0.0912	0.0006	0.02766	2.71E-04				76.33			
	3	2	0	0	1:28:07	0.0023	0.0456	0.0912	0.0006	0.02766	3.14E-04				73.4			
32	1	0	0	0	0:05:47	0.0006	0.0466	0.1004	0.0052	0.02936	5.08E-03	3.785E-03	1.187E-03	-49.24	66.82	105.29	5.36E+01	-41.14
	2	0	0	0	0:08:05	0.0014	0.0469	0.0969	0.0035	0.02856	3.53E-03				82.52			
	3	0	0	0	0:10:42	0.0006	0.0470	0.0977	0.0039	0.02936	2.74E-03				166.53			

Conf	1	0	0	0	0:05:02	0.0005	0.0474	0.0948	0.0024	0.02946	5.85E-03	6.332E-03	4.743E-04	-44.02	N/A	#DIV/0	#DIV/0!	N/A
sp	2	0	0	0	0:04:35	0.0009	0.0478	0.0956	0.0028	0.02906	6.34E-03				N/A			
	3	0	0	0	0:04:19	0.0006	0.0476	0.0952	0.0026	0.02936	6.80E-03				N/A			
Conf	1	0	0	0	1:29:31	0.0018	0.0465	0.0930	0.0015	0.02816	3.15E-04	3.624E-04	4.220E-05	-68.94	47.95	53.02	4.89E+00	-34.51
Ra	2	0	0	0	1:14:41	0.0017	0.0467	0.0934	0.0017	0.02826	3.78E-04				53.41			
	3	0	0	0	1:11:40	0.0017	0.0466	0.0932	0.0016	0.02826	3.94E-04				57.71			

Appendix E – Die Sinker Finishing Experiment Data

Run	Replicate	Time hh:mm:ss	Electrode Wear inches	6-pt best fit Radius	Max Diameter of Cut inches	Overcut	Actual Depth inches	Speed in/min	Mean Speed	Speed Std Dev.	Speed S/N	Ra	Mean Ra	Ra Std Dev.	Ra S/N
1	1	0:54:15	0.0028	0.0456	0.0912	0.0012	0.02716	5.01E-04	4.875E-04	4.015E-05	-66.30	47.73	45.34	2.30	-33.14
	2	0:52:17	0.0028	0.0456	0.0912	0.0012	0.02716	5.19E-04				45.14			
	3	1:01:23	0.0028	0.0456	0.0912	0.0012	0.02716	4.42E-04				43.14			
2	1	0:08:16	0.0022	0.0458	0.0916	0.0016	0.02776	3.36E-03	3.446E-03	2.266E-04	-49.29	63.28	60.03	3.10	-35.58
	2	0:08:32	0.002	0.0456	0.0912	0.0012	0.02796	3.28E-03				59.71			
	3	0:07:33	0.002	0.0457	0.0914	0.0014	0.02796	3.70E-03				57.11			
3	1	0:13:20	0.0018	0.0458	0.0916	0.0016	0.02816	2.11E-03	2.173E-03	7.369E-05	-53.27	64.18	60.88	3.06	-35.70
	2	0:13:08	0.0017	0.0456	0.0912	0.0012	0.02826	2.15E-03				58.14			
	3	0:12:32	0.0017	0.0457	0.0914	0.0014	0.02826	2.25E-03				60.33			
4	1	0:31:09	0.0014	0.0458	0.0916	0.0016	0.02856	9.17E-04	9.024E-04	1.426E-05	-60.89	50.8	47.02	5.21	-33.48
	2	0:31:20	0.0014	0.0455	0.0910	0.0010	0.02856	9.02E-04				41.08			
	3	0:32:09	0.0014	0.0456	0.0912	0.0012	0.02856	8.88E-04				49.18			
5	1	1:11:51	0.0029	0.0459	0.0918	0.0018	0.02706	3.77E-04	3.847E-04	1.420E-05	-68.31	47.09	52.88	6.75	-34.51
	2	1:12:10	0.0028	0.0456	0.0912	0.0012	0.02716	3.76E-04				51.27			
	3	1:07:43	0.0028	0.0457	0.0914	0.0014	0.02716	4.01E-04				60.29			
6	1	0:43:28	0.0016	0.0455	0.0910	0.0010	0.02836	6.52E-04	6.976E-04	3.927E-05	-63.16	57.41	52.67	7.60	-34.49
	2	0:39:10	0.0016	0.0455	0.0910	0.0010	0.02836	7.24E-04				43.91			
	3	0:39:36	0.0016	0.0455	0.0910	0.0010	0.02836	7.16E-04				56.7			
7	1	1:44:44	0.0023	0.0457	0.0914	0.0014	0.02766	2.64E-04	2.557E-04	7.673E-06	-71.85	36.17	36.08	0.83	-31.15
	2	1:49:17	0.0022	0.0456	0.0912	0.0012	0.02776	2.54E-04				36.86			
	3	1:51:04	0.0023	0.0457	0.0914	0.0014	0.02766	2.49E-04				35.2			
8	1	0:16:39	0.0018	0.0459	0.0918	0.0018	0.02816	1.69E-03	1.686E-03	2.304E-05	-55.46	93.2	69.96	20.75	-37.14
	2	0:16:30	0.0018	0.0460	0.0920	0.0020	0.02816	1.71E-03				53.29			
	3	0:16:57	0.0018	0.0460	0.0920	0.0020	0.02816	1.66E-03				63.38			
9	1	0:14:36	0.002	0.0457	0.0914	0.0014	0.02796	1.92E-03	1.888E-03	3.214E-04	-54.75	81.78	65.75	14.18	-36.49
	2	0:18:00	0.002	0.0455	0.0910	0.0010	0.02796	1.55E-03				60.62			
	3	0:12:50	0.0018	0.0456	0.0912	0.0012	0.02816	2.19E-03				54.84			
10	1	0:36:32	0.0016	0.0454	0.0908	0.0008	0.02836	7.76E-04	7.783E-04	5.053E-05	-62.21	61.74	52.62	8.72	-34.50
	2	0:38:55	0.0016	0.0453	0.0906	0.0006	0.02836	7.29E-04				51.76			
	3	0:34:18	0.0015	0.0455	0.0910	0.0010	0.02846	8.30E-04				44.36			
11	1	1:48:22	0.003	0.0457	0.0914	0.0014	0.02696	2.49E-04	2.437E-04	7.220E-06	-72.27	43.55	65.39	22.43	-36.64
	2	1:54:31	0.003	0.0458	0.0916	0.0016	0.02696	2.35E-04				88.37			
	3	1:49:13	0.003	0.0457	0.0914	0.0014	0.02696	2.47E-04				64.24			

12	1	0:12:32	0.0018	0.0458	0.0916	0.0016	0.02816	2.25E-03	2.262E-03	3.117E-05	-52.91	65.12	73.19	8.21	-37.32
	2	0:12:34	0.0018	0.0459	0.0918	0.0018	0.02816	2.24E-03				72.91			
	3	0:12:18	0.0017	0.0459	0.0918	0.0018	0.02826	2.30E-03				81.53			
13	1	1:02:27	0.0022	0.0454	0.0908	0.0008	0.02776	4.45E-04	4.658E-04	1.850E-05	-66.65	39.39	50.31	10.31	-34.15
	2	0:58:04	0.0022	0.0452	0.0904	0.0004	0.02776	4.78E-04				51.66			
	3	0:58:28	0.0022	0.0455	0.0910	0.0010	0.02776	4.75E-04				59.88			
14	1	0:11:17	0.002	0.0459	0.0918	0.0018	0.02796	2.48E-03	2.454E-03	7.568E-05	-52.21	68.49	69.43	0.87	-36.83
	2	0:11:48	0.002	0.0459	0.0918	0.0018	0.02796	2.37E-03				70.2			
	3	0:11:07	0.002	0.0459	0.0918	0.0018	0.02796	2.52E-03				69.61			
15	1	0:17:45	0.0018	0.0458	0.0916	0.0016	0.02816	1.59E-03	1.596E-03	2.126E-05	-55.94	71.12	74.03	2.63	-37.39
	2	0:17:48	0.0018	0.0458	0.0916	0.0016	0.02816	1.58E-03				76.24			
	3	0:17:15	0.002	0.0458	0.0916	0.0016	0.02796	1.62E-03				74.73			
16	1	0:53:35	0.0014	0.0457	0.0914	0.0014	0.02856	5.33E-04	5.286E-04	9.213E-06	-65.54	51.7	47.18	4.15	-33.50
	2	0:55:08	0.0014	0.0458	0.0916	0.0016	0.02856	5.18E-04				46.29			
	3	0:53:13	0.0015	0.0458	0.0916	0.0016	0.02846	5.35E-04				43.55			
17	1	0:08:53	0.0018	0.0457	0.0914	0.0014	0.02816	3.17E-03	3.043E-03	2.048E-04	-50.38	73.18	67.80	4.82	-36.64
	2	0:10:02	0.0018	0.0454	0.0908	0.0008	0.02816	2.81E-03				66.37			
	3	0:08:56	0.0018	0.0455	0.0910	0.0010	0.02816	3.15E-03				63.86			
18	1	0:33:11	0.0018	0.0457	0.0914	0.0014	0.02816	8.49E-04	8.841E-04	3.204E-05	-61.08	49.74	50.14	6.97	-34.06
	2	0:31:46	0.0016	0.0457	0.0914	0.0014	0.02836	8.93E-04				57.31			
	3	0:31:08	0.0016	0.0458	0.0916	0.0016	0.02836	9.11E-04				43.38			
19	1	1:26:06	0.0026	0.0455	0.0910	0.0010	0.02736	3.18E-04	3.160E-04	2.440E-05	-70.06	54.07	52.96	6.98	-34.53
	2	1:33:24	0.0028	0.0453	0.0906	0.0006	0.02716	2.91E-04				59.32			
	3	1:20:53	0.0025	0.0454	0.0908	0.0008	0.02746	3.40E-04				45.49			
20	1	0:11:41	0.002	0.0459	0.0918	0.0018	0.02796	2.39E-03	2.399E-03	1.149E-05	-52.40	70.03	66.70	15.13	-36.63
	2	0:11:33	0.0021	0.0459	0.0918	0.0018	0.02786	2.41E-03				50.18			
	3	0:11:39	0.0021	0.0459	0.0918	0.0018	0.02786	2.39E-03				79.89			
21	1	1:10:38	0.003	0.0456	0.0912	0.0012	0.02696	3.82E-04	4.011E-04	1.684E-05	-67.95	42.3	49.11	6.35	-33.87
	2	1:06:25	0.0026	0.0454	0.0908	0.0008	0.02736	4.12E-04				50.15			
	3	1:07:46	0.0022	0.0454	0.0908	0.0008	0.02776	4.10E-04				54.87			
22	1	0:10:30	0.0016	0.0458	0.0916	0.0016	0.02836	2.70E-03	2.780E-03	7.163E-05	-51.13	83.47	80.82	4.27	-38.16
	2	0:10:06	0.0017	0.0458	0.0916	0.0016	0.02826	2.80E-03				75.9			
	3	0:09:59	0.0016	0.0458	0.0916	0.0016	0.02836	2.84E-03				83.09			
23	1	0:16:25	0.0018	0.0457	0.0914	0.0014	0.02816	1.72E-03	1.748E-03	3.559E-05	-55.15	65.27	77.25	14.44	-37.86
	2	0:15:46	0.0018	0.0457	0.0914	0.0014	0.02816	1.79E-03				73.19			
	3	0:16:09	0.0018	0.0458	0.0916	0.0016	0.02816	1.74E-03				93.28			
24	1	0:50:34	0.0015	0.0456	0.0912	0.0012	0.02846	5.63E-04	5.550E-04	1.310E-05	-65.12	50.18	56.02	6.70	-35.01
	2	0:50:37	0.0015	0.0455	0.0910	0.0010	0.02846	5.62E-04				63.34			
	3	0:52:43	0.0015	0.0456	0.0912	0.0012	0.02846	5.40E-04				54.53			
25	1	1:07:23	0.0026	0.0459	0.0918	0.0018	0.02736	4.06E-04	4.110E-04	8.873E-06	-67.73	42.19	48.65	6.45	-33.79
	2	1:04:43	0.0027	0.0457	0.0914	0.0014	0.02726	4.21E-04				48.69			
	3	1:06:57	0.0028	0.0457	0.0914	0.0014	0.02716	4.06E-04				55.08			
26	1	1:07:23	0.0026	0.0459	0.0918	0.0018	0.02736	4.06E-04	4.110E-04	8.873E-06	-67.73	69.32	84.62	15.74	-38.65
	2	1:04:43	0.0027	0.0457	0.0914	0.0014	0.02726	4.21E-04				100.7			
	3	1:06:57	0.0028	0.0457	0.0914	0.0014	0.02716	4.06E-04				83.78			

27	1	0:17:22	0.0018	0.0458	0.0916	0.0016	0.02816	1.62E-03	1.577E-03	4.478E-05	-56.05	75.79	69.81	5.33	-36.89
	2	0:18:19	0.0019	0.0457	0.0914	0.0014	0.02806	1.53E-03				65.57			
	3	0:17:48	0.0019	0.0458	0.0916	0.0016	0.02806	1.58E-03				68.06			
28	1	0:44:51	0.0016	0.0458	0.0916	0.0016	0.02836	6.32E-04	6.316E-04	1.772E-06	-63.99	61.5	59.78	12.16	-35.65
	2	0:45:03	0.0016	0.0458	0.0916	0.0016	0.02836	6.30E-04				46.85			
	3	0:44:49	0.0016	0.0456	0.0912	0.0012	0.02836	6.33E-04				70.98			
29	1	0:16:53	0.0018	0.0460	0.0920	0.0020	0.02816	1.67E-03	1.585E-03	7.980E-05	-56.02	64.54	61.19	3.83	-35.74
	2	0:18:32	0.002	0.0460	0.0920	0.0020	0.02796	1.51E-03				57.01			
	3	0:17:42	0.002	0.0460	0.0920	0.0020	0.02796	1.58E-03				62.01			
30	1	0:47:06	0.0014	0.0458	0.0916	0.0016	0.02856	6.06E-04	6.082E-04	7.762E-06	-64.32	51.95	52.83	0.80	-34.46
	2	0:47:19	0.0015	0.0456	0.0912	0.0012	0.02846	6.01E-04				53.05			
	3	0:46:09	0.0015	0.0455	0.0910	0.0010	0.02846	6.17E-04				53.5			
31	1	1:28:23	0.0018	0.0455	0.0910	0.0010	0.02816	3.19E-04	2.995E-04	2.529E-05	-70.54	47.36	45.31	2.51	-33.13
	2	1:43:15	0.002	0.0456	0.0912	0.0012	0.02796	2.71E-04				46.05			
	3	1:30:29	0.002	0.0455	0.0910	0.0010	0.02796	3.09E-04				42.51			
32	1	0:18:21	0.0018	0.0458	0.0916	0.0016	0.02816	1.53E-03	1.580E-03	3.953E-05	-56.03	75.97	74.05	1.88	-37.39
	2	0:17:34	0.0017	0.0458	0.0916	0.0016	0.02826	1.61E-03				72.22			
	3	0:17:39	0.0018	0.0459	0.0918	0.0018	0.02816	1.60E-03				73.96			
33	1	0:09:45	0.0016	0.0459	0.0918	0.0018	0.02836	2.91E-03	2.700E-03	1.967E-04	-51.42	82.47	74.71	10.82	-37.53
	2	0:10:32	0.0018	0.0458	0.0916	0.0016	0.02816	2.67E-03				79.3			
	3	0:11:11	0.0018	0.0459	0.0918	0.0018	0.02816	2.52E-03				62.35			
Sp	1	0:08:04	0.0018	0.0463	0.0926	0.0026	0.02816	3.49E-03	3.434E-03	6.873E-05	-49.29	N/A	N/A	N/A	N/A
	2	0:08:11	0.0017	0.0465	0.0930	0.0030	0.02826	3.45E-03				N/A			
	3	0:08:25	0.0017	0.0465	0.0930	0.0030	0.02826	3.36E-03				N/A			
Ra	1	1:10:30	0.0017	0.0460	0.0920	0.0020	0.02826	4.01E-04	4.104E-04	1.877E-05	-67.75	30.23	30.34	0.71	-29.64
	2	1:11:12	0.0016	0.0463	0.0926	0.0026	0.02836	3.98E-04				29.7			
	3	1:05:11	0.0018	0.0461	0.0922	0.0022	0.02816	4.32E-04				31.1			

Appendix F – Hemispherical Geometry Data

Wafer #	Hemi	Cond (ohm-cm)	Elect.	P	A	B	SV	R	U	VPULS	M	C	V	RF	Time	Speed	Depth	Ra	Avg Ra
1	1	1 to 10	1	3	50	50	50	0.2	0.1	28	14	0	-200	25	4:09:49	0.00024	0.057	129.07	125.9
			2	1.5	3.2	25	65	0.2	0.4	23.62	4	5	-120	25	0:59:46	0.00098	0.058	125.44	
			3	0.5	1.6	25	65	0.4	1.6	23.63	4	3	-80	25	0:54:01	0.0011	0.059	123.43	
1	2	1 to 10	1	6	25	100	50	0.2	0.4	15	1	0	-200	25	81:18:04	0	0.057	245.43	204.5
			2	1.5	3.2	25	65	0.2	0.4	23.62	4	5	-120	25	0:51:35	0.00114	0.058	214.27	
			3	0.5	1.6	25	65	0.4	1.6	23.63	4	3	-80	25	0:44:53	0.001	0.059	153.93	
1	3	1 to 10	1	12	50	50	50	0.2	0.8	23.62	14	0	-200	26	4:32:00	0.0002	0.055	82.12	84.02
			2	2	6.4	12.8	65	0.2	0.2	23.62	4	6	-200	25	0:07:36	0.00764	0.058	94.19	
			3	0.5	0.8	6.4	70	0.4	1.6	9.45	4	1	-200	30	0:53:30	0.0011	0.059	75.76	
2	4	1 to 10	1	16	100	50	50	0.2	0.1	23.62	14	0	-200	26	4:43:52	0.002	0.054	Not taken	N/A
			2	2	6.4	12.8	65	0.2	0.2	23.62	4	6	-200	25	0:05:55	0.0098	0.058	Not taken	
			3	0.5	1.6	6.4	70	0.4	1.6	9.45	4	13	-200	30	0:14:28	0.00409	0.059	Not taken	
3	5	0.016	1	16	100	50	50	0.2	0.1	23.62	14	0	-200	26	0:04:58	0.01087	0.054	Not taken	N/A
			2	2	6.4	12.8	65	0.2	0.2	23.62	4	6	-200	25	Did not cut			Not taken	
			3	0.5	1.6	6.4	70	0.4	1.6	9.45	4	13	-200	30	Did not cut			Not taken	
3	6	0.016	1	3	50	50	50	0.2	0.2	23.62	14	0	-120	25	0:20:05	0.00268	0.054	31.82	36.50
			2	1.5	3.2	25	65	0.2	0.4	23.62	4	5	-120	25	0:02:57	0.01965	0.058	37.6	
			3	0.5	0.8	6.4	70	0.4	0.4	15	4	1	-80	30	0:47:03	0.00126	0.059	40.07	
4	7	0.016	1	3	50	50	50	0.2	0.2	23.62	14	0	-120	25	0:20:22	0.00244	0.05	17.02	18.92
			2	1.5	3.2	25	65	0.2	0.4	23.62	4	5	-120	25	0:06:53	0.00843	0.058	19.15	
			3	0.5	0.8	6.4	70	0.4	0.4	15	4	1	-80	30	1:48:45	0.00055	0.059	20.58	

Wafer #	Hemi	Cond (ohm-cm)	Elect	P	A	B	SV	R	U	VPULS	M	C	V	RF	Time	Speed	Depth	Ra	Avg Ra
4	8	0.016	1	2	6.4	50	65	0.2	0.2	23.62	4	6	-120	25	0:31:44	0.00157	0.05	16.69	21.41
			2	1.5	3.2	25	65	0.2	0.4	23.62	4	5	-120	25	0:07:40	0.00756	0.058	23.46	
			3	0.5	0.8	6.4	70	0.4	0.4	15	4	1	-80	25	1:48:38	0.00055	0.059	24.07	
4	9	0.016	1	1.5	3.2	25	65	0.2	0.4	23.62	4	5	-120	25	0:20:55	0.0024	0.05	13.53	13.63
			2	1.5	3.2	25	65	0.2	0.4	23.62	4	5	-120	25	0:08:47	0.00661	0.058	12.96	
			3	0.5	0.8	6.4	70	0.4	0.4	15	4	1	-80	25	2:31:58	0.00043	0.059	14.4	
5	10	0.016	1	1.5	3.2	25	65	0.2	0.2	23.62	4	5	-120	25	0:29:53	0.00165	0.05	37.24	37.68
			2	1.5	3.2	25	65	0.2	0.2	23.62	4	5	-120	25	0:10:05	0.00575	0.058	33.53	
			3	0.5	1.6	6.4	70	0.4	0.4	15	4	13	-80	25	0:25:38	0.00228	0.059	42.27	
5	11	0.016	1	1.5	3.2	25	65	0.2	0.8	23.62	4	5	-120	25	0:17:16	0.00267	0.05	28.24	28.62
			2	1.5	3.2	25	65	0.2	0.4	23.62	4	5	-120	25	0:08:06	0.00717	0.058	25.74	
			3	0.5	1.6	6.4	70	0.4	0.4	15	4	13	-80	25	0:25:14	0.00232	0.059	31.87	
5	12	0.016	1	1.5	3.2	25	65	0.2	0.4	23.62	4	5	-120	25	0:17:02	0.00291	0.05	10.59	10.52
			2	1.5	3.2	25	65	0.2	0.4	23.62	4	5	-120	25	0:08:36	0.00673	0.058	13.10	
			3	0.5	0.8	6.4	70	0.4	1.6	15	4	1	-80	25	2:44:13	0.00035	0.059	7.86	